

Features of myelin oligodendrocyte glycoprotein (MOG) required for the detection of autoantibodies from patients with MOG-antibody-associated disorders

Dissertation



Zur Erlangung des Doktorgrades der
Naturwissenschaften

(Dr. rer. nat.)

an der Fakultät für Biologie

der Ludwig-Maximilians-Universität München

Caterina Macrini

München 2021

Diese Dissertation wurde angefertigt unter der Leitung von Prof. Dr. Edgar
Meinl am Institut für Klinische Neuroimmunologie (Biomedizinisches Centrum,
Martinsried)
Ludwig-Maximilians-Universität München

Erstgutachterin: Prof. Dr. Elisabeth Weiß
Zweitgutachterin: Prof. Dr. Laura Busse

Tag der Abgabe: 22.02.21

Tag der mündlichen Prüfung: 22.06.21

EIDESSTATTLICHE ERKLÄRUNG

Ich versichere hiermit an Eides statt, dass die vorgelegte Dissertation von mir selbständig und ohne unerlaubte Hilfe angefertigt worden ist. Die vorliegende Dissertation wurde weder ganz, noch teilweise bei einer anderen Prüfungskommission vorgelegt. Ich habe noch zu keinem früheren Zeitpunkt versucht, eine Dissertation einzureichen oder anderweitig an einer Doktorprüfung teilzunehmen.

München, 03. November 2021

Caterina Macrini

*To Giulio Regeni,
And to his dreams.
Verità per Giulio Regeni*

TABLE OF CONTENTS

Table of contents	vii
Abbreviations	ix
List of Figures	xi
1 List of publications	xiii
1.1 Macrini et al., BRAIN, 2021	xiii
1.2 Gerhards et al., Acta Neuropathologica Communications, 2020	xiii
1.3 Winklmeier et al., Neurology Neuroimmunology & Neuroinflammation, 2019.....	xiii
1.4 Marti Fernandez et al., Frontiers in Immunology, 2019	xiv
1.5 Bronge et al., Journal of Autoimmunity, 2019	xiv
1.6 Spadaro et al., Annals of Neurology, 2018	xiv
Declaration of contribution as a co-author	xvii
Publication 1.4: Marti Fernandez et al., Frontiers in Immunology.	xvii
Publication 1.6: Spadaro et al., Annals of Neurology	xviii
Summary	1
Aims of the thesis	3
2 Introduction	5
2.1 Inflammatory demyelinating diseases of the central nervous system	5
2.2 General mechanisms of action of autoantibodies in the brain	5
2.3 Multiple sclerosis	6
2.3.1 Disease course and clinical symptomatology	6
2.3.2 Genetic and environmental risk factors in MS	7
2.3.3 Immunopathogenesis of MS.....	9
2.4 Neuromyelitis optica spectrum disorders	11
2.4.1 Clinical manifestations.....	11
2.4.2 Anti-AQP4 antibodies and their role in the immunopathogenesis. 12	

2.5	Acute disseminated encephalomyelitis	14
2.5.1	Disease features	14
2.6	MOG-antibody associated disorders	15
2.6.1	MOG protein: structure and glycosylation	15
2.6.2	Detection methods of MOG-antibodies	19
2.6.3	A new distinct group among CNS demyelinating diseases	21
2.6.4	Pathogenicity of MOG-antibodies	23
3	Results	25
3.1	Publication 1.1: Macrini et al. (2021), (accepted on 08.01.2021)	25
3.2	Publication 1.4: Marti Fernandez et al. (2019)	79
3.3	Publication 1.6: Spadaro et al. (2018)	91
4	Discussion	107
4.1	Details of antigen recognition of MOG-Abs	107
4.2	Pathogenic activity of MOG-Abs from patients	114
4.3	Conclusions	116
5	Reference List	119
6	Acknowledgments	139
7	Curriculum Vitae	143

ABBREVIATIONS

aa	Amino acid
Abs	Antibodies
ADEM	Acute disseminated encephalomyelitis
ADCC	Antibody-dependent cellular cytotoxicity
APC	Antigen presenting cell
AQP4	Aquaporin-4
BBB	Blood-brain barrier
CBA	Cell-based assay
CDC	Complement-dependent cytotoxicity
CNS	Central nervous system
CSF	Cerebrospinal fluid
EAE	Experimental autoimmune encephalitis
EBNA	Epstein-Barr virus nuclear antigen 1
EBV	Epstein-Barr virus
ELISA	Enzyme-linked immunosorbent assay
FRET	Förster resonance energy transfer
GFAP	Glial fibrillary acidic protein
GWAS	Genome-wide association studies
HLA	Human leucocyte antigen
hMOG	Human myelin oligodendrocyte glycoprotein
IgG	Immunoglobulin G
LFB	Luxol fast blue
mAb	Monoclonal antibody
MAC	Membrane attack complex

MBP	Myelin basic protein
MFI	Mean fluorescent intensity
MHC	Major histocompatibility complex
MOG	Myelin oligodendrocyte glycoprotein
mMOG	Mouse myelin oligodendrocyte glycoprotein
MOGAD	MOG-antibody-associated disorders
MRI	Magnetic resonance image
MS	Multiple sclerosis
NGF	Nerve growth factor
NMDAR	N-Methyl-D-aspartate receptor
NMOSD	Neuromyelitis optica spectrum disorders
OAPs	Orthogonal arrays of particles
OCB	Oligoclonal bands
ON	Optic neuritis
PPMS	Primary progressive multiple sclerosis
RRMS	Relapsing remitting multiple sclerosis
TM	Transverse myelitis

LIST OF FIGURES

Figure 1: Schematic illustration of MOG localization and structure.	18
Figure 2: Schematic representation of the testing for MOG antibodies.	112
Figure 3: Pathogenic mechanisms of affinity-purified MOG antibodies deriving from patients.....	114

1 LIST OF PUBLICATIONS

1.1 Macrini et al., BRAIN, 2021

Features of MOG required for recognition by patients with MOG-antibody-associated disorders, BRAIN, 2021

Caterina Macrini, Ramona Gerhards, Stephan Winklmeier, Lena Bergmann, Simone Mader, Melania Spadaro, Atay Vural, Michaela Smolle, Reinhard Hohlfeld, Tania Kümpfel, Stefan F. Lichtenthaler, Henri G. Franquelim, Dieter Jenne, Edgar Meinl

1.2 Gerhards et al., Acta Neuropathologica Communications, 2020

OMGP as a novel target for pathogenic autoimmunity in the CNS, Acta Neuropathologica Communications, 2020; 8(1): 207

Ramona Gerhards, Lena Kristina Pfeffer, Jessica Lorenz, Laura Starost, Luise Nowack, Franziska S. Thaler, Miriam Schlüter, Heike Rübsamen, Caterina Macrini, Stephan Winklmeier, Simone Mader, Mattias Bronge, Hans Grönlund, Regina Feederle, Hung-En Hsia, Stefan F Lichtenthaler, Juliane Merl-Pham, Stefanie M Hauck, Tanja Kuhlmann, Isabel J. Bauer, Eduardo Beltran, Lisa-Ann Gerdes, Aleksandra Mezydło, Amit Bar-Or, Brenda Banwell, Mohsen Khademi, Tomas Olsson, Reinhard Hohlfeld, Hans Lassmann, Tania Kümpfel, Naoto Kawakami, Edgar Meinl

1.3 Winklmeier et al., Neurology Neuroimmunology & Neuroinflammation, 2019

Identification of circulating MOG-specific B cells in patients with MOG antibodies, Neurology Neuroimmunology & Neuroinflammation, 2019; 6(6): 625

Stephan Winklmeier, Miriam Schlüter, Melania Spadaro, Franziska S. Thaler, Atay Vural, Ramona Gerhards, Caterina Macrini, Simone Mader, Aslı Kurne,

Berin Inan, Rana Karabudak, Feyza Gül Özbay, Gunes Esendagli, Reinhard Hohlfeld, Tania Kümpfel, Edgar Meinl

1.4 Marti Fernandez et al., Frontiers in Immunology, 2019

The Glycosylation Site of Myelin Oligodendrocyte Glycoprotein Affects Autoantibody Recognition in a Large Proportion of Patients, Frontiers in Immunology, 2019; 10: 1189

Iris Marti Fernandez, Caterina Macrini, Markus Krumbholz, Paul J. Hensbergen, Agnes L. Hipgrave Ederveen, Stephan Winklmeier, Atay Vural, Asli Kurne, Dieter Jenne, Frits Kamp, Lisa Ann Gerdes, Reinhard Hohlfeld, Manfred Wuhler, Tania Kümpfel, Edgar Meinl

1.5 Bronge et al., Journal of Autoimmunity, 2019

Myelin oligodendrocyte glycoprotein revisited - sensitive detection of MOG-specific T-cells in multiple sclerosis, Journal of Autoimmunity, 2019; 102: 38-49

Mattias Bronge, Sabrina Ruhrmann, Claudia Carvalho-Queiroz, Ola B. Nilsson, Andreas Kaiser, Erik Holmgren, Caterina Macrini, Stephan Winklmeier, Edgar Meinl, Lou Brundin, Mohsen Khademi, Tomas Olsson, Guro Gafvelin, Hans Grönlund

1.6 Spadaro et al., Annals of Neurology, 2018

Pathogenicity of human antibodies against myelin oligodendrocyte glycoprotein, Annals of Neurology 2018; 84(2): 315-28

Melania Spadaro, Stephan Winklmeier, Eduardo Beltrán, Caterina Macrini, Romana Höftberger, Elisabeth Schuh, Franziska S. Thaler, Lisa-Ann Gerdes, Sarah Laurent, Ramona Gerhards, Simone Brändle, Klaus Dornmair, Constanze Breithaupt, Markus Krumbholz, Markus Moser, Gurumoorthy

Kirshnamoorthy, Frits Kamp, Dieter Jenne, Reinhard Hohlfeld, Tania Kümpfel,
Hans Lassmann, Naoto Kawakami, Edgar Meinel

DECLARATION OF CONTRIBUTION AS A CO-AUTHOR

The publications Marti Fernandez et al. (2020) and Spadaro et al. (2018), items 1.4 and 1.6, respectively, are part of this cumulative thesis. I contributed to these publications as follows:

PUBLICATION 1.4: MARTI FERNANDEZ ET AL., FRONTIERS IN IMMUNOLOGY.

The Glycosylation Site of Myelin Oligodendrocyte Glycoprotein Affects Autoantibody Recognition in a Large Proportion of Patients, *Frontiers in Immunology*, 2019

Iris Marti Fernandez, Caterina Macrini, Markus Krumbholz, Paul J. Hensbergen, Agnes L. Hipgrave Ederveen, Stephan Winklmeier, Atay Vural, Asli Kurne, Dieter Jenne, Frits Kamp, Lisa Ann Gerdes, Reinhard Hohlfeld, Manfred Wuhrer, Tania Kümpfel, Edgar Meinl

My contribution to this work:

In this work, I performed repetitions of the cell-based assay with the MOG unglycosylated variants. I extensively worked on the writing of the manuscript together with I. Marti Fernandez and on its revision. I contributed especially on the preparation of the figures (Fig. 1, 2 and 3), the statistical analysis and the completion of Table 2.

Prof. Meinl

Prof. Weiß

PUBLICATION 1.6: SPADARO ET AL., ANNALS OF NEUROLOGY

Pathogenicity of human antibodies against myelin oligodendrocyte glycoprotein, Annals of Neurology 2018

Melania Spadaro, Stephan Winklmeier, Eduardo Beltrán, Caterina Macrini, Romana Höftberger, Elisabeth Schuh, Franziska S. Thaler, Lisa-Ann Gerdes, Sarah Laurent, Ramona Gerhards, Simone Brändle, Klaus Dornmair, Constanze Breithaupt, Markus Krumbholz, Markus Moser, Gurumoorthy Kirshnamoorthy, Frits Kamp, Dieter Jenne, Reinhard Hohlfeld, Tania Kümpfel, Hans Lassmann, Naoto Kawakami, Edgar Meinl

My contribution to this work:

In this work, I prepared the samples used for circular dichroism spectroscopy. I also performed cell-based assays on live and fixed cells expressing MOG as requested for revision purposes. I performed cell-based assays to characterize the anti-MOG responses to MOG derived from different species, which was included in Table 1. I contributed to the editing of the manuscript.

Prof. Meinl

Prof. Weiß

SUMMARY

Millions of people worldwide are currently affected by an inflammatory disease of the central nervous system; among those the most common and known is multiple sclerosis (MS). The diagnosis of those diseases can be very difficult, since the different pathologies have overlapping clinical symptoms.

Myelin oligodendrocyte glycoprotein-associated disorders (MOGAD) is an emerging pathology within this group. MOGAD patients present in their serum autoantibodies against the MOG protein. The clinical features of patients with MOGAD include optic neuritis (ON) and transverse myelitis (TM), which are also typical features of AQP4+ neuromyelitis optica spectrum disorder (NMOSD), another CNS autoimmune disease.

However, since MOGAD has been categorized only recently as a separate entity within this group, there is the urgent need to understand more of the interaction between autoantibodies and their target antigen, in order to develop a reliable diagnostic test. Furthermore, little is still known about the pathomechanisms that the MOG antibodies exert in the CNS.

In this thesis, we successfully elaborated that the intracellular part of MOG, specifically its second hydrophobic domain is essential for the autoantibodies to bind to its extracellular part. The need of this intracellular domain explains why the cell-based assay is currently the gold standard for the MOG antibodies' detection in human samples. Furthermore, we showed that the MOG antibodies deriving from patients bind the MOG protein bivalently. Since monovalent binding is known to activate the complement more efficiently than bivalent binding, this suggests that a therapeutic approach inhibiting complement might be less efficient than it was in patients with AQP4-Abs, where a monovalent binding has been shown. Altogether, the results compiled in this thesis deepen our knowledge about details of antigen-recognition of autoantibodies to MOG and have implications for our concepts of pathogenicity of MOGAD.

AIMS OF THE THESIS

The following points are the main objectives of the thesis:

- Determination of the essential domains of MOG required for the autoantibodies from patients with MOGAD in order to bind to the external portion of MOG
- Localization of the C-terminus of MOG
- Determination of monovalent versus bivalent binding of human MOG antibodies
- Contributed to the definition of the effects of the glycosylation of MOG on the antibody binding in (Marti Fernandez *et al.*, 2019)
- Contributed to the characterization of the effects of MOG affinity purified antibodies from MOGAD patients in transfer experiments in rodents in (Spadaro *et al.*, 2018)

2 INTRODUCTION

2.1 Inflammatory demyelinating diseases of the central nervous system

Inflammatory demyelinating diseases of the central nervous system (CNS) are a group of heterogeneous diseases characterized by the immune system attacking components of the CNS. This happens because the cellular components of the immune system are not capable to distinguish between self-antigens and external or pathological ones. The cause that can lead to this dysfunction cannot be attributed to a single and very specific event. The diagnosis of those diseases that fall into this group can be very difficult, since the different pathologies can have overlapping clinical symptoms or overlapping brain magnetic resonance imaging (MRI) and serological findings. Our work mostly focuses on the action of antibodies autoreactive in the brain. In the next paragraphs, I am going to briefly describe the type of pathological mechanisms autoantibodies can exert in the CNS. Furthermore, I will discuss in details some of the most common inflammatory diseases of this group, like multiple sclerosis (MS), neuromyelitis optica spectrum disorders (NMOSD), acute disseminated encephalomyelitis (ADEM) and MOG-antibody associated disorders (MOGAD).

2.2 General mechanisms of action of autoantibodies in the brain

Different mechanisms of action of autoantibodies in the brain have been described. For instance, autoantibodies can bind to antigens present on neuronal cells like oligodendrocytes or glial cells. While they bind their target antigen, their Fc portion can activate the complement. Upon the formation of the membrane attack complex (MAC), cell death can follow. This type of mechanism of action is called complement-mediated cytotoxicity (CDC). Another common mechanism is the antibody-dependent cell-mediated cytotoxicity (ADCC), where cells (NK, macrophages, neutrophils) bind the antibodies with their FC receptors, and through degranulation or release of cytotoxic factors manage to kill the antibody-targeted cells. Without causing

cell death, the binding of autoantibodies on their target can interfere with receptor crosstalk or lead to the internalization of the antigen, subsequently leading to a down or upregulation of cellular pathways (Brimberg *et al.*, 2015).

2.3 Multiple sclerosis

2.3.1 Disease course and clinical symptomatology

Around 2.5 million people are affected by multiple sclerosis (MS). MS is the most common inflammatory demyelinating disease of the CNS and it is the main cause of disability in young adults with an age of onset between 20 and 40 years (Koch-Henriksen and Sorensen, 2010; Dendrou *et al.*, 2015). The main features of this disease are ovoid shaped multifocal lesions disseminated in the white matter of the optic nerves, brainstem, cerebellum and in the grey matter (Popescu *et al.*, 2013). Those lesions are characterized by demyelination, presumably due to the combined attack of the innate and adaptive immune system (mostly macrophages, microglia, CD4+ and CD8+ T cells, B cells and antibodies) (Sospedra and Martin, 2005; Dendrou *et al.*, 2015). MS has heterogeneous clinical manifestations and disease courses, mostly due to the different CNS lesions in space and time (Kearney *et al.*, 2015). Patients with MS can display weakness, pain, cognitive difficulties, sensory and visual impairments and motor dysfunction (Compston and Coles, 2008). For the diagnosis of this disease, clinicians need to evaluate the clinical history of the subject together with MRI scans of the brain to visualize possible lesions and a lumbar puncture to analyse the presence of oligoclonal bands (OCBs) in the cerebrospinal fluid (CSF). OCBs are immunoglobulins (Ig) produced intrathecally in the CSF but not in the serum. They are shown by isoelectric focussing and are present in 95% of MS patients (McDonald *et al.*, 2001; Rammohan, 2009; Stangel *et al.*, 2013; Thompson *et al.*, 2018).

Clinically isolated syndrome (CIS) can be defined as the first manifestation that can lead to the development of MS. It is a neurological dysfunction that can originate from a demyelinating or inflammatory event in the areas of the optic nerve, the spinal cord or the brainstem (Miller *et al.*, 2012). Before the re-evaluation of the McDonald criteria in 2017, a CIS patient needed the

occurrence of a second lesion after the first attack to be considered an MS patient (McDonald *et al.*, 2001). With the new indications, if the MRI shows the presence of old asymptomatic lesions or symptomatic lesions in another CNS location, and if the current symptoms last at least 24 hours, the subject is directly categorized as an MS patient. What is essential in the diagnosis of MS is that the lesions are always disseminated in time and space (Thompson *et al.*, 2018). Around 85% of patients are affected by the most common type of MS, the relapsing-remitting multiple sclerosis (RRMS). A minority of patients (10%) begins with a primary progressive (PPMS) course of the disease with no acute attacks, but a steady progression towards disability (Sospedra and Martin, 2005). The RRMS form, instead, is characterized by different cycles of acute relapses, followed by partial remission. In some cases the CNS lesions can occur even without clinical symptoms, however every lesion paves the way to some degree of physical impairments (Hemmer *et al.*, 2002; Dendrou *et al.*, 2015). Approximately 80% of RRMS patients (around 10 to 20 years after the first diagnosis) develop secondary progressive multiple sclerosis (SPMS). In this phase the acute relapses and connected inflammatory activity diminish, the CNS atrophy increases and overall the course of the disease is more similar to the PPMS. This means that there must be an underlying pathophysiological mechanism, unrelated to the inflammatory process typical for RRMS, that leads to the neurological decline and that the currently available treatments are not capable to stop (Hemmer *et al.*, 2002; Dendrou *et al.*, 2015; Feinstein *et al.*, 2015).

2.3.2 Genetic and environmental risk factors in MS

The cause of MS is still not known. However, it is believed that the disease develops in genetically predisposed people and is triggered by environmental factors (Dendrou *et al.*, 2015). It has been observed that the risk of developing the disease increases 20 to 50-fold in first degree related people, in contrast to the overall population (Hollenbach and Oksenberg, 2015). Nonetheless, MS is not caused by a single gene mutation. In fact, genome wide association studies (GWAS) unravelled variants of several genes that can contribute to a higher chance to develop MS. In particular, these studies showed the

correlation between MS and variants of the human leucocyte antigen (HLA) class II gene, which seem to account for 10-60% of the genetic risk of MS (Hillert and Olerup, 1993). Among those variants, the more significant ones are the following: HLA-DRB1*1501, HLA-DRB1*0301 and HLA-DRB1*1303. In contrast to HLA-DRB1*1501, which is linked only to MS, the other two allele variants are associated also with other autoimmune diseases like rheumatoid arthritis, psoriasis and Graves' disease (Gough and Simmonds, 2007; Hemmer *et al.*, 2015). Overall, since HLA genes encode for proteins that process and present antigens to T cells, those HLA variations might affect T cell activation, by triggering an autoimmune response specifically towards the CNS (Hemmer *et al.*, 2015). In addition, mutations in several other genes (like the ones encoding for the α -chain of the IL-2 and IL-7 receptor) have also been linked to a higher susceptibility of MS (Gregory *et al.*, 2007; Hartmann *et al.*, 2014). The mutations of these genes could have a broader and more general effect to the immune system regulation and threshold of its activation (Dendrou *et al.*, 2015).

As mentioned above, MS in genetically predisposed people is most likely triggered also by exogenous factors. This was particularly visible in migration studies. In fact, it is known that MS prevalently affects Caucasians in countries far from the equator (North America, South Australia and Northern Europe), and it is rarely seen in Africans and Asians (Noseworthy *et al.*, 2000; Baecher-Allan *et al.*, 2018). However, when a subject in its adolescent years was moving from a low risk-country to a high-risk one, it had increased the chances to develop the disease. The reasons behind the geographical impact could be due to factors like sunlight exposure and vitamin D levels (van der Mei *et al.*, 2003; Munger *et al.*, 2004). It seems that high vitamin D levels can have protective effects towards autoimmune diseases and vitamin D in general has immunomodulatory properties (Munger *et al.*, 2004). Other exogenous factors that are connected with triggering MS are the Epstein-Barr virus (EBV) and smoking. Even though the underlying mechanisms are not fully understood, it has been shown that smokers and subjects with high levels of antibodies against EBV nuclear antigen 1 (EBNA1) have a higher risk to develop MS (Nielsen *et al.*, 2007; Wingerchuk, 2012). Even the effect of hormones on the immune system has been considered as a possible factor influencing the

onset of the disease, since MS occurs 2.8 times more often in women than in men (Greer and McCombe, 2011).

2.3.3 Immunopathogenesis of MS

As previously described, one of the hallmarks of MS are multifocal lesions of the white and grey matter. The lesions are damaged portions of the myelin sheath by infiltrated macrophages containing myelin debris, CD4+ T cells, CD8+ T cells, B cells and plasma cells (Popescu *et al.*, 2013). This means that all those cells and more in general the dysregulated immune system play a central role in the pathogenesis of the disease. Histopathological findings helped classifying MS lesions in four different patterns. In MS type I and type II lesions the inflammation is fundamentally driven by T cells and macrophages. In type II lesions complement and antibody deposition are also present. Those two patterns show similarity with autoimmune encephalitis. MS lesions type III and IV, instead, lack complement and antibodies and display apoptotic oligodendrocytes. Possibly the demyelination in these cases is caused by toxins or viruses and does not have an autoimmune origin (Lucchinetti *et al.*, 2000).

MS is believed to be a CD4+ T cell mediated disease, however there are arguments in favour and against this statement. What clearly speaks in favour of this hypothesis is that many of the genes that have been found to increase the susceptibility to the disease are variants of the HLA class II molecules. Those molecules are known to be specific for the antigen presentation to CD4+ cells (Hohlfeld *et al.*, 2016a). Likewise, the animal model of MS, known as experimental autoimmune encephalomyelitis (EAE), further supports the aforementioned hypothesis. EAE can be induced in mice or rats by the injection of myelin proteins together with adjuvants. The animals subsequently show MS-like symptoms. It was demonstrated that the effectors in the EAE model are CD4+ Th1 cells producing IFN- γ , IL-2 and CD4+ Th17 cells producing IL-17, IL-21 and IL-22 (Zamvil and Steinman, 1990; Hohlfeld *et al.*, 2016a). A further prove came from an alternative strategy that was used to induce EAE. Adoptive transfer of myelin basic protein (MBP) or MOG specific CD4+ T cells into naïve recipients also was sufficient to trigger EAE (Ben-Nun

et al., 1981; Gold *et al.*, 2006). However, against the initial hypothesis, there are different arguments. Firstly, in the MS lesions CD8+ T cells are more present than CD4+ T cells. Secondly, CD8+ T cells locally expand at the site of the lesion, but due to experimental difficulties, it has not been possible to further investigate the precise function that they might have (Hohlfeld *et al.*, 2016b). Finally, autoreactive myelin specific CD4+ T cells can also be found in the blood and the CSF of healthy individuals, meaning that these cells are not a prerogative of only MS patients (O'Connor *et al.*, 2001; Hemmer *et al.*, 2002).

B cells have received more and more attention in the pathogenesis of MS. This increased attention is partially due to the efficacy of anti-CD20 monoclonal antibody specific therapies (rituximab, ocrelizumab), which deplete the B cell pool without affecting long-lived plasma cells, meaning that the production of antibodies is intact (Hauser, 2015; Hohlfeld *et al.*, 2016b). As previously said, one of the hallmarks of MS is the presence of oligoclonal bands in the CSF of patients. Moreover, clonally expanded B cells are found in the brain parenchyma, in the CSF and in aggregates in the meninges (Owens *et al.*, 2003; Serafini *et al.*, 2004; Lovato *et al.*, 2011). Intriguingly, transcriptome analysis of the B cells in the CSF compared to proteome analysis of the OCBs, showed an overlap between the two, indicating that those B cells present in the CSF are the ones producing the oligoclonal immunoglobulins G (IgGs) (Obermeier *et al.*, 2011).

More than a T cell driven disease only, MS is a disease where T and B cells interplay and have both a role in the pathogenesis. What has been hypothesized is that myelin-reactive T cells, which detect myelin components, are activated by antigen presenting cells (APCs) and once activated, they disrupt the blood-brain barrier (BBB). Once the BBB is breached, they damage and inflame the CNS. The breach in the BBB allows also other cells to penetrate the CNS. Among those are B cells, which can be activated in the periphery or directly in the CNS compartment. Independently from their activation location, B cells can act as APCs and recruit further T cells or in the CNS they can differentiate into plasmablasts and plasma cells, which are able to secrete antibodies. The antibodies in the CNS could target myelin

components as well or could activate the complement machinery to further disrupt the myelin sheath and increase the degree of demyelination (Hemmer *et al.*, 2002; Sospedra and Martin, 2005). This theory would be backed up by MS lesions type II, where complement and antibody deposition can be found, or by animal experiments that show that antigen presentation by B cells augments inflammation through further T cell activation (Parker Harp *et al.*, 2015).

2.4 Neuromyelitis optica spectrum disorders

2.4.1 Clinical manifestations

NMOSD differs from MS. Patients with NMOSD have an average age of disease onset at 39 years. The disease is more prevalent in women than in men (8:1), and it seems to have a higher incidence in the Asian and Black population compared to the Caucasian one (Wingerchuk *et al.*, 2007a; Jarius and Wildemann, 2010; Pandit *et al.*, 2015). Initially it was mistaken as a severe manifestation of MS; however, the absence of OCBs, the characteristic lesion pattern observed by MRI scans and the course of the disease were the initial proofs that NMOSD is a different disease than MS. The main clinical features of NMOSD are ON and longitudinally extensive myelitis (at T2 level, extending sometimes over more than three vertebral segments). Patients, even if rarely, can also show brainstem encephalitis or diencephalic syndrome (Jarius *et al.*, 2014; Weinshenker and Wingerchuk, 2017; Mader *et al.*, 2020). NMOSD usually does not have a monophasic course, it is actually characterised by several attacks, which in contrary to MS, tend to be more persistent and long lasting. Furthermore, there is no complete recovery from the attacks, leading to the accumulation of deficits, which can ultimately result in blindness and paralysis. However, NMOSD is unlikely to transition into a secondary progressive clinical course like MS (Wingerchuk *et al.*, 2007b; Kleiter *et al.*, 2016; Pandit and Mustafa, 2017).

The discovery of a very specific biomarker in the serum of patients with NMOSD led to a better definition of the disease. In fact, in around 80% of the people with NMOSD, serum autoantibodies are present against the protein

aquaporin-4 (AQP4), which is highly present in the spinal cord and the optic nerve (Lennon *et al.*, 2004; Lennon *et al.*, 2005; Mader *et al.*, 2010; Waters *et al.*, 2012; Weber *et al.*, 2018). Currently, AQP4-antibodies are included as markers for diagnosing NMOSD (with 99% specificity). AQP4 antibodies therefore help with the decision regarding the therapeutic intervention (Wingerchuk *et al.*, 2006).

2.4.2 Anti-AQP4 antibodies and their role in the immunopathogenesis

Aquaporins are a family of water channel proteins localized in the cell membrane (Carbrey and Agre, 2009). AQP4 is one of the members of this family and it is known for its high water permeability (Yang and Verkman, 1997). This particular protein is mostly expressed in the CNS, however, it can also be found in the kidneys, skeletal muscles and the epithelium of the airways (Frigeri *et al.*, 1995a; Frigeri *et al.*, 1995b). At the CNS level, AQP4 is the most abundant water channel and is concentrated at astrocyte end-feet, which are in proximity to the endothelium of the vessels that form the BBB or it also localized in the ependymal cells of the ventricles in contact with the CSF (Nielsen *et al.*, 1997; Rash *et al.*, 1998). AQP4 is present in two isoforms, one starting from methionine-1, called M1 AQP4 and the other one is shorter starting at methionine-23, named M23 AQP4 (Lu *et al.*, 1996). Both isoforms form tetramers and each monomer is composed of eight helical domains: six of them are membrane spanning, and the leftover two are just short segments adjacent to a narrow aqueous pore (Ho *et al.*, 2009). M1 and M23 AQP4 can form heterodimers, which can further aggregate on the cell membrane and form substructures called orthogonal arrays of particles (OAPs). It has been shown that M23 AQP4 tends to assemble in bigger OAPs than M1 AQP4 (Landis and Reese, 1974; Yang *et al.*, 1996; Wolburg *et al.*, 2011). The ratio between M23 and M1 AQP4 plays a role in the size and the shape of the OAPs. M23 usually is in the core of the 3D structure and M1 is more at the borders, where it is basically limiting the size (Furman *et al.*, 2003; Crane *et al.*, 2011; Rossi *et al.*, 2012).

In general, AQP4 facilitates water movement between brain and blood and between CSF and brain. Knockout mice showed that a lack of AQP4 in models

for brain tumour would increase brain edema (Papadopoulos *et al.*, 2004). In case of hydrocephalus, the absence of this protein would increase the size of the ventricles (Bloch *et al.*, 2006; Verkman *et al.*, 2006). Also astrocytes can be affected by the absence of AQP4, leading to general inflammation and to problems of neuroexcitation (Binder *et al.*, 2006; Verkman *et al.*, 2006; Li *et al.*, 2011).

As mentioned in the previous paragraph, around 80% of people with NMOSD have antibodies against AQP4 in their serum. Histopathological analysis of the brain lesions showed IgGs and massive perivascular complement deposition, with partial myelin preservation but severe astrocyte disruption. In fact, NMOSD is usually referred to as an immune astrocytopathy indicated by glial fibrillary acidic protein (GFAP) loss (Lucchinetti *et al.*, 2014). *In vitro* studies tried to explain the mechanisms behind the damage of astrocytes mediated by AQP4 IgGs. When the autoantibodies bind AQP4, they cause complement activation leading to CDC or they activate other immune cells (effector cells), like natural killer (NK) cells and granulocytes which cause ADCC (Hinson *et al.*, 2009; Ratelade *et al.*, 2013). Studies on the binding of the antibodies to their target antigen showed that in the case of CDC, AQP4 IgGs monovalently bind with high affinity to the OAPs, leading to an organized clustering of the antibodies that favours complement activation (Soltys *et al.*, 2019).

Based on histopathological stainings of human lesions, it is believed that AQP4 antibodies that bind to their target antigen on astrocytic end-feet, leading to complement activation and subsequent astrocytic damage. The damage of these cells calls for the recruitment of other inflammatory cells like granulocytes (neutrophils and eosinophils) or macrophages. This leads to degranulation or cytokines release, which further damages the BBB and secondarily oligodendrocytes, leading to demyelination. *In vivo* studies tried to elucidate the details of all the passages that culminate in the lesion formation. Several groups showed in rodents that peripheral administration of patients' AQP4 antibodies in combination with injection of myelin-reactive T cells or with pre-treatment of Freund' adjuvant (both compromise the integrity of the BBB) lead to the creation of CNS lesions with activated complement

deposition and myelin loss. Thus, this indicates the pathogenicity of AQP4 autoantibodies (Bennett *et al.*, 2009; Bradl *et al.*, 2009; Saadoun *et al.*, 2010). However, from these studies it is hard to understand if the AQP4 autoantibodies alone, without the co-injection of human complement or without the prior breaching of the BBB by myelin-reactive T cells, could be able to breach the BBB and start the inflammatory response needed for the antibody pathogenicity. Nevertheless, some research would actually indicate that AQP4 antibodies do not need the help of T cells to cause lesions. In fact, in a recent study from Hillebrand and colleagues, the constant application of high affinity AQP4 IgGs over an extended period of time was sufficient to allow the antibodies to enter the CNS via circumventricular organs and meningeal or parenchymal blood vessels and to create lesions different from each other depending on the antibodies site of entry. However, this antibody was a monoclonal antibody and did derive from NMOSD patients. The group also showed that the co-presence of encephalitogenic T cells induces the formation of lesions in a more efficient way (Hillebrand *et al.*, 2019). Most of the studies we referred so far indicated the central role of complement and so of CDC, since complement deposition was always visible in correspondence to the affected sites. Furthermore, clinical trials using eculizumab, a monoclonal antibody capable of blocking the complement machinery, showed promising results, since it managed to decrease the risk of relapses in patients with NMOSD (Pittock *et al.*, 2019). Nevertheless, thanks to *in vivo* investigations, also the importance of ADCC in the pathogenesis of NMOSD became clear. In particular, in NMOSD lesions NK cells are not usually present, instead macrophages, neutrophils and eosinophils are quite abundant (Saadoun *et al.*, 2012a). In fact, the inhibition of neutrophils and eosinophils reduced the lesion size and severity in mice brains injected with AQP4 antibodies (Saadoun *et al.*, 2012b; Zhang and Verkman, 2013)

2.5 Acute disseminated encephalomyelitis

2.5.1 Disease features

ADEM is a demyelinating disease that mostly affects children at an age between 5 and 8 years old (Menge *et al.*, 2005). ADEM has usually a

monophasic disease course with 57-89% of patients reaching a full recovery and no recurrence, however around 5-25% of ADEM cases are considered recurring cases (Marchioni *et al.*, 2005; Tenenbaum *et al.*, 2007). If the disease has a recurring course, it is harder to diagnose and to differentiate from MS. The development of ADEM has been associated with infections. It has been shown that in around 75% of the cases, the first neurological symptoms were usually anticipated by an infection or fever (Murthy *et al.*, 2002; Menge *et al.*, 2007a), meaning that molecular mimicry could be the possible underlying mechanism that leads to the occurrence of ADEM. The main pathological features of this disease are acute multifocal bilateral lesions in the white matter, but also the deep grey matter can be affected especially in the cortex and the basal ganglia. Histopathological findings showed infiltration of lymphocytes and monocytes in the lesion area (Mikaeloff *et al.*, 2004; Krupp *et al.*, 2007; Tenenbaum *et al.*, 2007; Baumann *et al.*, 2015). The subsequent neurological manifestations are ataxia, hemiparesis, vision impairment, lethargy, seizures and coma (Murthy *et al.*, 2002; Tenenbaum *et al.*, 2002; Anlar *et al.*, 2003; Tenenbaum *et al.*, 2007). Intriguingly, serum investigations showed that serum anti-MOG antibodies can be found in around 40 to 58% of ADEM patients (O'Connor *et al.*, 2007; Brilot *et al.*, 2009). The MOG IgGs disappear rapidly in these patients (Probstel *et al.*, 2011). In general, MOG antibodies can be considered a reliable prognostic marker to assess the chances for a relapse (Lopez-Chiriboga *et al.*, 2018).

2.6 MOG-antibody associated disorders

2.6.1 MOG protein: structure and glycosylation

MOG is a minor protein component of the myelin sheath (around 0.05%). It is localised on the outermost layer of myelin and on the processes of oligodendrocytes (Brunner *et al.*, 1989) (see Figure 1). In contrary to other myelin proteins such as MBP and myelin proteolipid protein (PLP), MOG has been found exclusively in the CNS of mammals (Dyer and Matthieu, 1994; Johns and Bernard, 1999). The MOG protein has a molecular weight of 26-28 kDa and is composed of 218 amino acids (plus 29 of the signal peptide); the amino acidic sequence is highly conserved among species (Linnington *et al.*,

1988; Delarasse *et al.*, 2006). The human gene encoding for MOG is located on the chromosome 6 within the HLA locus. The same counts for the mouse MOG, which is located on chromosome 17, within the gene locus of the major histocompatibility complex (MHC) (Pham-Dinh *et al.*, 1993).

MOG belongs to the Ig superfamily. X-ray crystallography showed that the extracellular domain at the N-terminus is characterized by an Ig-V fold consisting of two antiparallel beta-sheets (Breithaupt *et al.*, 2003; Clements *et al.*, 2003). The extracellular domain is then followed by a transmembrane domain (until amino acid (aa) 150) that transverses the whole membrane, a cytosolic portion followed by a hydrophobic one (from aa 182 to 202) that dips into the membrane without spanning the whole double layer, ending with its C-terminus intracellularly (Pham-Dinh *et al.*, 1993; Kroepfl *et al.*, 1996) (refer to Figure 1). In humans, 15 different spliced variants of MOG have been detected. They are divided in α and β isoforms depending from which exon the amino acids of the C-terminus are coming from. Furthermore, the C-terminus and the presence or absence of some of the domains are determining the localization of the different isoforms and their occurrence at different stages of brain development. For example, MOG isoforms have been found on the cell surface (α/β -1), in the endoplasmic reticulum or in endosomes. In contrast, isoforms missing the first transmembrane domain are secreted (α/β -4 isoform) (Delarasse *et al.*, 2006; Boyle *et al.*, 2007).

There are several monoclonal antibodies against MOG, however, the most famous is the mouse 8-18C5 (IgG1 isotype), raised against rat cerebellar glycoproteins. Its fame comes from the fact that Linnington and colleagues showed that this specific antibody helped in the determination of a novel antigen, which then corresponded with MOG (Linnington *et al.*, 1984). Apart from defining the 3D structure of the external domain of MOG, an X-ray crystallography study from Breithaupt and colleagues also clarified which parts of the protein are needed for the binding of the 8-18C5, as illustrated in Figure 1. The FG loop (aa 101-108) was identified as essential epitope for the interaction with the 8-18C5. Furthermore, it is a conserved epitope since also other monoclonal antibodies against MOG bound to the same region (Breithaupt *et al.*, 2003). In another paper from Breithaupt and colleagues, it

was shown that within the FG loop, the aa histidine 103 and serine 104 are, which protrude from this loop, are essential for the 8-18C5 binding (Breithaupt *et al.*, 2008).

Insights on which amino acids of the extracellular part of MOG structures are important for the binding of human MOG antibodies came from the study of Mayer and colleagues (Mayer *et al.*, 2013). In this case, by using single point mutations, seven distinct binding patterns were discovered for MOG autoantibodies from patients with different demyelinating diseases. In particular, the CC'-loop (aa 41-46) and FG loop were the most frequently detected ones. In particular, many of the patients' antibodies showed that proline 42 is essential for their binding. This also explained why many of the human MOG antibodies were not detected by rodent MOG, since rodent MOG shows a serine at aa 42 instead of a proline. This was further confirmed by mutating the Pro42 with a serine (Mayer *et al.*, 2013). Lastly, also a large study from Austral-Asia indicated the pivotal role of proline 42 for recognition by patient antibodies to MOG (Tea *et al.*, 2019).

MOG has also one N-glycosylation site at asparagine 31, which is located in the loop (BC) connecting the two antiparallel β -sheets (Breithaupt *et al.*, 2003) (Figure 1). A detailed analysis of the impact of the glycosylation of MOG on recognition by MOG Abs is part of this thesis (see paragraph 3.2).

The function of the MOG protein is still not known. Knockout mice developed without any clear abnormality in the myelin or any histological difference compared to wild-type mice (Delarasse *et al.*, 2003). Nevertheless, over the years, different studies that tried to elucidate the role of MOG have been conducted. It is believed that MOG could act as an adhesion molecule that compacts the myelin layers, or as cellular receptor or as regulator of microtubule stability (Johns and Bernard, 1999; Clements *et al.*, 2003; Marta *et al.*, 2005). Other functions have been postulated. For example, MOG could have a role in the axonal growth and survival since it is capable to interact and sequester the nerve growth factor (NGF) (von Budingen *et al.*, 2015). Purified MOG binds to the complement component C1q, meaning that it can be involved in the regulation of the classical complement pathway (Johns and Bernard, 1997). Another study illustrated that the presence of MOG on cells

could act as a receptor that allows the entry of rubella virus (Cong *et al.*, 2011). Finally, if MOG shows fucosylated N-glycans at Asn31, then it happens to be a ligand for a c-type lectin receptor (DC-SIGN), which is expressed on dendritic cells and macrophages. Intriguingly, if MOG gets de-fucosylated, the interaction of MOG with DC-SIGN is interrupted, leading to inflammasome activation and inflammation guided by T-cells. Thus, this shows that MOG has potent regulatory function (Garcia-Vallejo *et al.*, 2014).

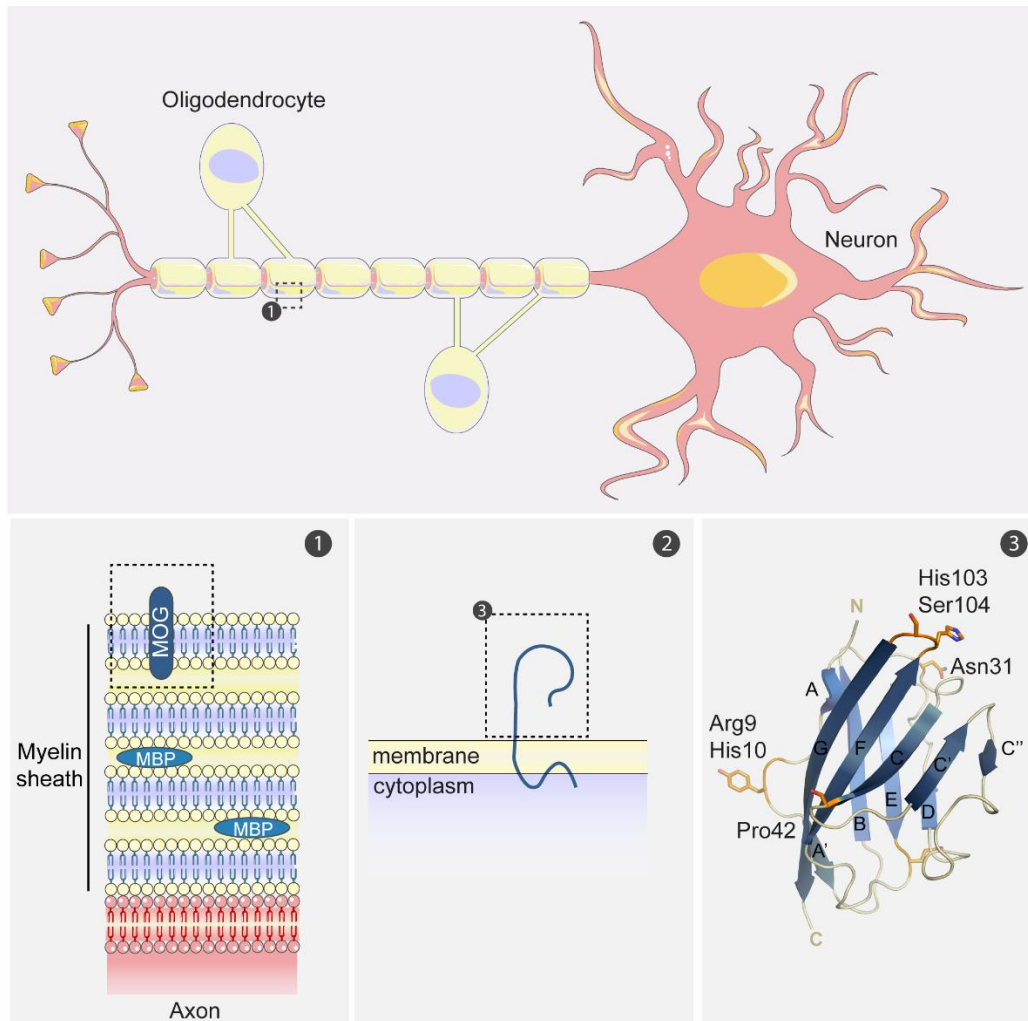


Figure 1: Schematic illustration of MOG localization and structure. 1) MOG localizes in the outermost layer of the myelin sheaths, which is wrapped around the neurons. 2) At the N-terminus MOG has an extracellular domain, which is characterized by an Ig-V fold. This is followed by a transmembrane domain, a cytosolic one and then by a hydrophobic domain that does not span the whole membrane layer. The C-terminus is localized intracellularly. 3) The extracellular domain has been studied with X-ray crystallography (Breithaupt *et al.*, 2003). This method showed that the external portion is an Ig-V fold consisting of two antiparallel β -sheets. The FG loop, and especially the aa His103 and Ser104 are essentials for the binding of the monoclonal antibody against MOG (8-18C5). The Pro42 has been also indicated important for the binding of human antibodies (Mayer *et al.*, 2013; Tea *et al.*, 2019). This figure was created using Servier Medical Art templates, which are licensed under a Creative Commons Attribution 3.0 Unported License.3) Was adapted from (Mayer *et al.*, 2013).

Even if the main biological role of MOG is still not fully understood, what is sure is that MOG has a primary role as immunogen. It can exert a demyelinating immune response in several animal models, where autoantibodies against MOG are involved. This, together with the accessible position of the protein for antibodies on the myelin, brought many research groups to investigate the possible pathogenic role of MOG-antibodies in demyelinating diseases of the CNS (Iglesias *et al.*, 2001; Peschl *et al.*, 2017b; Spadaro *et al.*, 2018). For further details on the pathogenicity refer to paragraph 2.6.4.

2.6.2 Detection methods of MOG-antibodies

The improvement of detection methods for MOG antibodies led to the definition of a new inflammatory CNS disease: MOGAD.

In 1968 for the first time, antibodies against MOG with demyelinating potential were identified in guinea pigs (Seil *et al.*, 1968; Lebar *et al.*, 1976; Lebar *et al.*, 1979; Lebar *et al.*, 1989). With the production of a monoclonal antibody specific to MOG (mAb 8-18C5), it was possible to confirm that MOG antibodies were capable to induce demyelination in immunized rats with MBP (Lassmann *et al.*, 1988; Linington *et al.*, 1988). Several following studies illustrated the pathogenicity of MOG antibodies *in vitro* and *in vivo* in different species (Amor *et al.*, 1994; von Budingen *et al.*, 2004; Mader *et al.*, 2011; Dale *et al.*, 2014). A more detailed discussion on the pathogenicity of MOG antibodies will follow in paragraph 2.6.4.

The clinical relevance of MOG-antibodies and subsequent disease definition became clear only with the improvement of the detection techniques. At the beginning, MOG antibodies have been associated with MS as prognostic markers (Reindl *et al.*, 1999), but this could not be confirmed (Kuhle *et al.*, 2007). The reasons behind this tight association were related to the fact that the MOG IgGs were detected in patient samples via Western-blot or enzyme-linked immunosorbent assay (ELISA), and because MOG is used as immunogen in EAE (Mayer and Meinl, 2012; Jurynczyk *et al.*, 2017b). Summing up data coming from 16 studies conducted with immunoblotting and/or ELISA showed that around 20% of the MS patients presented with

MOG-antibodies (Karni *et al.*, 1999; Reindl *et al.*, 1999; Berger *et al.*, 2003; Mantegazza *et al.*, 2004; Menge *et al.*, 2007b; Wang *et al.*, 2008; Reindl and Waters, 2019). However, those studies have been considered as non-reliable because of the lack of consistency among each other and because the assays were detecting MOG antibodies even in the serum of healthy controls (~ 10%). Both assays are now considered unreliable for testing MOG antibodies, since they require the use of MOG peptides, or of a linear or a refolded protein, which then leads to detect antibodies not directed against native MOG-epitopes (Mayer and Meinl, 2012; Reindl and Waters, 2019). The turning point on the clinical relevance for MOG autoantibodies came only with the emerging of new methodologies utilizing correctly folded MOG. Firstly, K. O'Connor and colleagues utilized a soluble MOG-tetramer as a substrate in a radioimmunoassay (RIA) (with an in vitro translated and presumably correctly folded MOG), and showed that MOG antibodies were more frequent in cohorts of individuals affected by ADEM (19%), and only in 2% of people affected by MS (O'Connor *et al.*, 2007). Then, cell based assays (CBA) (already used for example to detect AQP4 antibodies in possible NMOSD cases) helped to define and clearly indicate which patients with MOG-Abs (Brilot *et al.*, 2009; McLaughlin *et al.*, 2009; Probstel *et al.*, 2011). In CBA, cells which display the α -1 MOG isoform on the surface are incubated with serum from patients. The antibodies that are bound to the MOG are subsequently detected with anti-human specific antibodies. The specificity was reported to be increased when anti-human IgG1 was used (Waters *et al.*, 2015). The binding is detected via flow cytometry or via microscopic evaluation of fluorescent signal (Waters *et al.*, 2015; Spadaro and Meinl, 2016). The first studies conducted with CBA gave inconclusive results. They showed that adult MS cases and healthy controls presented low MOG antibody titres (Haase *et al.*, 2001; Lalive *et al.*, 2006; Zhou *et al.*, 2006). Improvements of the CBA assay and inclusion of highly positive samples from children with acquired demyelinating diseases brought more clear results, showing that MOG-antibodies are rarely detected in adult MS patients and they are mostly related to non-MS demyelinating diseases (McLaughlin *et al.*, 2009; Spadaro *et al.*, 2015; Waters *et al.*, 2015; Spadaro *et al.*, 2016; Peschl *et al.*, 2017a). In detail, in 25 studies conducted with immunofluorescence based CBA, it has been shown that only 1.5% of

patients with MS have MOG-antibodies, most of these were paediatric cases (Peschl *et al.*, 2017a; Reindl and Waters, 2019). Furthermore, across 24 studies it was shown that MOG-antibodies are rarely found in AQP4+ NMOSD (0.5%) (Mader *et al.*, 2011; Woodhall *et al.*, 2013; Kitley *et al.*, 2014; Sato *et al.*, 2014; Reindl and Waters, 2019), but in 42% of the NMOSD patients AQP4 seronegative present MOG Ig (Hamid *et al.*, 2017). Therefore, the availability of a reliable and specific test helped to correlate MOG-antibodies not anymore to MS but to non-MS acquired demyelinating diseases like ADEM, AQP4-NMOSD, ON and myelitis, and to then highlight a common clinical phenotype essential to define MOGAD (Jurynczyk *et al.*, 2019; Wynford-Thomas *et al.*, 2019).

2.6.3 A new distinct group among CNS demyelinating diseases

Individuals are diagnosed with MOGAD when they present antibodies against MOG in their serum (Jurynczyk *et al.*, 2017b; Wynford-Thomas *et al.*, 2019). MOGAD onset is usually around the beginning of the thirties to mid-thirties with also a slightly higher occurrence in women (2-3:1), but MOG antibodies can also be very common in children diagnosed with ADEM as mentioned in paragraph 2.5.1 (Brilot *et al.*, 2009; Probstel *et al.*, 2011; Di Pauli and Berger, 2018; Waters *et al.*, 2019). The course of the disease can be monophasic (especially in ADEM cases) or characterized by relapses; if the MOG antibodies persist in the serum, there are increased chances of relapses. (Di Pauli and Berger, 2018; Weber *et al.*, 2018; Reindl and Waters, 2019; Waters *et al.*, 2019; Wynford-Thomas *et al.*, 2019; Mader *et al.*, 2020). The most common clinical features are ON (54-61%) with or without myelitis, ADEM, cortical encephalitis and N-Methyl-D-aspartate receptor (NMDAR) encephalitis (Reindl and Waters, 2019; Mader *et al.*, 2020). The CSF of patients affected by MOGAD is usually negative for oligoclonal bands, and there are no evidences of intrathecal production of MOG-Ig (Weber *et al.*, 2018; Wynford-Thomas *et al.*, 2019; Mader *et al.*, 2020).

Before the definition of MOGAD as a new inflammatory demyelinating disease of the CNS, many of the patients affected by it were diagnosed as MS or as NMOSD. However, the serological and MRI findings further helped to classify

the disease. MRI brain images showed that the lesions present in patients with MOGAD were particularly different to the ones found in typical MS, but difficult to distinguish from AQP4 IgG+ NMOSD (Jurynczyk *et al.*, 2017a; Reindl and Waters, 2019; Salama *et al.*, 2020). Radially expanding confluent slowly expanding smouldering lesions in the white matter characterize brains affected by MS (Hoftberger *et al.*, 2020). In MOGAD, brain scans show few (three or even less) fluffy lesions mostly in the thalamic or pons areas. As in AQP4 IgG+ NMOSD, T2 lesions in the spine can be found also in MOGAD. However, in this case they are usually shorter and confined to the grey matter (Weber *et al.*, 2018; Wynford-Thomas *et al.*, 2019; Mader *et al.*, 2020). As previously mentioned, ON is one of the hallmarks of MOGAD. From MRI images it has been possible to ascertain that in 35-41% of MOGAD cases both optic nerves are affected, especially in the retrobulbar region (in contrast to AQP4 IgG+ NMOSD, where the ON is originating intracranially) (Weber *et al.*, 2018).

The MRI findings of AQP4 IgG+ NMOSD and MOGAD look very similar, however the histopathology of these two disorders show clear differences and further distance MOGAD from MS. For instance, it has been demonstrated that AQP4 antibodies target preferentially astrocytes, making AQP4 IgG+ NMOSD an astrocytopathy, caused by antibodies and C9neo complement complex deposition. Infiltrating neutrophils and eosinophilic granulocytes, together with elevated concentration of GFAP in the CSF are also characteristic features of NMOSD (Misu *et al.*, 2013; Mader *et al.*, 2020). Whereas, in MOGAD, astrocytes are shown to be intact, likewise also axons and oligodendrocytes are preserved. One typical feature of MOGAD cases is primary demyelination (similar to MS type II pattern). In particular, two main patterns were identified. In one pattern, the demyelination happens in the proximity of vascular vessels. The other instead is a fusion pattern present mostly in the cortical-medullary junctions and in the white matter. Especially in the white matter, the demyelination can extend to a point, which leads to the formation of demyelinating plaques (Hoftberger *et al.*, 2020; Takai *et al.*, 2020). Demyelination sites are also characterised by the presence of infiltrates, mainly consisting of macrophages, B cells and T cells (predominantly CD4+). Complement deposition (C9neo complex) can also be

observed in these demyelinated areas, however, less abundant than in AQP4+ NMOSD (Spadaro *et al.*, 2015; Wang *et al.*, 2016; Takai *et al.*, 2020).

2.6.4 Pathogenicity of MOG-antibodies

Several *in vitro* and *in vivo* studies tried to define the effector mechanism of anti-MOG antibodies.

In vitro studies

In vitro studies suggested for example that MOG antibodies can activate complement, since they are mainly IgG1 isotypes (Waters *et al.*, 2015), meaning that their Fc region is capable to bind C1q and activate the cascade (Johns and Bernard, 1997; McLaughlin *et al.*, 2009). The activation of the complement cascade by MOG antibodies leads to the lysis of cells expressing MOG. In particular, only high titre autoantibodies were able to activate the cascade, whereas low titres or MOG- antibodies were incapable to initiate it and therefore to exert complement-mediated toxicity (Mader *et al.*, 2011). Peschl and colleagues came to similar conclusions. They purified the antibodies from MOG+ patients, and only one of them, with high titre and highly reactive, was capable to induce complement-mediated myelin loss in organotypic murine brain slices (Peschl *et al.*, 2017b).

In another study, it has been shown that MOG antibodies were capable to perform ADCC (Brilot *et al.*, 2009). Furthermore, MOG IgGs derived from patients were able to modify and disrupt the cytoskeleton of oligodendrocytes, without leading to cell death (Dale *et al.*, 2014). It has been demonstrated that this happens independently from complement activation, but subsequently to the binding of the autoantibodies to MOG. The MOG molecules repartition into detergent insoluble fractions of the membrane. The repartition leads to the phosphorylation and subsequent activation of proteins involved in cell stress response (EF-2, HSP74) and to dephosphorylation of protein involved in cytoskeleton stability (β -tubulin, annexin vi) (Kim and Pfeiffer, 1999; Marta *et al.*, 2003; Marta *et al.*, 2005; Dale *et al.*, 2014; von Budingen *et al.*, 2015).

Furthermore, MOG antibodies have been described to be able to mediate APC recognition of MOG through Fc binding, even in absence of the protein

itself. The APCs internalized and processed MOG, to subsequently present it to T cells, which then were activated and became encephalitogenic (Kinzel *et al.*, 2016).

In vivo studies

The *in vivo* studies conducted until now showed that MOG antibodies are not strongly pathogenic on their own, but they retain a second hit effect, where they induce worsening conditions in the presence of an ongoing inflammation process.

In 1988, the anti-MOG mAb 8-18C5 was injected in rat EAE models, deteriorated the clinical conditions of the animals, and increased the length of the disease. The effects here described, were not visible when 8-18C5 was injected in perfectly healthy or control immunized animals (Linington *et al.*, 1988).

Instead, the peripheral injection of concentrated human MOG antibodies into Lewis rats suffering from T cell induced EAE failed to show strong pathogenicity, but just caused demyelination and minor axonal loss (Zhou *et al.*, 2006). Also in another study where human MOG IgGs, deriving from NMO patients, were intrathecally injected into EAE mice, the main consequence was myelin loss with very little complement deposition (Saadoun *et al.*, 2014). In another case, intrathecal injection of human MOG antibodies accelerated the onset of EAE in mice (Flach *et al.*, 2016). However, in all those experiments listed above, a total IgG preparation was used for the injections, which may contain other autoantibodies in addition to MOG-Abs. Therefore, conducting a transfer experiment with MOG affinity purified antibodies could lead to a better understanding of their pathogenic mechanism. In the paper from (Spadaro *et al.*, 2018) present in paragraph 3.3, we detailed described how MOG affinity purified antibodies exert pathogenicity in combination with encephalitogenic T cells, and which epitopes are recognized by those pathogenic antibodies.

3 RESULTS

3.1 Publication 1.1: Macrini et al. (2021), (accepted on 08.01.2021)

The portions of text highlighted in yellow indicate the modifications applied based on the referees' comments during the peer-review process.

Features of MOG required for recognition by patients with MOG-antibody-associated disorders

Journal:	<i>Brain</i>
Manuscript ID	BRAIN-2020-01767.R2
Manuscript Type:	Original Article
Date Submitted by the Author:	21-Dec-2020
Complete List of Authors:	<p>Macrini, Caterina; Ludwig-Maximilians-University, Institute of Clinical Neuroimmunology Gerhards, Ramona; Ludwig-Maximilians-University, Institute of Clinical Neuroimmunology Winklmeier, Stephan; Ludwig-Maximilians-University, Institute of Clinical Neuroimmunology Bergmann, Lena; Biomedical Center and University Hospitals, LMU Munich, Physiological Chemistry Mader, Simone; Ludwig-Maximilians-University, Institute of Clinical Neuroimmunology Spadaro, Melania; Klinikum der Universität München Institut für Klinische Neuroimmunologie Vural, Atay; Koc University School of Medicine Smolle, Michaela; Biomedical Center and University Hospitals, LMU Munich, Physiological Chemistry Hohlfeld, Reinhard; LMU Munich, Institute of Clinical Neuroimmunology Kümpfel, Tania; University Hospital Munich Institute of Clinical Neuroimmunology Lichtenthaler, Stefan; Deutsches Zentrum für Neurodegenerative Erkrankungen München, Neuroproteomics Franquelim, Henri; Max-Planck-Institute of Biochemistry Jenne, Dieter; Ludwig-Maximilians-University and Helmholtz-Zentrum, Comprehensive Pneumology Center, Institute of Lung Biology and Disease (ILBD) Meinel, Edgar; Ludwig-Maximilians-University, Institute of Clinical Neuroimmunology</p>
Methodology:	NEUROBIOLOGY OF DISEASE
Subject area:	MULTIPLE SCLEROSIS, NEUROINFLAMMATION

Features of MOG required for recognition by patients with MOG-antibody-associated disorders

Running title: Recognition of MOG by autoantibodies

Caterina Macrini¹, Ramona Gerhards¹, Stephan Winklmeier¹, Lena Bergmann², Simone Mader¹, Melania Spadaro¹, Atay Vural³, Michaela Smolle^{2,8}, Reinhard Hohlfeld¹, Tania Kümpfel¹, Stefan F. Lichtenthaler^{4,5}, Henri G. Franquelim⁶, Dieter Jenne⁷, Edgar Meinl^{1*}

¹Institute of Clinical Neuroimmunology, Biomedical Center and University Hospitals, Ludwig-Maximilians-Universität München, 82152 Munich, Germany;

²Physiological Chemistry, Biomedical Center, Ludwig-Maximilians-Universität, 82152 Munich, Germany

³Department of Neurology, Koc University School of Medicine, 34450 Istanbul, Turkey

⁴German Center for Neurodegenerative Diseases (DZNE) Munich and Neuroproteomics, School of Medicine, Klinikum rechts der Isar, Technical University of Munich, 81675 Munich, Germany

⁵Munich Cluster for Systems Neurology (SyNergy), 81377 Munich, Germany

⁶Cellular and Molecular Biophysics, Max Planck Institute of Biochemistry, 82152 Munich, Germany

⁷Institute of Lung Biology and Disease (ILBD), Comprehensive Pneumology Center (CPC), Helmholtz Zentrum, 81377 Munich, Germany

⁸BioPhysics Core Facility, Biomedical Center, Ludwig-Maximilians-Universität, 82152 Munich, Germany

*Corresponding author: Dr. Edgar Meinl; Edgar.Meinl@med.uni-muenchen.de

Institute of Clinical Neuroimmunology, Biomedical Center and University Hospitals, Ludwig-Maximilians-Universität München, Großhaderner Str. 9, 82152 Planegg-Martinsried, Germany

Abstract

Antibodies (Abs) to myelin oligodendrocyte glycoprotein (MOG) define a distinct disease entity. Here we aimed to understand essential structural features of MOG required for recognition by autoantibodies from patients. We produced the N-terminal part of MOG in a conformationally correct form; this domain was insufficient to identify patients with MOG-Abs by ELISA even after site-directed binding. This was neither due to a lack of lipid embedding nor to a missing putative epitope at the C-terminus, which we confirmed to be an intracellular domain. When MOG was displayed on transfected cells, patients with MOG-Abs recognized full-length MOG much better than its N-terminal part with the first hydrophobic domain ($p < 0.0001$). Even antibodies affinity-purified with the extracellular part of MOG recognized full-length MOG better than the extracellular part of MOG after transfection. The second hydrophobic domain of MOG enhanced the recognition of the extracellular part of MOG by antibodies from patients as seen with truncated variants of MOG. We confirmed the pivotal role of the second hydrophobic domain by fusing the intracellular part of MOG from the evolutionary distant opossum to the human extracellular part; the chimeric construct restored the antibody-binding completely. Further, we found that in contrast to 8-18C5, MOG-Abs from patients bound preferentially as F(ab')₂ rather than Fab. It was previously found that bivalent binding of human IgG1, the prominent isotype of MOG-Abs, requires that its target antigen is displayed at a distance of 13-16 nm. We found that, upon transfection, molecules of MOG did not interact so closely to induce a Förster resonance energy transfer (FRET) signal, indicating that they are more than 6 nm apart. We propose that the intracellular part of MOG holds the monomers apart at a suitable distance for bivalent binding; this could explain why a cell-based assay is needed to identify MOG-Abs. Our finding that MOG-Abs from most patients require bivalent binding has implications for understanding the pathogenesis of MOG-antibody-associated-disorders. Since bivalently bound antibodies have been reported to only poorly bind C1q, we speculate that the pathogenicity of MOG-Abs is mostly mediated by other mechanisms than complement activation. Therefore, therapeutic inhibition of complement activation should be less efficient in MOG-Ab associated disorders than in patients with Abs to aquaporin-4.

Keywords:

Autoimmunity, antigen-recognition, demyelination, neuroinflammation, MOG

Abbreviations:

Abs = antibodies

CBA = cell based assay

CNS = central nervous system

Cyt = cytoplasmic

ED = external domain

ECFP = enhanced cyan fluorescent protein

EGFP = enhanced green fluorescent protein

ELISA = enzyme-linked immunosorbent assay

EYFP= enhanced yellow fluorescent protein

FL = full-length

FRET = Förster resonance energy transfer

IgG = immunoglobulin G

mAb = monoclonal antibody

MOG = myelin oligodendrocyte glycoprotein

MOGAD = MOG-antibody-associated disorders

TMD = transmembrane domain

1. Introduction

The identification of autoantibodies in patients with inflammatory diseases of the central nervous system (CNS) helps to establish a specific diagnosis, which is critical for understanding the pathogenesis and for therapy optimization (Brimberg *et al.*, 2015; Dalmau and Graus, 2018). The recognition of autoantibodies may eventually result in the definition of separate diseases. For example, consensus is now emerging that autoantibodies to myelin oligodendrocyte glycoprotein (MOG) define a separate disease entity, MOG-antibody-associated disorders (MOGAD) (Zamvil and Slavin, 2015; Juryńczyk *et al.*, 2017; Weber *et al.*, 2018; Reindl and Waters, 2019; Durozard *et al.*, 2020; Mader *et al.*, 2020; Takai *et al.*, 2020).

MOG is displayed on the outer surface of internodal myelin and due to this position it is a target of pathogenic antibodies. While it was demonstrated since the 1980s that autoantibodies to MOG induce demyelination in rodent and primate models of multiple sclerosis (Lington *et al.*,

1988; Genain *et al.*, 1995), the unequivocal identification of MOG-Abs in the blood of patients was achieved much later (O'Connor *et al.*, 2007). MOG-Abs were subsequently connected to acquired demyelinating diseases in children (Brilot *et al.*, 2009; McLaughlin *et al.*, 2009; Pröbstel *et al.*, 2011) and later also to adults with inflammation in the central nervous system (reviewed in (Reindl and Waters, 2019).

One reason for the difficulty to identify patients with MOG-Abs initially was the fundamental difference of MOG-Abs obtained in animal models and MOG-Abs in patients. In animal models, MOG-Abs were readily detected by ELISA (Litzenburger *et al.*, 1998; Pollinger *et al.*, 2009), whereas pathogenic monoclonal antibodies from animals recognized MOG both by ELISA and on the surface of transfected cells (Brehm *et al.*, 1999). To identify patients with MOG-Abs, there is now consensus that an assay using cells transfected with full-length MOG is needed (Tea *et al.*, 2019; Reindl *et al.*, 2020).

MOG is displayed on the membrane. The structure of its extracellular N-terminal part was determined by x-ray crystallography; it forms an Ig-V fold consisting of two antiparallel beta-sheets (Breithaupt *et al.*, 2003; Clements *et al.*, 2003). The prototype rodent anti-MOG mAb 8-18C5 binds to three loops linking the beta-sheets of this N-terminal part with a dominant contribution of His103 and Ser104 in the center of the FG loop (Breithaupt *et al.*, 2003; Breithaupt *et al.*, 2008). MOG-Abs derived from patients are heterogenous and bind to different loops linking the beta-sheets (Mayer *et al.*, 2013; Marti Fernandez *et al.*, 2019; Tea *et al.*, 2019). This N-terminal part of MOG has been recombinantly produced in its correctly folded form and was used for affinity-purification of selected patients' antibodies (Spadaro *et al.*, 2018) as well as detection of MOG-Abs in a few patients (Tea *et al.*, 2019). Thus, the precise conformation of MOG is essential to identify patients with MOG-Abs and correctly folded N-terminal part of MOG alone is not sufficient. The reason for this is currently unknown.

While there is consensus on the extracellular localization and structure of the N-terminal part of MOG, there is dissens about the localization of its C-terminus. Earlier papers indicated that the C-terminus is intracellular (Kroepfl *et al.*, 1996; della Gaspera *et al.*, 1998), whereas currently Uniprot (27.November.2020) and a recent detailed review with reference to Uniprot (Sinmaz *et al.*, 2016) presented a model where the C-terminus of MOG was localized extracellularly. Thus it is unclear, if this part of MOG contributes to antigen recognition in patients.

The aim of our study was to gain further insights into details of antigen-recognition by MOG-Abs from patients. Specifically, we wanted to understand why a cell-based assay (CBA) is

needed to identify patients with MOG-Abs and why the N-terminal external domain of MOG in the correct conformation is not sufficient. To investigate this, we produced the N-terminal part of MOG recombinantly in a correctly folded way and bound it in a site-directed manner to a solid-phase or to lipid-coated beads, then analysed the recognition by MOG-Abs. We revisited the localization of the C-terminal part of MOG with an Ab specific for the C-terminus. We analyzed in detail 14 patients with MOG-Abs using truncated variants of MOG and domain-swapping with parts of the evolutionary distant opossum. We prepared Fab and F(ab')₂ fragments to analyze monovalent versus bivalent binding and used Förster resonance energy transfer (FRET) to analyze whether MOG monomers interacted closely with each other.

Our different experimental approaches revealed that most MOG-Abs from patients, but not the prototypic rodent mAb 8-18C5, require the intramembraneous second hydrophobic domain for MOG recognition and bivalent binding is needed. We propose a model in which the second hydrophobic domain of MOG makes two kinks in the membrane around two conserved prolines and is localized within the inner cytosolic membrane leaflet, in agreement with previous reports (Kroepfl *et al.*, 1996; della Gaspera *et al.*, 1998). This structural feature would thereby facilitate lateral clustering and spacing of the extracellular N-terminal part of MOG that allows bivalent binding of autoantibodies. This could explain why a cell-based assay with full-length MOG is needed to identify patients with MOG-Abs. Importantly, the bivalent binding of MOG-Abs has implications for our concepts of pathogenicity of MOG-Abs and therapeutic strategies.

2. Materials and methods

2.1. MOG-variants

Constructs coding for the different variants of the intracellular part of MOG were synthesized from GeneArt (Thermo Fisher Scientific, Waltham, MA, United States) and then cloned into the pEGFP-N1 vector (Clontech Laboratories, Mountain View, CA, United States) fusing the c-terminus to an enhanced green fluorescent protein (EGFP) tag. The ED-MOG (1-155) construct was truncated at glycine 155, thus comprising the whole external domain, the first hydrophobic domain and part of the cytosolic domain (Waters *et al.*, 2015). The whole intracellular cytosolic portion was included in construct MOG-Cyt by ending the protein at the tyrosine 181. MOG-2TMD includes the whole second hydrophobic domain (until leucine 202) of FL-MOG. The

native C-terminus of this construct was substituted with a SGSGGGSGGGSGS linker. The numbering of these constructs is according to (Breithaupt *et al.*, 2003; Mayer *et al.*, 2013) starting with the first coding amino acids (GQF...) and not with the signal peptide.

The MOG sequence of opossum (*Monodelphis domestica*) was taken from the NCBI database and then ordered from Thermo Fisher Scientific GenArt service. The chimeric construct, named Human-Opossum MOG, was designed with human MOG sequence until glycine 155 followed by the cytosolic and second hydrophobic domain from the MOG sequence of the opossum. In this construct, the C-terminus consists of an SGSGGGSGGGSGS linker. Schemes of these constructs are included in **Fig. 4**. Mutants of the N-terminal extracellular part of MOG were described previously (Mayer *et al.*, 2013).

The MOG variants EYFP/CFP-FL-MOG and EYFP/CFP-ED-MOG, with the fluorescent dyes at the N-terminus were also synthesized from GenArt (Thermo Fisher Scientific) and then cloned into the pEGFP-N1 vector, with the consequent removal of the EGFP sequence portion at the C-terminus. The control constructs ECFP, EYFP and the fusion ECFP-EYFP were kindly provided by H. Eibel (Feiburg, Germany) and were described in (Smulski *et al.*, 2017).

2.2. List of Lipids

1,2-Dioleoyl-*sn*-glycero-3-phosphocholine (dioleoylphosphatidylcholine; DOPC) (Avanti Polar Lipids, Alabaster, AL, United States)

1,2-Dioleoyl-*sn*-glycero-3-phosphoethanolamine-*N*-(cap biotinyl) (18:1 Biotinyl Cap PE) (Avanti Polar Lipids)

1,2-Dioleoyl-*sn*-glycero-3-phosphoethanolamine labeled with Atto 488 (Atto488 DOPE) (Sigma Aldrich, St. Louis, MO, United States)

2.3. Recombinant production of correctly folded extracellular part of MOG

The extracellular part of human MOG (amino acids 1-125) with an Avi-tag allowing enzymatic biotinylation and a His-tag was recombinantly produced using the HEK-EBNA cells and the pTT5 vector (Perera *et al.*, 2013). MOG-1-125 was secreted in serum-free supernatant, purified via its His-tag and its correct folding was assessed using circular dichroism as described (Spadaro *et al.*, 2018; Marti Fernandez *et al.*, 2019). The glycan of this MOG-1-125 has a similar

size as the glycan of FL-MOG on transfected cells and its glycoforms have been described (Marti Fernandez *et al.*, 2019). This material was used for ELISA, for binding to lipid-coated beads and for affinity-purification of MOG-Abs.

2.4. Affinity purification of MOG-Abs from patients

The autoantibodies against MOG present in the plasma of patient #7 were affinity-purified using correctly folded extracellular part of MOG bound to streptavidin columns as previously described in (Spadaro *et al.*, 2018).

2.5. Enzyme-linked immunosorbent assays (ELISAs) detecting MOG-Abs and recombinant monoclonal antibodies

We applied two ELISAs. First, MOG-1-125 was bound to MaxiSorp (ThermoFischer, Waltham, MA, United States) and compared with BSA-coated wells. Second, MOG-1-125 was biotinylated at its Avi-tag with the BirA biotin ligase Kit (Avidity, Aurora, CO, United States) and then bound to streptavidin plates and compared to streptavidin wells, since we saw that adding BSA to streptavidin-coated plates resulted in essentially the same results as using streptavidin-coated plates alone. The ELISA assays were validated by a recombinant mAb against MOG (r8-18C5) and a control mAb against *Borrelia* (HK-3) (**Suppl. Fig. 1**), both having a human IgG1-Fc part (Brändle *et al.*, 2016; Spadaro *et al.*, 2018). Serum was diluted 1:200 and binding of antibodies was detected with an anti-human IgG conjugated to horseradish peroxidase (Jackson ImmunoResearch, West Grove, PA, United States).

2.6. Localization of the C-terminus of MOG

Two different cell lines were used for this part of our study: HeLa cells transiently transfected with FL-MOG or ED-MOG, each fused to EYFP at the N-terminus and the TE-671 cell line (rhabdomyosarcoma cells) stably transfected with FL-MOG without any fluorescent tag (Pröbstel *et al.*, 2011). HeLa cells were fixed with 2% PFA and permeabilized with Intracellular Staining Perm Wash Buffer (BioLegend, San Diego, CA, United States). TE671 cells were fixed and permeabilized with Cyto-Fast Fix/Perm Buffer Set (BioLegend, United States). To detect

MOG, the r8-18C5, which binds to the FG-loop in the extracellular part of MOG (Breithaupt *et al.*, 2003) and the commercially available Ab28766 (Abcam, Cambridge, UK, England), which binds the last 12 amino acids of MOG at the C-terminus (AGQFLEELRNPF), were applied.

2.7. Lipid coating of silica beads and binding of MOG

Silica beads (SiO₂-R-6.0) of 6.16 µm in diameter (microParticles, Berlin, Germany) were coated with a lipid bilayer as follows. First, a mixture of DOPC, Biotinyl CAP PE, Atto488 DOPE in chloroform was prepared at a 98:1:0.03 molar ratio inside a glass vial. A lipid film was formed on the walls of the vial by gently evaporating the solvent with a nitrogen stream and by subsequently drying under vacuum for 20 minutes. The lipid film was then rehydrated with 200 µl of PBS (Gibco, Thermo Scientific, Waltham, MA, United States), 100 µl beads solution (at 6 mg/ml of concentration) and resuspended via vortexing until the solution became turbid. Following this, The beads were coated with the lipids through 30 minutes of sonication in a bath sonicator until the solution cleared.

The extent of the coating was determined in the first place by checking the green fluorescent signal of Atto488 DOPE on the beads via confocal microscopy imaging with an LSM 780 microscope using a 40x/1.2 W C-Apochromat objective (Carl Zeiss AG, Oberkochen, Germany). We bound the biotinylated MOG-1-125 with neutravidin (Invitrogen, Carlsbad, CA, United States) to the Biotinyl CAP PE. We showed that it was displayed on the coated beads surface by detecting it with the r8-18C5 and Alexa Fluor 647 goat anti-human IgG (H+L) antibody (Invitrogen) as the secondary antibody. The fluorescent signal was detected via confocal microscope imaging and via flow cytometry with FACSverse (BD Biosciences, San Jose, CA, United States).

2.8. Quantification of anti-MOG reactivity on lipid coated beads

We quantified the anti-MOG reactivity of several sera and of the humanized r8-18C5 via flow cytometry (BD Biosciences, San Jose, CA, United States). We gated on all the fluorescent beads with an Atto488 signal >100 and then we calculated their MFI in the APC channel. The MFI ratio was obtained by dividing the MFI of the beads bound to biotinylated MOG-1-125 incubated with sera or r8-18C5 by the MFI of the fluorescent beads not bound by biotinylated-MOG-1-125

incubated with sera or r8-18C5. All the signals were quantified by using FlowJo software (LLC, BD life sciences).

To test for recognition by sera with MOG-Abs, the beads were resuspended in 400 μ l of FACS buffer, then 100 μ l were incubated with serum diluted 1:50 in FACS Buffer. Binding of antibodies in serum was detected with Alexa Fluor 647 goat anti-human IgG (H+L) antibody (Invitrogen). The fluorescent signal was detected via flow cytometry with FACSverse (BD Biosciences).

2.9. Cell based assay (CBA) to quantify recognition of MOG variants

The reactivity of the patients' antibody to the different MOG variants was detected in a live-cell-based assay as previously described (Mayer *et al.*, 2013; Spadaro *et al.*, 2018) with FACSverse flowcytometer (BD Biosciences). HeLa cells were transiently transfected via Lipofectamine 2000 (Thermo Fisher Scientific, Waltham, MA) with the different MOG constructs or with EGFP alone (control). To detect the binding of antibodies in serum (diluted 1:50) to the transfected cells, we used biotin-SP-conjugated goat anti-human IgG (1:500 diluted) (Jackson ImmunoResearch, West Grove, PA, United States) as secondary antibody. Subsequently, Alexa Fluor 647-conjugated streptavidin was added (1:2000). Dead cells were excluded from the experiment with Propidium Iodide staining (1:2000 in PBS).

All of our MOG-constructs were expressed as fusion proteins with EGFP allowing the direct quantification of MOG expression via the EGFP signal. We noted that the different MOG constructs were expressed to a different intensity (**Suppl. Fig. 2**). This was taken into consideration and the gating for the default quantification was set to EGFP 100-500, because all MOG-constructs showed a decent expression with this gating criteria (**Suppl. Fig. 2A**). Thus, the anti-MOG reactivity was quantified by gating the cells with EGFP-signal between 100-500 and determining their mean fluorescence intensity (MFI) in the APC channel. We subsequently calculated the MFI ratio of cells expressing MOG-EGFP and cells expressing EGFP alone. All the signals were quantified by using FlowJo software (LLC, BD life sciences, Ashland, OR, United States).

2.10. Consideration of different expression intensities of the applied MOG-mutants

We displayed all MOG-variants as EGFP-fusion proteins as this allowed a precise quantification of MOG expression. We noted that the six MOG mutants differed in their intensity of expression. MOG-2TMD and human-opossum-MOG showed the highest expression. (**Suppl. Fig. 2**). All MOG-constructs yielded a decent expression within the EGFP gate of 100-500 (**Suppl. Fig. 2**). Therefore this EGFP gate of 100-500 was our default setting for quantification of the reactivity towards the different constructs.

We show the reactivity towards each MOG-construct for all analyzed patients using two different gatings, EGFP>100 and EGFP 100-500 (**Suppl. Fig. 3A and 3B**). While in most instances the graphs in **Suppl. Fig. 3A and 3B** look similar, these two presentations provide complementary information in special instances. For example, for patient #22 the response to ED-MOG appears higher than FL-MOG in **Suppl. Fig. 3B**, but when considering the EGFP gates of 100-500, it becomes clear that this patient recognized ED-MOG and FL-MOG similarly. Thus, the apparently higher response to ED-MOG of patient #22 was only due to the higher percentage of cells expressing higher levels of ED-MOG than FL-MOG. This applies also to other patients like #14, #38, #41, #42 and #16, whose reactivity to ED-MOG would be missed completely with the gate setting of EGFP 100-500.

2.11. Förster resonance energy transfer (FRET) experiment to assess MOG dimerization

We performed our FRET experiments essentially as described in (Smulski *et al.*, 2017). Briefly, we transiently transfected HEK293T cells with the ECFP and EYFP MOG fusion constructs described in 2.3. The cells were subsequently analyzed 16-20 hours post-transfection. All FRET experiments were performed with a LSR Fortessa (BD Biosciences). The EYFP signal was detected using the 488 nm laser with a 540/30 filter, ECFP signal was detected using the 405 nm laser with a 450/40 filter and FRET signal was recorded using the 405 nm laser with a 540/30 filter. We defined the positive FRET gating by using cells expressing an ECFP–EYFP fusion protein as positive control. To define the FRET negative gating, cells were co-transfected with ECFP and EYFP .

2.12. Production of Fab and F(ab')₂ from patients' plasma and analysis of their MOG recognition

IgG was purified from plasma with Protein G HP SpinTrap columns (GE Healthcare Life Sciences, Chicago, IL). Subsequently, the IgG concentration was measured with a Human IgG ELISA kit (Mabtech, Nacka Strand, Sweden). The IgG concentration range of the purified plasma samples spanned between 2.5 and 7 mg/ml. Fab and F(ab')₂ fragments were then generated with the Pierce Fab/F(ab')₂Preparation Kit (Thermo Fisher Scientific, Waltham, MA, United States). The Fab fragments were further purified by Size Exclusion Chromatography to separate them from the pool of undigested IgGs using a SuperdexIncrease 200 10/-300 GL column (GE Healthcare Life Sciences, Chicago, IL, United States). Peak fractions were analyzed by SDS-PAGE and Coomassie staining, elution fractions containing only digested Fabs were finally pooled and used for downstream assays.

To detect binding of the Fab and F(ab')₂ fragments to MOG, a different secondary antibody from the one used for detection of anti-MOG in serum had to be used, since the secondary Ab used for evaluating serum includes reactivity to the Fc-part of the IgG, which is no longer present after the Fab and F(ab')₂ preparation. We used an Alexa Fluor 647 mouse anti-human Ig light chain κ antibody together with an Alexa Fluor 647 mouse anti-human Ig light chain λ antibody, both 1:100 diluted (BioLegend, San Diego, CA, United States). The fluorescent signal was further amplified by the use of a rat anti-mouse IgG Alexa Fluor 647 antibody diluted 1:500 (Jackson ImmunoResearch, West Grove, PA, United States). r8-18C5 was produced recombinantly with the human heavy chain from the J-element onwards, but a murine light chain (Brändle *et al.*, 2016; Spadaro *et al.*, 2018). Therefore, this Ab and its Fab and F(ab')₂ were detected with an anti-human IgG + IgA + IgM (H+L) (Jackson ImmunoResearch, West Grove, PA, United States) as secondary Ab.

2.13. Statistics

For statistical analysis, we used the GraphPad Prism7 programm (GraphPad software, San Diego, CA, United States). For the quantification of the reactivity of the 14 patients with MOG-Abs towards the six different MOG variants we set the reactivity towards FL-MOG to 100% and

normalized the reactivity towards the other constructs . We then used a one-way ANOVA Tukey's multiple test comparison to quantify the significance of the recognition of the different constructs.

2.14. Patients and control subjects

For the comparative analysis of MOG-recognition by ELISA versus cell-based assay we used serum samples from 18 patients with MOGAD (average age: 38 years old, 10 females, 9 males). To set the threshold, we analyzed 13 healthy donors. To set the threshold for our CBA we had included over the years 87 healthy controls (average age: 35 years old, 53 females, 34 males). For the analysis of the recognition of MOG-variants, we used serum samples and plasma samples of 14 patients with MOGAD (average age: 39 years old, 6 females, 8 males), who showed a strong MOG-reactivity in the CBA including 12 patients from the above comparison (indicated with filled circles in **Fig. 1**). For comparison, one patient who scored negative in the cell-based assay and the ELISA was included throughout (designated as C). Patients with MOG-Abs, #5, #7, #10, #14, #16 and #17 were described in (Spadaro *et al.*, 2018); and #22, #23, #24, #38, #39, #41, #42, #43 in (Winklmeier *et al.*, 2019). Informed consent was obtained from each donor according the Declaration of Helsinki and the ethical committee of the medical faculty of the LMU approved the study.

2.15. Data availability

The data presented in the manuscript are available from the corresponding author on request.

3. Results

3.1. The extracellular part of MOG displayed site-directed on an ELISA plate allows detection of MOG antibodies only in few patients

The epitopes of MOG recognized by autoantibodies from patients are located in the loops that link the β -sheets of the extracellular part of MOG (Mayer *et al.*, 2013; Tea *et al.*, 2019). We produced this extracellular part in a correctly folded form and confirmed the beta-sheet conformation by circular dichroism (Spadaro *et al.*, 2018; Marti Fernandez *et al.*, 2019). We used this part of MOG for two ELISA variants. In one, MOG-1-125 was bound to typical MaxiSorp plates and in the other MOG-1-125 was enzymatically biotinylated at the Avi-tag of its C-terminus and bound in a site-directed manner to streptavidin plates. Both ELISAs were validated with r8-18C5 (**Suppl. Fig. 1**). We analysed 18 patients with MOG-Abs and compared the anti-MOG-reactivity obtained by CBA using full-length MOG with the recognition of MOG by the two ELISA variants (**Fig. 1**). The MaxiSorp ELISA detected MOG-Abs in 4/18 patients, while the streptavidin-biotinylated MOG-ELISA detect 9/18 patients with MOG-Abs. Thus, an ELISA using site-directed binding of MOG-1-125 is superior to a random binding of MOG-1-125. However, even this improved ELISA did not detect half of the patients who scored positive in a CBA with MOG-transfected cells.

3.2. The C-terminus of MOG is intracellular

Since MOG-1–125 used in the ELISA assay had a sensitivity to detect MOG-Abs in patients' sera, we specifically revisited whether the C-terminus of MOG (from amino acid 203 to 218) is intracellular or extracellular. We used ab28766, specific for the last 12 amino acids of MOG (**Fig. 2A**), and the mAb r8-18C5 that binds to a defined loop on the extracellular part of MOG around amino acid 103 (Breithaupt *et al.*, 2003) (**Fig. 2A**). Both antibodies were tested on HeLa cells transiently transfected with FL-MOG or ED-MOG tagged at the N-terminus with EYFP to ensure that the fluorescent tag does not interfere with the binding of the Ab to the C-terminus. Additionally, TE-671 cells (rhabdomyosarcoma cells) stably transfected with FL-MOG without any tag (Pröbstel *et al.*, 2011) were used (**Fig. 2B-I**).

The mAb r8-18C5 bound to FL-MOG and ED-MOG in HeLa cells as well as the FL-MOG in TE-671 cells, in both living and fixed conditions. (**Fig. 2B, 2C, 2F, 2G**). In contrast, the ab28766, failed to detect MOG in both cell lines when living cells were analyzed (**Fig. 2D and 2H**). However, once the cells (HeLa and TE671) were fixed and permeabilized, the ab28766 bound to EYFP-FL-MOG in HeLa cells and also to the FL-MOG stably expressed on the TE-671 cells (**Fig. 2E and 2I**). As a further control for the specificity of the applied antibodies, we used HeLa cells transfected with ED-MOG (lacking the C-terminus). These cells were not recognized by the ab28766, neither in the viable nor fixed and permeabilized conditions (**Fig. 2D and 2E**). We conclude that the C-terminus of the MOG protein is intracellular. Thus, the patient samples that recognized FL-MOG in live CBAs had bound to the N-terminal extracellular part of MOG.

3.3. Displaying MOG-1-125 in a fluid lipidic environment does not improve antibody detection

Having seen the drastic difference between MOG-1-125 bound to an ELISA plate and FL-MOG displayed on transfected cells, we tested the effect of embedding of MOG in a lipid environment on Ab recognition. Thus, we explored the impact of a fluid lipidic environment on the detection of ED-MOG, by designing a new assay.

We coated silica beads of dimensions similar to cells (6 μm of diameter) with a lipid mixture that would mimic the lipid bilayer that forms the cell membrane (**Fig. 3A**). To monitor the lipid-coating of the beads, the mixture contained fluorescently labelled lipids with Atto488 and biotinylated lipids for a neutravidin bridge to attach biotinylated MOG-1-125. The biotinylated MOG-1-125 is correctly folded as assessed by circular dichroism (Spadaro *et al.*, 2018; Marti Fernandez *et al.*, 2019) and is expected to move freely along the lipid bilayer when linked to the biotinylated lipid via neutravidin (Ramm *et al.*, 2018). MOG-1-125 bound to lipid-coated beads, could be detected by r8-18C5 (**Fig. 3A, 3C and 3D**). However, the intensity of the binding was lower in comparison to FL-MOG or ED-MOG expressed in transiently transfected cells (**Fig. 3D**). We incubated these beads with sera of five patients (#5, #14, #16, #17 and #22) (**Fig. 3E**). Three of these patients (#5, #17 and #22) weakly recognized MOG displayed by these beads. Those three patients were also detected by the site directed ELISA (**Fig. 1B**). Nevertheless, the MOG-1-125 in the site directed ELISA was also capable of binding the antibodies of patient #16. Therefore, we

conclude that the embedding of MOG-1-125 in a fluid lipidic environment does not improve the antibody detection.

3.4. The second hydrophobic domain of MOG is crucial for MOG recognition by most patients

We tested sera from 14 patients with MOG-Abs for recognition of HeLa cells transfected with FL-MOG or ED-MOG. For comparison, we also show the reactivity of one MOG negative patient (#C) to all of our mutants (**Fig. 4 and 5, Suppl. Fig. 3**). All of the 14 MOG+ patients recognized FL-MOG much better than ED-MOG ($p < 0.0001$) (**Fig. 5B**). **Fig. 4** shows details of representative patients. **Fig. 5 and Suppl. Fig. 3** show the summary of all analysed patients and related statistics. Overall, only five patients out of the 14 MOG+ (36%) were detected by cells transfected with ED-MOG (**Fig. 5A and Suppl. Fig. 3A**). Thus, not only in the ELISA assay, but even in the CBA was ED-MOG poorly recognized by most patients, deeming it insufficient to detect MOG-Abs. The detailed recognition of epitopes of MOG was determined for 12 of the 14 patients and they recognized different epitopes as seen with point-mutations of the loops linking the beta-sheets of the N-terminal part of MOG (**Suppl. Fig. 5**). Thus, the strong recognition of FL-MOG as compared to ED-MOG is not related to certain epitopes on the extracellular part of MOG, but is rather a general feature of MOG-Abs from patients.

We went on to narrow-down the intracellular domains of MOG, which increase the antibody detection of the extracellular domain. Hence, we designed two MOG variants. The first one is composed of the extracellular part, the first transmembrane domain and the cytoplasmic part until the second hydrophobic domain (Tyr181); named MOG-Cyt (**Fig. 4**). Secondly, we cloned a longer variant of MOG that included the second hydrophobic domain (until leucine 202), called MOG-2TMD (**Fig. 4**). These variants were tested for recognition by autoantibodies from our 14 patients (**Fig. 5 and Suppl. Fig. 3**).

The raw data in the dot-plots already indicate that the three representative patients #5, #7 and #14 strongly recognized MOG-2TMD, but only weakly MOG-Cyt (**Fig. 4**). Considering all patients, MOG-Cyt was far less recognized than MOG-2TMD or FL-MOG ($p < 0.0001$) (**Fig. 5; Suppl. Fig. 3A**). In particular, the reactivity towards MOG-Cyt dropped in 13/14 patients even below 20% compared to FL-MOG (**Fig. 5B**). Together, this part of our analysis identified the

second hydrophobic domain of MOG as the crucial non-extracellular part of MOG to enhance recognition of its extracellular part by autoantibodies from patients.

To further elaborate the impact of the second hydrophobic part of MOG for antigen-recognition, we analysed the recognition of full-length MOG from the evolutionary distant opossum (*Monodelphis domestica*) and of a chimeric construct composed of the extracellular and first hydrophobic domain of human MOG fused to the cytoplasmic and second hydrophobic domain from opossum (**Fig. 4**). The group of patients with MOG-Abs recognized opossum MOG weaker than human FL-MOG ($p < 0.0001$) (**Fig. 5A**). We also observed a heterogeneous recognition of opossum-MOG by patients: compared to human FL-MOG, out of 14 MOG+ patients, seven showed a weak cross-reactivity to opossum-MOG (recognition below 20%). Two patients recognized it similarly (#39 and #10), and another two recognized the opossum-MOG even better than the human MOG (#7 and #22) (**Fig. 4 and Suppl. Fig. 3**). Strikingly, the human-opossum construct was detected by all 14 MOG+ patients. Of note, the four patients (#14, #38, #41 and #42) who did not show cross reactivity to opossum-MOG had also detected the human-opossum construct (**Fig. 5, Suppl. Fig. 3A**). Human-opossum MOG was better recognized than ED-MOG by all 14 patients ($p < 0.0001$) (**Suppl. Fig. 3A**). Thus, the intracellular part of opossum-MOG greatly enhances recognition of the extracellular part of human MOG. In contrast to patients with MOG-Abs, the mAb r8-18C5 recognized all these MOG variants similarly, as elaborated in a dose-response (**Suppl. Fig. 4**).

3.5. MOG-Abs affinity-purified with the extracellular part of MOG still recognize preferentially full-length MOG

We have affinity-purified MOG-Abs using MOG-1-125 from patient #7, who showed a typical and strong recognition of FL-MOG while a weak recognition of ED-MOG (**Fig. 4**). Remarkably, not only the serum antibodies, but also the MOG-Abs affinity-purified with the recombinantly produced MOG-1-125 recognized FL-MOG much better than ED-MOG in transfected cells. (**Suppl. Fig. 6A**). We noted that this type of affinity-purification does not extract all MOG-Abs, a substantial amount was still present in the flow-through. We compared the affinity-purified antibodies with the starting material (plasma) and the flow-through with respect to recognition of mutated variants of the extracellular part of MOG, which are known to identify MOG epitopes (Mayer *et al.*, 2013). This showed that the MOG-Abs that were affinity-purified

with the ED-MOG recognized the same epitopes on the extracellular part of MOG as the crude plasma and as the antibodies in the flow-through (**Suppl. Fig. 6B**). Together, these experiments indicate that **MOG-Abs of the same antigenic immunoreactivity within one patient strongly recognize FL-MOG and weakly ED-MOG.**

3.6. Bivalent recognition of MOG required by antibodies from patients

We analysed the importance of bivalent binding for the differential recognition of FL-MOG and ED-MOG. To this end, we generated with pepsin and papain digestion Fab and F(ab')₂ fragments of the r8-18C5 as well as IgGs of four patients (#14, #16, #17 and #22). We picked a highly reactive MOG patient (#14), one medium reactive (#16), one patient (#17), whose antibodies were also detected in the ELISA assay (**Fig. 1**), and patient #22, whose antibodies were also detected by ELISA and bound strongly to ED-MOG and FL-MOG (**Fig. 4**). F(ab')₂ fragments were obtained by pepsin digestion; F(ab) fragments were obtained by digestion with papain and subsequent size exclusion chromatography (SEC) to separate the undigested pool of antibodies from the Fab fragments (**Fig. 6A**).

We compared the reactivities of Fab and F(ab')₂ fragments on cells transfected with FL-MOG or ED-MOG. The F(ab')₂ fragments from the four patients behaved in the same manner as the purified IgGs (**Fig. 6B**). The Fab preparations of all four analyzed patients showed little or no recognition of either FL-MOG or ED-MOG (**Fig. 6B**). In contrast, the Fab from r8-18C5 clearly bound to both FL-MOG and ED-MOG. A dose response of r8-18C5 and its Fab and F(ab')₂ fragments demonstrated that the recognition of Fab is slightly weaker than of F(ab')₂, but Fab and F(ab')₂ of this mAb did not differentiate between FL-MOG and ED-MOG (**Suppl. Fig. 7**). Together, this part illustrates that MOG-Abs from patients, but not the mAb r8-18C5, strictly require bivalent recognition to bind to MOG. The need for bivalent binding and the importance of the second hydrophobic together are presented in our model in **Fig. 7**.

3.7. FRET does not show dimerization of ED-MOG or FL-MOG

We investigated whether FL-MOG or ED-MOG formed dimers detected by FRET. To this end, we co-transfected HEK-293T cells with ECFP-FL-MOG and EYFP-FL-MOG or with ECFP-ED-MOG and EYFP-ED-MOG. These experiments revealed that neither FL-MOG, nor ED-MOG

came so close to each other that this would result in a FRET signal. In contrast, the positive control, fusion protein ECFP-EYFP yielded a strong FRET signal (**Suppl. Fig. 8**).

4. Discussion

We report that the second hydrophobic domain of MOG enhances recognition of its N-terminal extracellular part in most patients and propose that this is the reason why a cell-based assay with FL-MOG is the gold-standard to identify patients with MOG-Abs. Most MOG-Abs from patients recognize loops that link the beta-sheets of the IgV-like fold of the extracellular N-terminal part of MOG (Mayer *et al.*, 2013). This part of MOG (MOG-1-125) can be produced in a conformationally correctly folded way (Spadaro *et al.*, 2018; Marti Fernandez *et al.*, 2019; Tea *et al.*, 2019), but this is not sufficient to identify MOG-Abs positive patients. This was seen in a recent study, where MOG was bound in a random way to an ELISA plate (Tea *et al.*, 2019). Our study confirms this and shows that a site-directed display of MOG on the ELISA is superior, but still insufficient to identify all patients with MOG-Abs.

We found that MOG-1-125 embedded in a fluidic lipid environment is recognized by the anti-MOG mAb r8-18C5 and weakly by patients, but far less efficient than MOG in transfected cells. Therefore we worked out details of MOG-recognition in transfected cells and found that most patients recognized FL-MOG much better than ED-MOG. This is in accordance with a previous report (Waters *et al.*, 2015). We went on to dissect the contribution of the intracellular part of MOG for the enhanced recognition of FL-MOG with different truncated variants of MOG and this revealed that the second hydrophobic domain of MOG is crucial for the detection of MOG by patients with MOG-Abs.

We continued to analyze whether this enhanced recognition of MOG by the intracellular part is based on a specific sequence of MOG or rather based on the overall structure of MOG. While wrapped myelin is found in vertebrates, MOG is found only in mammals. We expressed MOG from opossum, the evolutionary most distant animal from whom a MOG-sequence was available in the NCBI database. Most patients did not or only weakly recognize MOG from opossum. This was expected, since many patients do not even show cross-reactivity to rodent MOG (Mayer *et al.*, 2013; Peschl *et al.*, 2017; Spadaro *et al.*, 2018). Importantly, when we constructed a chimeric MOG, with the N-terminal ED part from human MOG and the C-terminal part from

opossum MOG, this MOG-construct was recognized as strongly as the full-length human MOG. We observed this enhanced recognition of MOG by the second transmembranous domain of MOG in patients who recognize different epitopes on the extracellular part of MOG. This argues that the second hydrophobic domain does not induce the exposure of a specific epitope, but induces an overall structure of MOG that is better recognized by autoantibodies.

We tested whether the enormous difference in recognition of ED-MOG versus FL-MOG could be attributed at least partially to an extracellular display of the C-terminal part of MOG. All of our experiments using both transiently and stably transfected cells, came to the same conclusion, namely that the C-terminus is intracellular. Our observation is in line with earlier reports (Kroepfl *et al.*, 1996; della Gaspera *et al.*, 1998), but at variance with the current prediction of Uniprot (27.November.2020), and a model presented in a recent review with reference to Uniprot (Sinmaz *et al.*, 2016). Our model in **Fig. 7** includes the specific amino acid composition of the second hydrophobic domain of MOG and their adjacent amino acids: the second hydrophobic domain has two prolines. A proline might indicate a kink in the α -helix (von Heijne, 1991; Nilsson *et al.*, 1998). A similar monotopic domain displaying an analogous structure with two hydrophobic helices and a proline in the middle (helix-break-helix) is also seen for caveolin (Aoki *et al.*, 2010) and for the transmembrane protein PEN-2, a subunit of the Alzheimer's disease- and Notch-signaling-related protease γ -secretase (Pittock *et al.*, 2019; Zhou *et al.*, 2019). Also, the three positively charged amino acids next to the hydrophobic domain that were expected to bind to negatively charged lipids intracellularly and the cysteine at the end of the hydrophobic domain that might be palmitoylated (Smotrys and Linder, 2004) are linked to the intracellular localization of the C-terminus of MOG. These four amino acids are also conserved from opossum to human (**Suppl. Fig. 9**). Further, we found that all patients with MOG-Abs recognized the mutant MOG-2TMD, which does not include the C-terminus, at least as strongly as FL-MOG. Together, this part of our study establishes that the C-terminus of MOG is intracellular and in contrast to the second hydrophobic domain, not involved in binding of patient antibodies to FL-MOG.

To offer further insight into details of MOG-recognition, we analyzed whether FL-MOG or ED-MOG form close dimers detectable by FRET and we analyzed monovalent versus bivalent binding to FL-MOG and ED-MOG. We found that neither ED-MOG nor FL-MOG give a FRET signal. The intensity of a FRET signal is inversely proportional to the sixth power of the inter-dye distance and this energy transfer process can serve as a spectroscopic ruler in the 1-6 nm range

(Stryer and Haugland, 1967). Thus, our FRET experiments show that ED-MOG or FL-MOG are further apart from each other than 6 nm. To allow bivalent binding of IgG1 (the typical isotype of MOG-Abs), the target antigen has to be at a relatively strict distance of about 13-16 nm as recently corroborated with DNA origami technology (Shaw *et al.*, 2019). In a crystallographic paper, ED-MOG was reported to form a head-to-tail dimer (Clements *et al.*, 2003); in the same paper, MOG extracted from myelin appeared by Western-blot largely monomeric, but also a minor proportion of dimeric forms of MOG were observed indicating that MOG may form dimers under special crystallization conditions and also in myelin. Our FRET experiments do not exclude dimer formation of MOG under certain situations, but show that under our experimental conditions, cells transfected with MOG for a CBA, MOG does not associate closer than 6 nm. In accordance with our FRET data, MOG from transfected cells appeared as a monomer when Western blots of transfected cells were performed (Mayer *et al.*, 2013; Marti Fernandez *et al.*, 2019).

We found that MOG-Abs from four patients bound strongly in the form of F(ab')₂, but poorly or not at all as Fab, indicating that these MOG-antibodies largely require bivalent binding to be detected. The dependence on bivalent binding is most likely due to concentration and affinity. In particular, it argues that the affinity of human MOG-Abs is lower than of 8-18C5 and therefore a gain of avidity due to bivalent binding is needed for a clear binding to MOG. Also, in vitro-translated extracellular part of MOG constructed to form tetramers is recognized by MOG-Abs from patients (O'Connor *et al.*, 2007). We speculate that FL-MOG is better recognized than ED-MOG, because the intracellular part of MOG induces a clustering of MOG with a spacing of the extracellular part of MOG that allows bivalent Ab-binding, illustrated in **Fig. 7**. The second hydrophobic domain could hold the monomers apart at a suitable distance that would facilitate the bivalent binding of the MOG-Abs, presumably involving lipid rafts (Kim and Pfeiffer, 1999). This model is in accordance with previous studies that showed that crosslinking of MOG-Abs induces signaling (Marta *et al.*, 2005) and lateral diffusion of transfected MOG in the membrane is anomalous and slowed down (Gielen *et al.*, 2005; Gielen *et al.*, 2008). We are aware that our model in **Fig. 7** might not be the only possible explanation for the enhanced recognition and bivalent binding of MOG-Abs when the second hydrophobic domain is present. It could also be that the second hydrophobic domain creates an empty space around the MOG molecules which favors the binding of MOG-Abs.

We assume that the few patients whose MOG-Abs give some signal using MOG-1-125 bound to an ELISA plate or to ED-MOG in transfected cells, have such a strong affinity that allows monovalent binding. This view is also strengthened by features of the mAb r8-18C5, which has a strong affinity to MOG, binds also as Fab to MOG, recognizes ED-MOG and FL-MOG in transfected cells similarly and also MOG by ELISA. Together, we show that MOG-Abs from most patients require bivalent binding to be detected. We propose that bivalent binding is facilitated with cells transfected with FL-MOG (or MOG-2TMD), but not when ED-MOG is transfected or when MOG-1-125 is bound to an ELISA plate.

Patients with antibodies to MOG or AQP4 show clinically overlapping features, but consensus is emerging that anti-MOG and anti-AQP4 constitute separate diseases (Zamvil and Slavin, 2015; Fujihara, 2019; Mader *et al.*, 2020). While this study indicates that MOG-Abs from most patients require bivalent binding for antigen-recognition, autoantibodies to AQP4 have been reported to bind also as monomer (Crane *et al.*, 2011). Monovalent binding of IgG provides a more efficient platform for C1q binding and complement activation than bivalent binding (Diebold *et al.*, 2014; Soltys *et al.*, 2019). Previous work has shown that complement-mediated activation by MOG-Abs in vitro was restricted to high titre positive patients (Mader *et al.*, 2011). Thus, MOG-Abs may activate complement, but they do this far less efficient than by AQP4-Abs. This view is supported by histopathological examinations: although C9neo deposition can be observed in patients with MOG-Abs (Spadaro *et al.*, 2015; Jarius *et al.*, 2016; Kortvelyessy *et al.*, 2017; Hoftberger *et al.*, 2020) or after transfer of their MOG-Abs (Spadaro *et al.*, 2018), it is far less pronounced than in patients with antibodies to AQP4 (Lucchinetti *et al.*, 2002; Bradl *et al.*, 2009; Takai *et al.*, 2020). In particular, patients with AQP4-Abs have large perivascular complement deposition that is missing in MOGAD (Weber *et al.*, 2018; Mader *et al.*, 2020).

While IgGs from patients with AQP4-Abs readily induce disease upon transfer (Bradl *et al.*, 2009), this has been difficult to achieve with IgG preparations from MOG-Abs positive patients and it took affinity purification of antibodies from selected patients to achieve this (Spadaro *et al.*, 2018). These affinity-purified Abs that transfer disease also recognize MOG by ELISA as shown here. Recognition of MOG by ELISA by a few patients was interpreted as an indicator of high affinity (Tea *et al.*, 2019), suggesting that these patients' antibodies might bind monovalently. Along this line, only a single patient with high-titre antibodies to MOG was able to induce complement-dependent tissue injury in an ex vivo organotypic brain slice model (Peschl *et al.*, 2017) and no complement-dependent changes were observed upon intracerebral injection of pooled

IgG from MOG positive patients (Saadoun *et al.*, 2014). Complement-independent pathomechanisms of MOG-Abs include also cytoskeletal alterations (Dale *et al.*, 2014) and antibody-mediated cellular cytotoxicity (Brilot *et al.*, 2009).

The observations from pathology and our finding that MOG-Abs largely bind bivalently have therapeutic implications. This suggests that the anti-complement therapy with eculizumab, which is very successful in patients with anti-AQP4 (Pittock *et al.*, 2019) might be less effective in patients with MOG-Abs. Autoantibodies may induce pathology by multiple mechanisms other than complement activation, including endocytosis and FcR activation (Ludwig *et al.*, 2017; Dalmau and Graus, 2018). In animal models of hemolytic anemia, low-affinity bivalently binding autoantibodies were highly pathogenic (Fossati-Jimack *et al.*, 1999). MOG-Abs affinity-purified from patients were pathogenic by enhancing activation of cognate T cells (Spadaro *et al.*, 2018), presumably by accumulating in CNS-resident phagocytes (Flach *et al.*, 2016) and enhancing T cell activation via FcR-dependent opsonization of MOG (Kinzel *et al.*, 2016).

Together, we report that MOG-Abs from most patients require the intracellular part of MOG to recognize its extracellular part and show a bivalent binding to MOG. These features of human MOG-Abs explain why a cell-based assay with FL-MOG is the gold-standard to identify such patients and have implications for our concept about pathogenicity of human MOG-Abs.

5. Acknowledgements

We are grateful to Heike Rübsamen for technical assistance and Prof. Hartmut Wekerle for the continuous support. We are grateful to Prof. Hermann Eibel for kindly providing the FRET control constructs. We thank Samantha Ho together with Drs Naoto Kawakami and Klaus Dornmair for comments on the manuscript. FRET experiments were supported by Dr. L. Richter, Core Facility Flow Cytometry at the Biomedical Center, LMU Munich.

6. Funding

This study was funded by the DFG (SFB TR128) and under Germany's Excellence Strategy within the framework of the Munich Cluster for Systems Neurology (EXC 2145 SyNergy– ID

390857198), the Werner Reichenberger Stiftung and the Verein zur Therapieforschung für MS-Kranke.

7. Competing interests

The authors declare no competing interests.

For Peer Review

8. Figure legends

Fig. 1: Comparison of MOG-reactivity by ELISA and cell-based assay (CBA). The anti-MOG-reactivity of 18 patients with MOG-Abs was determined by CBA using FL-MOG and by ELISA. CBA was performed as described (Spadaro *et al.*, 2018) and the anti-MOG reactivity is shown as MFI ratio, calculated as described in the materials and methods section. For ELISA, MOG-1-125 was bound to MaxiSorp plates and Δ OD was calculated after subtraction of the OD of BSA coated MaxiSorp plates (A). Alternatively, MOG-1-125 was biotinylated at its C-terminal Avi-tag and bound to streptavidin plates. For ELISA, the anti-MOG reactivity is expressed as Δ OD (streptavidin + MOG) – (streptavidin only) (B). The horizontal dashed lines represent the mean of the anti-MOG reactivity of a total of 87 healthy controls + 3SDs. The vertical dashed lines represent the mean + 3SDs of 13 healthy controls. Samples included in the analysis of recognition of MOG-variants are shown with filled circles.

Fig. 2: Localization of the C-terminus of MOG. A) Schematic representation of the binding of the recombinant humanized r8-18C5 (blue) and ab28766 (yellow). B) Localization of the C-terminus of MOG. In the upper row (B-E), HeLa cells were transiently transfected with EYFP alone (closed grey graph), with FL-MOG (vermillion line), or ED-MOG (light blue line). FL-MOG and ED-MOG were fused to EYFP at the N-terminus. These cells were tested live (B, D) as well as after fixation and permeabilization (C, E) with r8-18C5 (B, C) and ab28766 (D, E). Gates were set to an EYFP signal >100. In the lower row (F-I), TE671 cells stably transfected with FL-MOG (vermillion line) or the empty vector (closed grey graph) were tested live (F, H) as well as after fixation and permeabilization (G, I) with r8-18C5 (F, G) and ab28766 (H, I). MFI values are given for each histogram.

Fig. 3: Detection of MOG-1-125 displayed on lipid-coated beads. A) Schematic representation of the lipid coated silica beads model. Glass bead of 6 μ m in diameter were coated with a lipid mixture that formed a bilayer. The correctly folded MOG-1-125 is displayed on this bilayer. The magnification shows a segment of a single lipid coated bead. MOG-1-125 biotinylated is attached to the Biotinyl CAP PE via one of the free subunits of the neutravidin. MOG-1-125 is bound by the r8-18C5 (blue), which is detected by the Alexa Fluor 647 anti human IgG (magenta). B, C) Confocal microscopy image of lipid coated beads, to asses the extent of the coating. B) The

Atto488 DOPE lipids gave green fluorescence to the whole membrane coating. **C)** MOG displayed on these beads is detected by r8-18C5 and visualized with a red-labelled secondary antibody. **B+C)** were taken with a 40X water objective; scale bar indicates 10 μm . **D)** Detection of increasing concentrations of r8-18C5 by cells transfected with FL-MOG (vermillion), ED-MOG (light blue line) and by lipid-coated beads displaying MOG-1-125 (dark green line). **E)** Binding of sera (diluted 1:50) of five patients with MOG-Abs to MOG-1-125 coated beads. The closed gray graphs represent background-bindings of the beads, the black line represents binding to beads displaying MOG-1-125. MFI values for each histogram are given.

Fig. 4: MOG variants used for transient transfection and their recognition by selected patients. The upper row shows cartoons of MOG-variants used. Rows 2-5 show dot-plots obtained with serum diluted 1:50 of the indicated patients. Patients #14, #5, and #7 represent the majority of the patients, because they show a greater recognition of FL-MOG compared to ED-MOG. Patient #22 has an unusual binding behavior, since it strongly recognizes ED-MOG. The lowest row shows the reactivity of the MOG-specific control mAb r8-18C5 (0.5 $\mu\text{g/ml}$). The two vertical lines in each dot-plot indicate an EGFP intensity of 100-500 (dotted one) that is used as threshold for the quantitative analysis in **Fig. 5**.

Fig. 5: Differential detection of MOG variants and quantification. **A)** Sera from 14 patients with MOG-Abs and one negative control (C) were tested for reactivity towards the six MOG-variants. The mAb r8-18C5 (0.5 $\mu\text{g/ml}$) was used as a control. For the quantitative evaluation, the cells with EGFP signal between 100-500 were considered (**Fig. 4**). Error bars indicate SEM of 2 experiments. **B)** The reactivity of all the MOG variants normalized to FL-MOG (set as 100%) is shown with EGFP gating of 100-500. ED-MOG, MOG-Cyt and opossum-MOG were significantly less capable to detect the MOG+ patients when compared to FL-MOG, MOG-2TMD and human-opossum-MOG ($p < 0.0001$). The EGFP gating of 100-500 highlights also a difference in the reactivity between MOG-2TMD and FL-MOG ($p < 0.05$), but MOG-2TMD is still capable of detecting all 14 MOG+ patients.

Fig. 6: Recognition of FL-MOG and ED-MOG by F(ab')₂ and Fab preparations. **A)** Preparation of F(ab')₂ and Fab. IgGs purified with protein-G columns were digested with pepsin to obtain the F(ab')₂ and with papain to yield Fab. Since the Fab preparations obtained after papain

digestion still contained undigested IgG, the Fab fragments were further purified by size exclusion chromatography (SEC). Elution fractions were separated by non-reducing SDS-PAGE and stained with Coomassie. Relevant elution fractions were then pooled and analyzed again on an SDS-PAGE gel. Here, #14 is shown as a representative example. **B)** HeLa cells were transfected with EGFP, FL-MOG or ED-MOG. Binding of IgGs from plasma (400 µg/ml), F(ab')₂ (800 µg/ml) and Fab (800 µg/ml) of the indicated patients was determined with secondary antibodies specific for Ig-kappa and Ig-lambda as described in the materials and methods section. The mAb r8-18C5 (0.1 µg/ml) was used as a control. The anti-MOG reactivities were calculated on transfected cells with EGFP signal >500. MFI values are given for each histogram. Representative measurements from two experiments with similar results are shown.

Fig. 7: Model illustrating how the second hydrophobic domain of MOG enhances recognition of its extracellular part by autoantibodies from patients. We show in this paper that MOG-Abs from patients require bivalent binding and the second hydrophobic domain for MOG binding. We therefore propose the model shown here in which the second hydrophobic domain of MOG facilitates bivalent binding of MOG-Abs. The magnified figure shows how the second hydrophobic domain is embedded in the membrane in a homotypic manner with both sides of this hydrophobic domain in the cytoplasm. The two prolines (P) in the middle induce kinks inside the membrane. Positively charged amino acids arginine (R) and lysine (K) adjacent to the hydrophobic domain might interact with the cytosolic interface of the membrane. The cysteine (C) at the end of the hydrophobic domain might be palmitoylated. The presence of the second hydrophobic domain brings MOG molecules to a distance that allows bivalent binding of autoantibodies. The absence of the second hydrophobic domain in the ED-MOG protein leads to the weak and monovalent binding of MOG-Abs.

9. Reference list

Aoki S, Thomas A, Decaffmeyer M, Brasseur R, Epand RM. The role of proline in the membrane re-entrant helix of caveolin-1. *J Biol Chem* 2010; 285(43): 33371-80.

Bradl M, Misu T, Takahashi T, Watanabe M, Mader S, Reindl M, *et al.* Neuromyelitis optica: Pathogenicity of patient immunoglobulin in vivo. *Annals of Neurology* 2009; 66 630-43.

Brändle SM, Obermeier B, Senel M, Bruder J, Mentele R, Khademi M, *et al.* Distinct oligoclonal band antibodies in multiple sclerosis recognize ubiquitous self-proteins. *Proc Natl Acad Sci U S A* 2016; 113(28): 7864-9.

Brehm U, Piddlesden SJ, Gardinier MV, Linington C. Epitope specificity of demyelinating monoclonal autoantibodies directed against the human myelin oligodendrocyte glycoprotein (MOG). *Journal of neuroimmunology* 1999; 97(1-2): 9-15.

Breithaupt C, Schafer B, Pellkofer H, Huber R, Linington C, Jacob U. Demyelinating myelin oligodendrocyte glycoprotein-specific autoantibody response is focused on one dominant conformational epitope region in rodents. *J Immunol* 2008; 181(2): 1255-63.

Breithaupt C, Schubart A, Zander H, Skerra A, Huber R, Linington C, *et al.* Structural insights into the antigenicity of myelin oligodendrocyte glycoprotein. *Proceedings of the National Academy of Sciences of the United States of America* 2003; 100(16): 9446-51.

Brilot F, Dale RC, Selter RC, Grummel V, Kalluri SR, Aslam M, *et al.* Antibodies to native myelin oligodendrocyte glycoprotein in children with inflammatory demyelinating central nervous system disease. *Ann Neurol* 2009; 66(6): 833-42.

Brimberg L, Mader S, Fujieda Y, Arinuma Y, Kowal C, Volpe BT, *et al.* Antibodies as Mediators of Brain Pathology. *Trends in immunology* 2015; 36(11): 709-24.

Clements CS, Reid HH, Beddoe T, Tynan FE, Perugini MA, Johns TG, *et al.* The crystal structure of myelin oligodendrocyte glycoprotein, a key autoantigen in multiple sclerosis. *Proc Natl Acad Sci U S A* 2003; 100(19): 11059-64.

Crane JM, Lam C, Rossi A, Gupta T, Bennett JL, Verkman AS. Binding affinity and specificity of neuromyelitis optica autoantibodies to aquaporin-4 M1/M23 isoforms and orthogonal arrays. *J Biol Chem* 2011; 286(18): 16516-24.

Dale RC, Tantsis EM, Merheb V, Kumaran RY, Sinmaz N, Pathmanandavel K, *et al.* Antibodies to MOG have a demyelination phenotype and affect oligodendrocyte cytoskeleton. *Neurol Neuroimmunol Neuroinflamm* 2014; 1(1): e12.

Dalmau J, Graus F. Antibody-Mediated Encephalitis. *N Engl J Med* 2018; 378(9): 840-51.

della Gaspera B, Pham-Dinh D, Roussel G, Nussbaum JL, Dautigny A. Membrane topology of the myelin/oligodendrocyte glycoprotein. *European journal of biochemistry* 1998; 258(2): 478-84.

Diebold CA, Beurskens FJ, de Jong RN, Koning RI, Strumane K, Lindorfer MA, *et al.* Complement is activated by IgG hexamers assembled at the cell surface. *Science* 2014; 343(6176): 1260-3.

Durozard P, Rico A, Boutiere C, Maarouf A, Lacroix R, Cointe S, *et al.* Comparison of the Response to Rituximab between Myelin Oligodendrocyte Glycoprotein and Aquaporin-4 Antibody Diseases. *Ann Neurol* 2020; 87(2): 256-66.

Flach AC, Litke T, Strauss J, Haberl M, Gomez CC, Reindl M, *et al.* Autoantibody-boosted T-cell reactivation in the target organ triggers manifestation of autoimmune CNS disease. *Proc Natl Acad Sci U S A* 2016; 113(12): 3323-8.

Fossati-Jimack L, Reininger L, Chicheportiche Y, Clynes R, Ravetch JV, Honjo T, *et al.* High pathogenic potential of low-affinity autoantibodies in experimental autoimmune hemolytic anemia. *J Exp Med* 1999; 190(11): 1689-96.

Fujihara K. Neuromyelitis optica spectrum disorders: still evolving and broadening. *Curr Opin Neurol* 2019; 32(3): 385-94.

Genain CP, Nguyen MH, Letvin NL, Pearl R, Davis RL, Adelman M, *et al.* Antibody facilitation of multiple sclerosis-like lesions in a nonhuman primate. *The Journal of clinical investigation* 1995; 96(6): 2966-74.

Gielen E, Smisdom N, De Clercq B, Vandeven M, Gijsbers R, Debyser Z, *et al.* Diffusion of myelin oligodendrocyte glycoprotein in living OLN-93 cells investigated by raster-scanning image correlation spectroscopy (RICS). *Journal of fluorescence* 2008; 18(5): 813-9.

Gielen E, Vercammen J, Sýkora J, Humpolickova J, Vandeven M, Benda A, *et al.* Diffusion of sphingomyelin and myelin oligodendrocyte glycoprotein in the membrane of OLN-93 oligodendroglial cells studied by fluorescence correlation spectroscopy. *Comptes rendus biologiques* 2005; 328(12): 1057-64.

Hoftberger R, Guo Y, Flanagan EP, Lopez-Chiriboga AS, Endmayr V, Hochmeister S, *et al.* The pathology of central nervous system inflammatory demyelinating disease accompanying myelin oligodendrocyte glycoprotein autoantibody. *Acta Neuropathol* 2020.

Jarius S, Metz I, König FB, Ruprecht K, Reindl M, Paul F, *et al.* Screening for MOG-IgG and 27 other anti-glial and anti-neuronal autoantibodies in 'pattern II multiple sclerosis' and brain biopsy findings in a MOG-IgG-positive case. *Mult Scler* 2016; 22: 1541-9.

Juryńczyk M, Messina S, Woodhall MR, Raza N, Everett R, Roca-Fernandez A, *et al.* Clinical presentation and prognosis in MOG-antibody disease: a UK study. *Brain* 2017; 140(12): 3128-38.

Kim T, Pfeiffer SE. Myelin glycosphingolipid/cholesterol-enriched microdomains selectively sequester the non-compact myelin proteins CNP and MOG. *Journal of neurocytology* 1999; 28(4-5): 281-93.

Kinzel S, Lehmann-Horn K, Torke S, Hausler D, Winkler A, Stadelmann C, *et al.* Myelin-reactive antibodies initiate T cell-mediated CNS autoimmune disease by opsonization of endogenous antigen. *Acta Neuropathol* 2016; 132(1): 43-58.

Kortvelyessy P, Breu M, Pawlitzki M, Metz I, Heinze HJ, Matzke M, *et al.* ADEM-like presentation, anti-MOG antibodies, and MS pathology: TWO case reports. *Neurol Neuroimmunol Neuroinflamm* 2017; 4(3): e335.

Kroepfl JF, Viise LR, Charron AJ, Linington C, Gardinier MV. Investigation of myelin/oligodendrocyte glycoprotein membrane topology. *J Neurochem* 1996; 67(5): 2219-22.

Linington C, Bradl M, Lassmann H, Brunner C, Vass K. Augmentation of demyelination in rat acute allergic encephalomyelitis by circulating mouse monoclonal antibodies directed against a myelin/oligodendrocyte glycoprotein. *Am J Pathol* 1988; 130(3): 443-54.

Litzenburger T, Fässler R, Bauer J, Lassmann H, Linington C, Wekerle H, *et al.* B lymphocytes producing demyelinating autoantibodies: development and function in gene-targeted transgenic mice. *The Journal of experimental medicine* 1998; 188(1): 169-80.

Lucchinetti CF, Mandler RN, McGavern D, Brück W, Gleich G, Ransohoff RM, *et al.* A role for humoral mechanisms in the pathogenesis of Devic's neuromyelitis optica. *Brain* 2002; 125(Pt 7): 1450-61.

Ludwig RJ, Vanhoorelbeke K, Leypoldt F, Kaya Z, Bieber K, McLachlan SM, *et al.* Mechanisms of Autoantibody-Induced Pathology. *Front Immunol* 2017; 8: 603.

Mader S, Gredler V, Schanda K, Rostasy K, Dujmovic I, Pfaller K, *et al.* Complement activating antibodies to myelin oligodendrocyte glycoprotein in neuromyelitis optica and related disorders. *J Neuroinflammation* 2011; 8: 184.

Mader S, Kumpfel T, Meinl E. Novel insights into pathophysiology and therapeutic possibilities reveal further differences between AQP4-IgG- and MOG-IgG-associated diseases. *Curr Opin Neurol* 2020; 33(3): 362-71.

Marta CB, Montano MB, Taylor CM, Taylor AL, Bansal R, Pfeiffer SE. Signaling cascades activated upon antibody cross-linking of myelin oligodendrocyte glycoprotein: potential implications for multiple sclerosis. *J Biol Chem* 2005; 280(10): 8985-93.

Marti Fernandez I, Macrini C, Krumbholz M, Hensbergen PJ, Hipgrave Ederveen AL, Winklmeier S, *et al.* The Glycosylation Site of Myelin Oligodendrocyte Glycoprotein Affects Autoantibody Recognition in a Large Proportion of Patients. *Front Immunol* 2019; 10: 1189.

Mayer MC, Breithaupt C, Reindl M, Schanda K, Rostasy K, Berger T, *et al.* Distinction and temporal stability of conformational epitopes on myelin oligodendrocyte glycoprotein recognized by patients with different inflammatory central nervous system diseases. *J Immunol* 2013; 191(7): 3594-604.

McLaughlin KA, Chitnis T, Newcombe J, Franz B, Kennedy J, McArdel S, *et al.* Age-dependent B cell autoimmunity to a myelin surface antigen in pediatric multiple sclerosis. *J Immunol* 2009; 183(6): 4067-76.

Nilsson I, Saaf A, Whitley P, Gafvelin G, Waller C, von Heijne G. Proline-induced disruption of a transmembrane alpha-helix in its natural environment. *J Mol Biol* 1998; 284(4): 1165-75.

O'Connor KC, McLaughlin KA, De Jager PL, Chitnis T, Bettelli E, Xu C, *et al.* Self-antigen tetramers discriminate between myelin autoantibodies to native or denatured protein. *Nat Med* 2007; 13(2): 211-7.

Perera NC, Wiesmuller KH, Larsen MT, Schacher B, Eickholz P, Borregaard N, *et al.* NSP4 is stored in azurophil granules and released by activated neutrophils as active endoprotease with restricted specificity. *J Immunol* 2013; 191(5): 2700-7.

Peschl P, Schanda K, Zeka B, Given K, Bohm D, Ruprecht K, *et al.* Human antibodies against the myelin oligodendrocyte glycoprotein can cause complement-dependent demyelination. *J Neuroinflammation* 2017; 14(1): 208.

Pittock SJ, Berthele A, Fujihara K, Kim HJ, Levy M, Palace J, *et al.* Eculizumab in Aquaporin-4-Positive Neuromyelitis Optica Spectrum Disorder. *N Engl J Med* 2019; 381(7): 614-25.

Pollinger B, Krishnamoorthy G, Berer K, Lassmann H, Bosl MR, Dunn R, *et al.* Spontaneous relapsing-remitting EAE in the SJL/J mouse: MOG-reactive transgenic T cells recruit endogenous MOG-specific B cells. *The Journal of experimental medicine* 2009; 206(6): 1303-16.

Pröbstel AK, Dornmair K, Bittner R, Sperl P, Jenne D, Magalhaes S, *et al.* Antibodies to MOG are transient in childhood acute disseminated encephalomyelitis. *Neurology* 2011; 77(6): 580-8.

Ramm B, Glock P, Mucksch J, Blumhardt P, Garcia-Soriano DA, Heymann M, *et al.* The MinDE system is a generic spatial cue for membrane protein distribution in vitro. *Nat Commun* 2018; 9(1): 3942.

Reindl M, Schanda K, Woodhall M, Tea F, Ramanathan S, Sagen J, *et al.* International multicenter examination of MOG antibody assays. 2020; 7(2).

Reindl M, Waters P. Myelin oligodendrocyte glycoprotein antibodies in neurological disease. *Nat Rev Neurol* 2019; 15(2): 89-102.

Saadoun S, Waters P, Owens GP, Bennett JL, Vincent A, Papadopoulos MC. Neuromyelitis optica MOG-IgG causes reversible lesions in mouse brain. *Acta Neuropathol Commun* 2014; 2(1): 35.

Shaw A, Hoffecker IT, Smyrlaki I, Rosa J, Grevys A, Bratlie D, *et al.* Binding to nanopatterned antigens is dominated by the spatial tolerance of antibodies. *Nat Nanotechnol* 2019; 14(2): 184-90.

Sinmaz N, Nguyen T, Tea F, Dale RC, Brilot F. Mapping autoantigen epitopes: molecular insights into autoantibody-associated disorders of the nervous system. *J Neuroinflammation* 2016; 13(1): 219.

Smotrys JE, Linder ME. Palmitoylation of intracellular signaling proteins: regulation and function. *Annu Rev Biochem* 2004; 73: 559-87.

Smulski CR, Decossas M, Chekkat N, Beyrath J, Willen L, Guichard G, *et al.* Hetero-oligomerization between the TNF receptor superfamily members CD40, Fas and TRAILR2 modulate CD40 signalling. *Cell Death Dis* 2017; 8(2): e2601.

Soltys J, Liu Y, Ritchie A, Wemlinger S, Schaller K, Schumann H, *et al.* Membrane assembly of aquaporin-4 autoantibodies regulates classical complement activation in neuromyelitis optica. *J Clin Invest* 2019; 129(5): 2000-13.

Spadaro M, Gerdes LA, Mayer MC, Ertl-Wagner B, Laurent S, Krumbholz M, *et al.* Histopathology and clinical course of MOG-antibody associated encephalomyelitis. *Annals of Clinical and Translational Neurology* 2015; 2: 295-301.

Spadaro M, Winklmeier S, Beltran E, Macrini C, Hoftberger R, Schuh E, *et al.* Pathogenicity of human antibodies against myelin oligodendrocyte glycoprotein. *Ann Neurol* 2018; 84(2): 315-28.

Stryer L, Haugland RP. Energy transfer: a spectroscopic ruler. *Proc Natl Acad Sci U S A* 1967; 58(2): 719-26.

Takai Y, Misu T, Kaneko K, Chihara N, Narikawa K, Tsuchida S, *et al.* Myelin oligodendrocyte glycoprotein antibody-associated disease: an immunopathological study. *Brain* 2020; 143(5): 1431-46.

Tea F, Lopez JA, Ramanathan S, Merheb V, Lee FXZ, Zou A, *et al.* Characterization of the human myelin oligodendrocyte glycoprotein antibody response in demyelination. *Acta Neuropathol Commun* 2019; 7(1): 145.

von Heijne G. Proline kinks in transmembrane alpha-helices. *J Mol Biol* 1991; 218(3): 499-503.

Waters P, Woodhall M, O'Connor KC, Reindl M, Lang B, Sato DK, *et al.* MOG cell-based assay detects non-MS patients with inflammatory neurologic disease. *Neurol Neuroimmunol Neuroinflamm* 2015; 2(3): e89.

Weber MS, Derfuss T, Metz I, Bruck W. Defining distinct features of anti-MOG antibody associated central nervous system demyelination. *Ther Adv Neurol Disord* 2018; 11: 1756286418762083.

Winklmeier S, Schluter M, Spadaro M, Thaler FS, Vural A, Gerhards R, *et al.* Identification of circulating MOG-specific B cells in patients with MOG antibodies. *Neurol Neuroimmunol Neuroinflamm* 2019; 6(6): 625.

Zamvil SS, Slavin AJ. Does MOG Ig-positive AQP4-seronegative opticospinal inflammatory disease justify a diagnosis of NMO spectrum disorder? *Neurol Neuroimmunol Neuroinflamm* 2015; 2(1): e62.

Zhou R, Yang G, Guo X, Zhou Q, Lei J, Shi Y. Recognition of the amyloid precursor protein by human gamma-secretase. *Science* 2019; 363(6428).

Figure 1

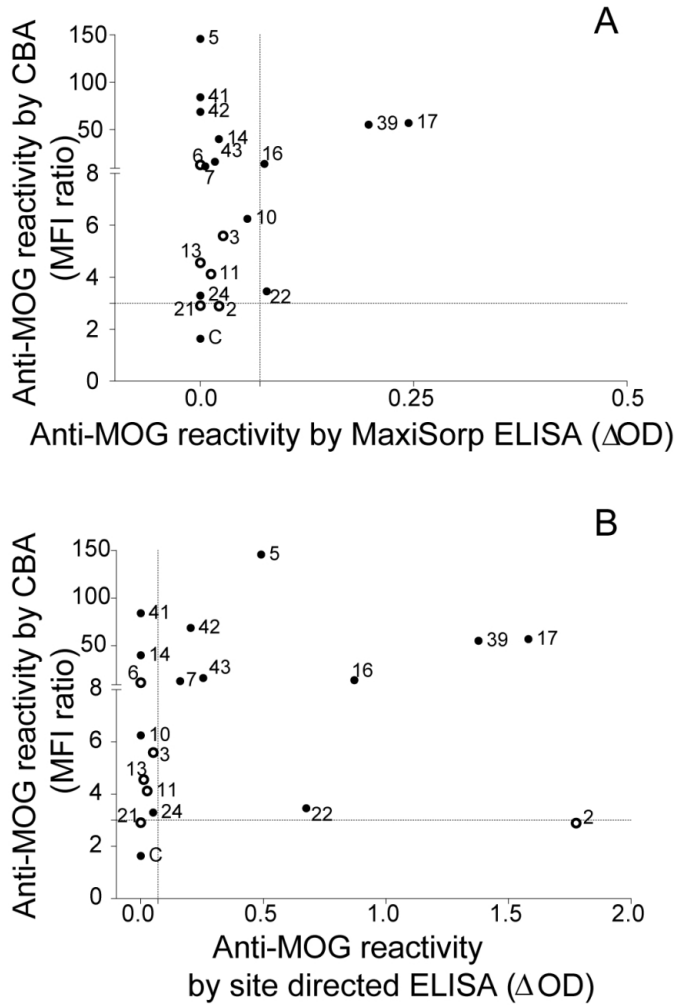


Fig. 1: Comparison of MOG-reactivity by ELISA and cell-based assay (CBA). The anti-MOG-reactivity of 18 patients with MOG-Abs was determined by CBA using FL-MOG and by ELISA. CBA was performed as described (Spadaro et al., 2018) and the anti-MOG reactivity is shown as MFI ratio, calculated as described in the materials and methods section. For ELISA, MOG-1-125 was bound to MaxiSorp plates and a delta OD was calculated after substraction of the OD of BSA coated MaxiSorp plates (A). Alternatively, MOG-1-125 was biotinylated at its C-terminal Avi-tag and bound to streptavidin plates. For ELISA, the anti-MOG reactivity is expressed as Δ OD (streptavidin + MOG) - (streptavidin only) (B). The horizontal dashed lines represent the mean of the anti-MOG reactivity of a total of 87 healthy controls + 3SDs. The vertical dashed lines represent the mean + 3SDs of 13 healthy controls. Samples included in the analysis of recognition of MOG-variants are shown with filled circles.

88x141mm (300 x 300 DPI)

Figure 2

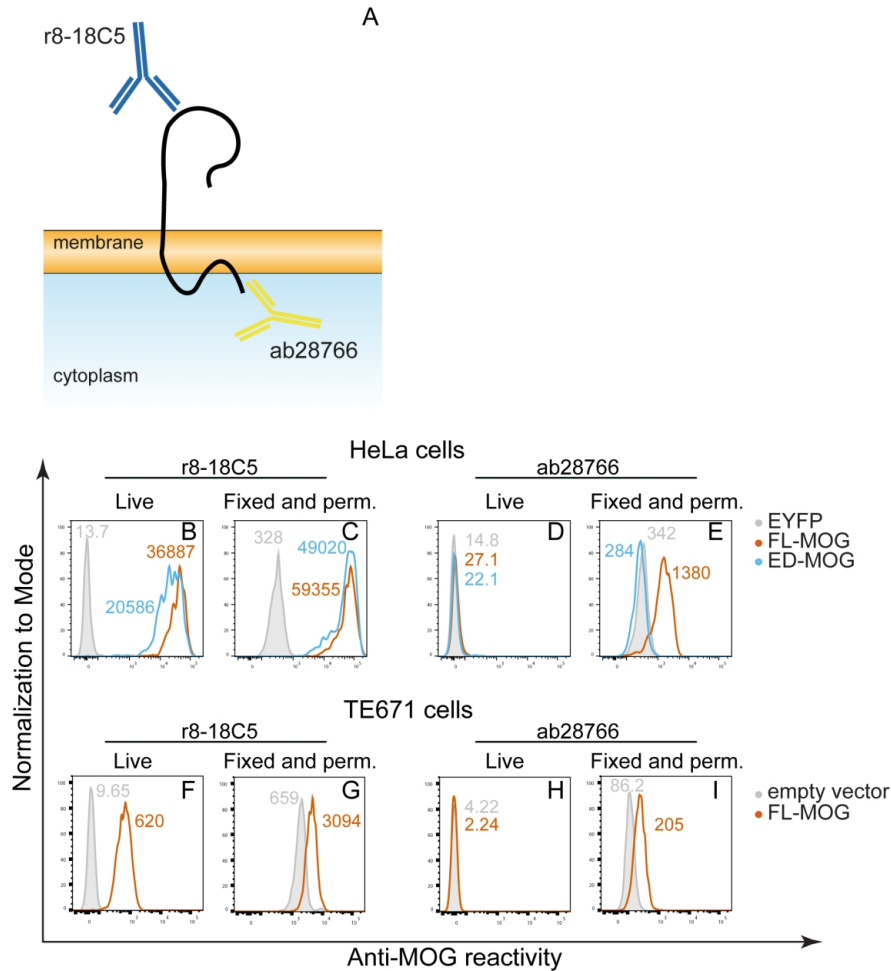


Fig. 2: Localization of the C-terminus of MOG. A) Schematic representation of the binding of the recombinant humanized r8-18C5 (blue) and ab28766 (yellow). B) Localization of the C-terminus of MOG. In the upper row (B-E), HeLa cells were transiently transfected with EYFP alone (closed grey graph), with FL-MOG (vermillion line), or ED-MOG (light blue line). FL-MOG and ED-MOG were fused to EYFP at the N-terminus. These cells were tested live (B, D) as well as after fixation and permeabilization (C, E) with r8-18C5 (B, C) and ab28766 (D, E). Gates were set to an EYFP signal >100. In the lower row (F-I), TE671 cells stably transfected with FL-MOG (vermillion line) or the empty vector (closed grey graph) were tested live (F, H) as well as after fixation and permeabilization (G, I) with r8-18C5 (F, G) and ab28766 (H, I). MFI values are given for each histogram.

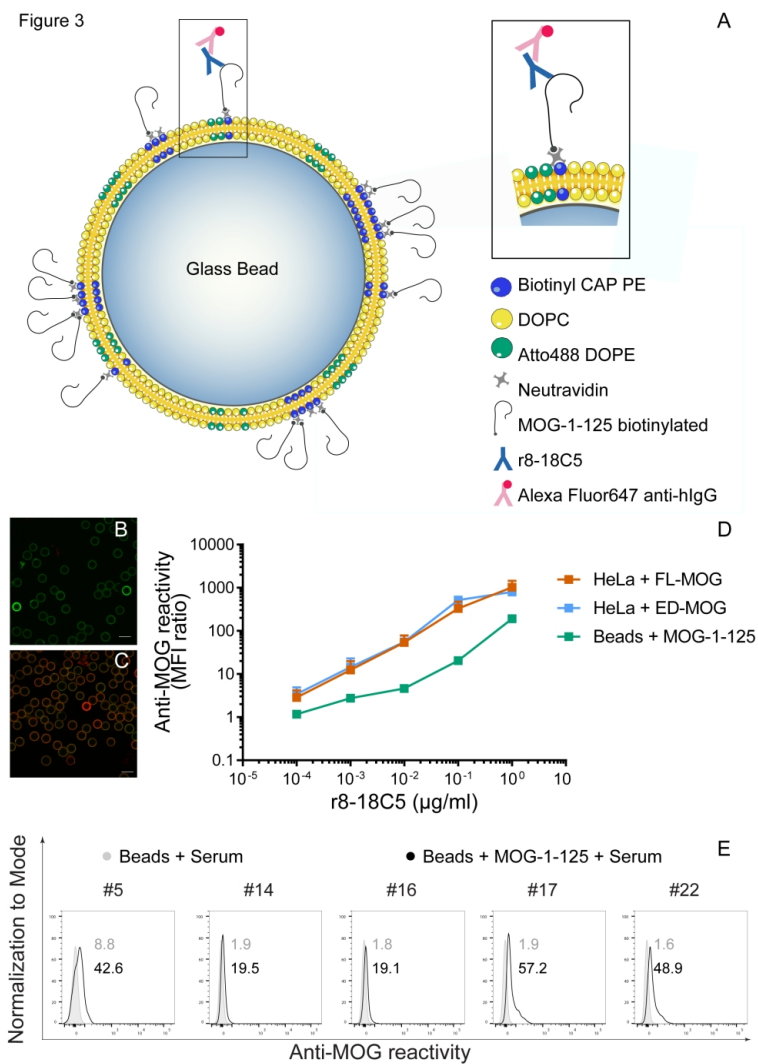


Fig. 3: Detection of MOG-1-125 displayed on lipid-coated beads. A) Schematic representation of the lipid coated silica beads model. Glass bead of 6 μm in diameter were coated with a lipid mixture that formed a bilayer. The correctly folded MOG-1-125 is displayed on this bilayer. The magnification shows a segment of a single lipid coated bead. MOG-1-125 biotinylated is attached to the Biotinyl CAP PE via one of the free subunits of the neutravidin. MOG-1-125 is bound by the r8-18C5 (blue), which is detected by the Alexa Fluor 647 anti human IgG (magenta). B, C) Confocal microscopy image of lipid coated beads, to assess the extent of the coating. B) The Atto488 DOPE lipids gave green fluorescence to the whole membrane coating. C) MOG displayed on these beads is detected by r8-18C5 and visualized with a red-labelled secondary antibody. B+C were taken with a 40X water objective; scale bar indicates 10 μm . D) Detection of increasing concentrations of r8-18C5 by cells transfected with FL-MOG (vermillion), ED-MOG (light blue line) and by lipid-coated beads displaying MOG-1-125 (dark green line). E) Binding of sera (diluted 1:50) of five patients with MOG-Abs to MOG-1-125 coated beads. The closed gray graphs represent background-bindings of the beads, the black line represents binding to beads displaying MOG-1-125. MFI values for each histogram are given.

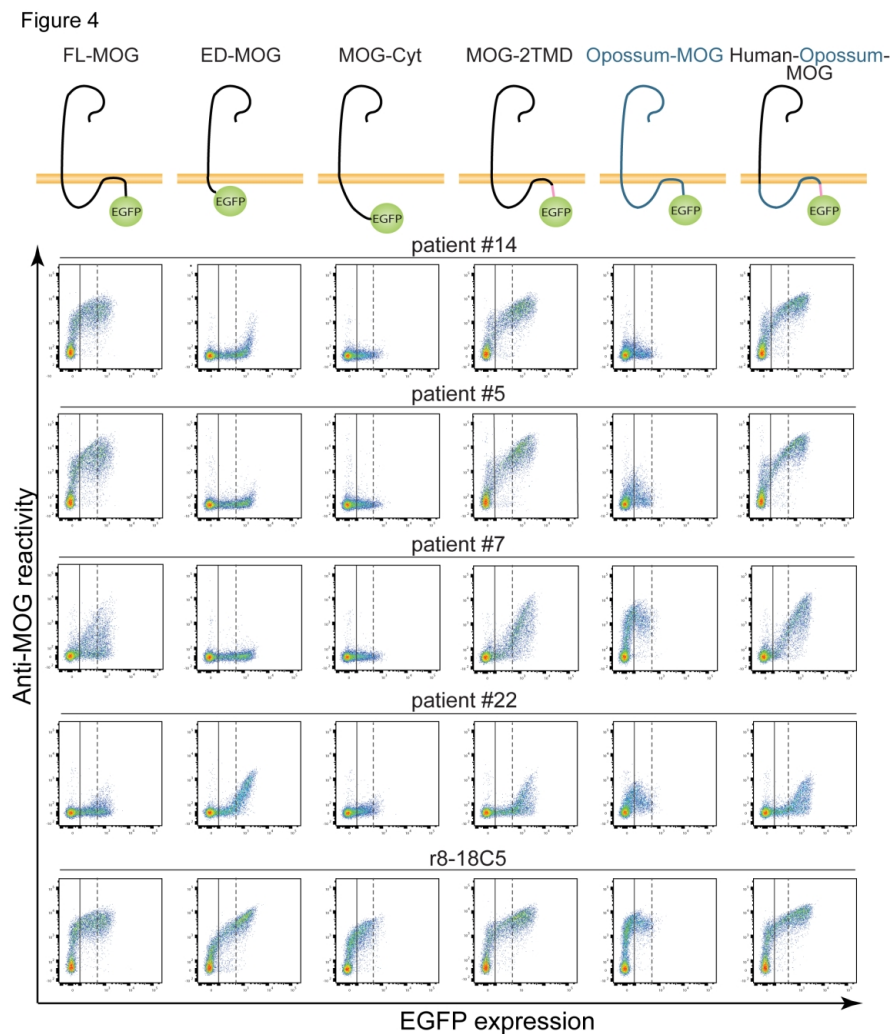


Fig. 4: MOG variants used for transient transfection and their recognition by selected patients. The upper row shows cartoons of MOG-variants used. Rows 2-5 show dot-plots obtained with serum diluted 1:50 of the indicated patients. Patients #14, #5, and #7 represent the majority of the patients, because they show a greater recognition of FL-MOG compared to ED-MOG. Patient #22 has an unusual binding behavior, since it strongly recognizes ED-MOG. The lowest row shows the reactivity of the MOG-specific control mAb r8-18C5 (0.5 $\mu\text{g/ml}$). The two vertical lines in each dot-plot indicate an EGFP intensity of 100-500 (dotted one) that is used as threshold for the quantitative analysis in Fig. 5.

Figure 5

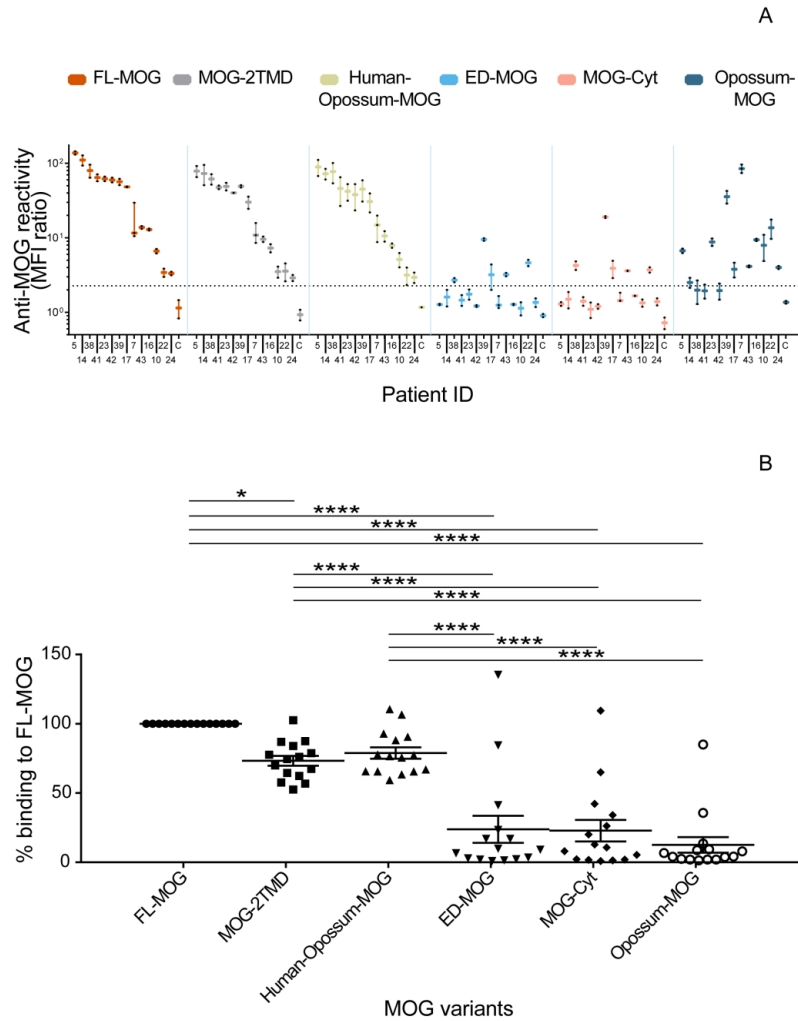


Fig. 5: Differential detection of MOG variants and quantification. A) Sera from 14 patients with MOG-Abs and one negative control (C) were tested for reactivity towards the six MOG-variants. The mAb r8-18C5 (0.5 $\mu\text{g/ml}$) was used as a control. For the quantitative evaluation, the cells with EGFP signal between 100-500 were considered (Fig. 4). Error bars indicate SEM of 2 experiments. B) The reactivity of all the MOG variants normalized to FL-MOG (set as 100%) is shown with EGFP gating of 100-500. ED-MOG, MOG-Cyt and opossum-MOG were significantly less capable to detect the MOG+ patients when compared to FL-MOG, MOG-2TMD and human-opossum-MOG ($p < 0.0001$). The EGFP gating of 100-500 highlights also a difference in the reactivity between MOG-2TMD and FL-MOG ($p < 0.05$), but MOG-2TMD is still capable of detecting all 14 MOG+ patients.

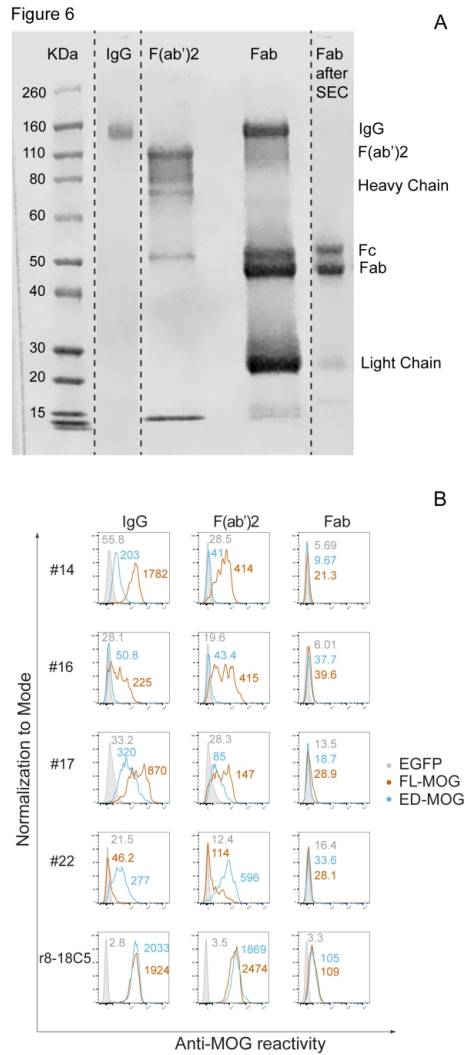


Fig. 6: Recognition of FL-MOG and ED-MOG by F(ab')₂ and Fab preparations. A) Preparation of F(ab')₂ and Fab. IgGs purified with protein-G columns were digested with pepsin to obtain the F(ab')₂ and with papain to yield Fab. Since the Fab preparations obtained after papain digestion still contained undigested IgG, the Fab fragments were further purified by size exclusion chromatography (SEC). Elution fractions were separated by non-reducing SDS-PAGE and stained with Coomassie. Relevant elution fractions were then pooled and analyzed again on an SDS-PAGE gel. Here, #14 is shown as a representative example. B) HeLa cells were transfected with EGFP, FL-MOG or ED-MOG. Binding of IgGs from plasma (400 µg/ml), F(ab')₂ (800 µg/ml) and Fab (800 µg/ml) of the indicated patients was determined with secondary antibodies specific for Ig-kappa and Ig-lambda as described in the materials and methods section. The mAb r8-18C5 (0.1 µg/ml) was used as a control. The anti-MOG reactivities were calculated on transfected cells with EGFP signal >500. MFI values are given for each histogram. Representative measurements from two experiments with similar results are shown.

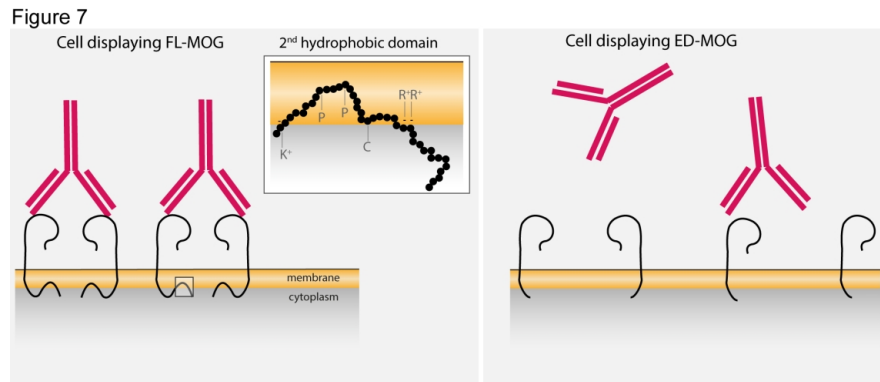
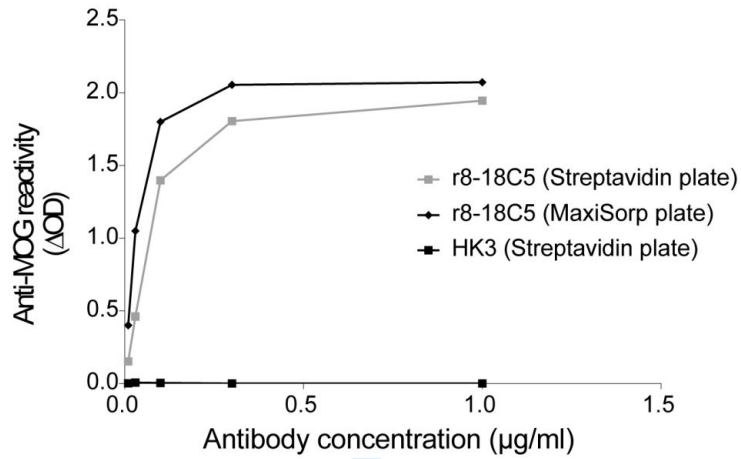
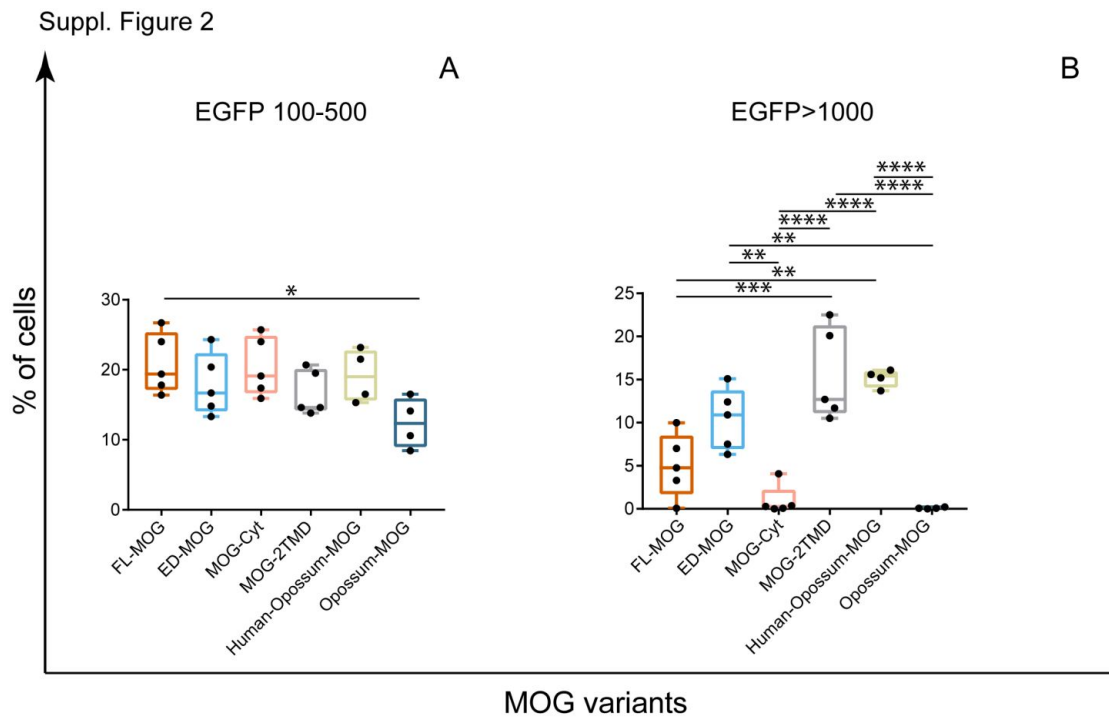


Fig. 7: Model illustrating how the second hydrophobic domain of MOG enhances recognition of its extracellular part by autoantibodies from patients. We show in this paper that MOG-Abs from patients require bivalent binding and the second hydrophobic domain for MOG binding. We therefore propose the model shown here in which the second hydrophobic domain of MOG facilitates bivalent binding of MOG-Abs. The magnified figure shows how the second hydrophobic domain is embedded in the membrane in a homotypic manner with both sides of this hydrophobic domain in the cytoplasm. The two prolines (P) in the middle induce kinks inside the membrane. Positively charged amino acids arginine (R) and lysine (K) adjacent to the hydrophobic domain might interact with the cytosolic interface of the membrane. The cysteine (C) at the end of the hydrophobic domain might be palmitoylated. The presence of the second hydrophobic domain brings MOG molecules to a distance that allows bivalent binding of autoantibodies. The absence of the second hydrophobic domain in the ED-MOG protein leads to the weak and monovalent binding of MOG-Abs.

Suppl. Figure 1



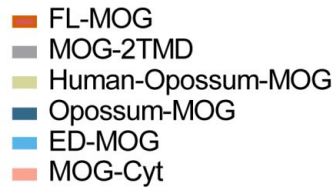
Suppl. Figure 1: Validation of the MOG ELISAs with r8-18C5. MOG-1-125 was bound to MaxiSorp plates and delta OD was calculated by subtracting the OD of BSA coated MaxiSorp plates (black rhombus). Alternatively, MOG was biotinylated at its C-terminal Avi-tag and bound to streptavidin plates and delta OD was determined by subtraction of streptavidin coated wells (grey square). Binding of the MOG-specific r8-18C5 and the control mAb HK3 was compared. The control mAb HK3 is shown for the Streptavidin plate. The background level of this control mAb was similar on the MaxiSorp plate (not shown).



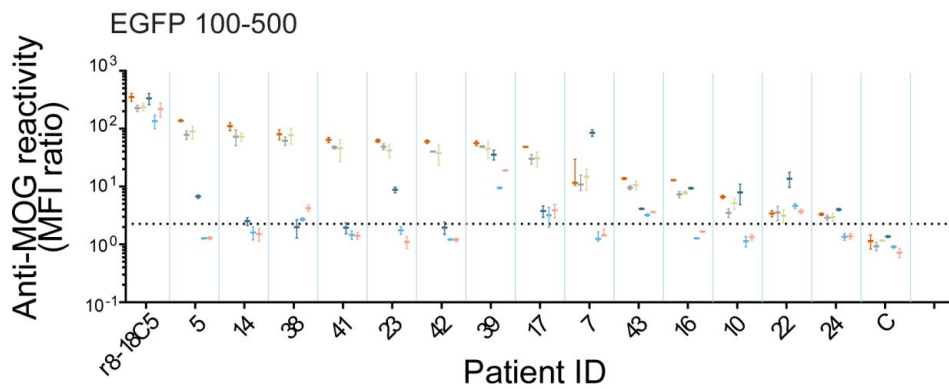
Suppl. Figure 2: Different intensity of expression of MOG-variants after transfection.

HeLa cells were transiently transfected with the indicated MOG-variants, which were all expressed as a fusion protein with EGFP. After 24h, the intensity of expression of the transfected variants was assessed by measuring the EGFP signal by FACS. The raw data is shown in the dot-plot in **Figure 4**. Here, the percentages of cells with EGFP signals of 100-500 (**A**) and >1000 (**B**) are displayed. Error bars indicate SEM of 4-5 replicates. When the gates are set to EGFP 100-500 (**A**) all the constructs have a similar expression. Only FL-MOG is significantly more expressed than opossum-MOG ($p < 0.05$). **B**) When the gates are set to include only the highest expressing cells (EGFP >1000), the different intensities of expression are revealed. The intensity of expression was calculated using one-way ANOVA Tukey's multiple comparisons statistical test.

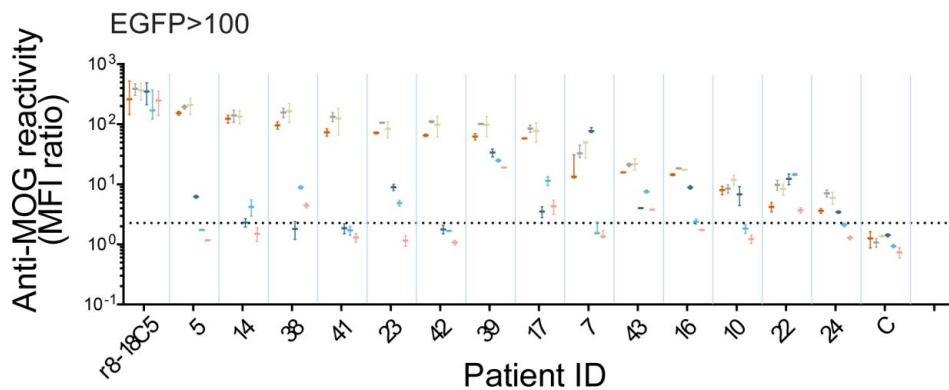
Suppl. Figure 3



A



B

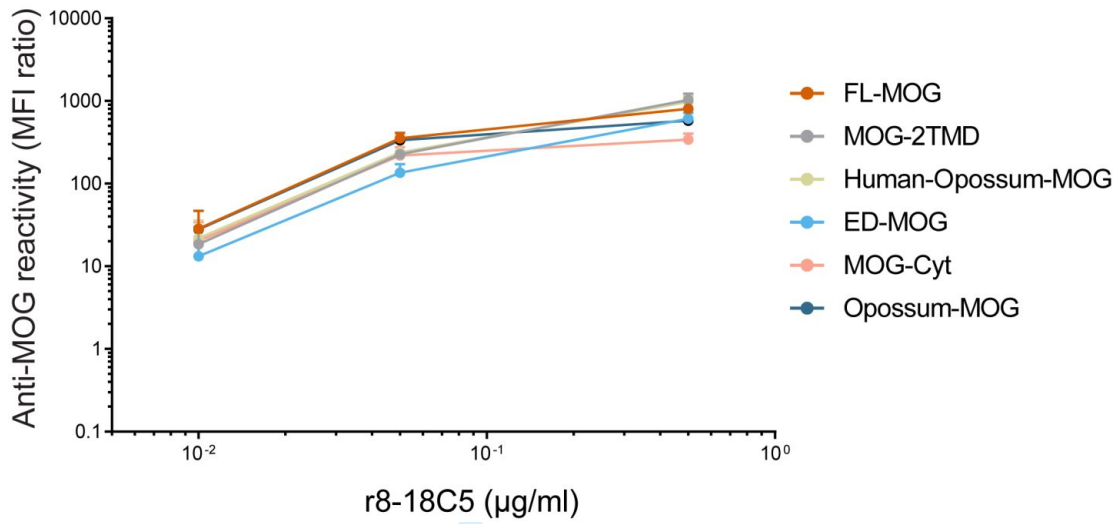


Suppl. Figure 3: Individual responses of patients with MOG-Abs to different MOG variants quantified with two different gate settings. The serum response (diluted 1:50) of the analyzed patients to cells transfected with the indicated MOG-variants was determined. The anti-MOG response is given as MFI ratio as described in the materials and methods section and displayed here in a logarithmic scale. The mAb r8-18C5 and a control sample (C) were run in parallel. The mean + SEM of two experiments is shown. The horizontal grey dotted lines in **A**) and **B**) represent the cut-off used to determine MOG+ sera to FL-MOG and it is 2.27 (mean + 3SD of controls). Since the different MOG-variants were expressed in different intensities (details in **Suppl. Figure 2**), we used different gating strategies to take this into consideration. In **A**) cells

with an EGFP signal of 100-500 were included, in **B**) cells with an EGFP signal >100 . While in most instances, the graphs in **A** and **B** look similarly, these two presentations provide complementary information in special instances. For example, for patient #22 the response to ED-MOG appears higher in **B**), but when considering the gates of 100-500, it becomes clear that this patient recognizes ED-MOG and FL-MOG similarly (**A**).

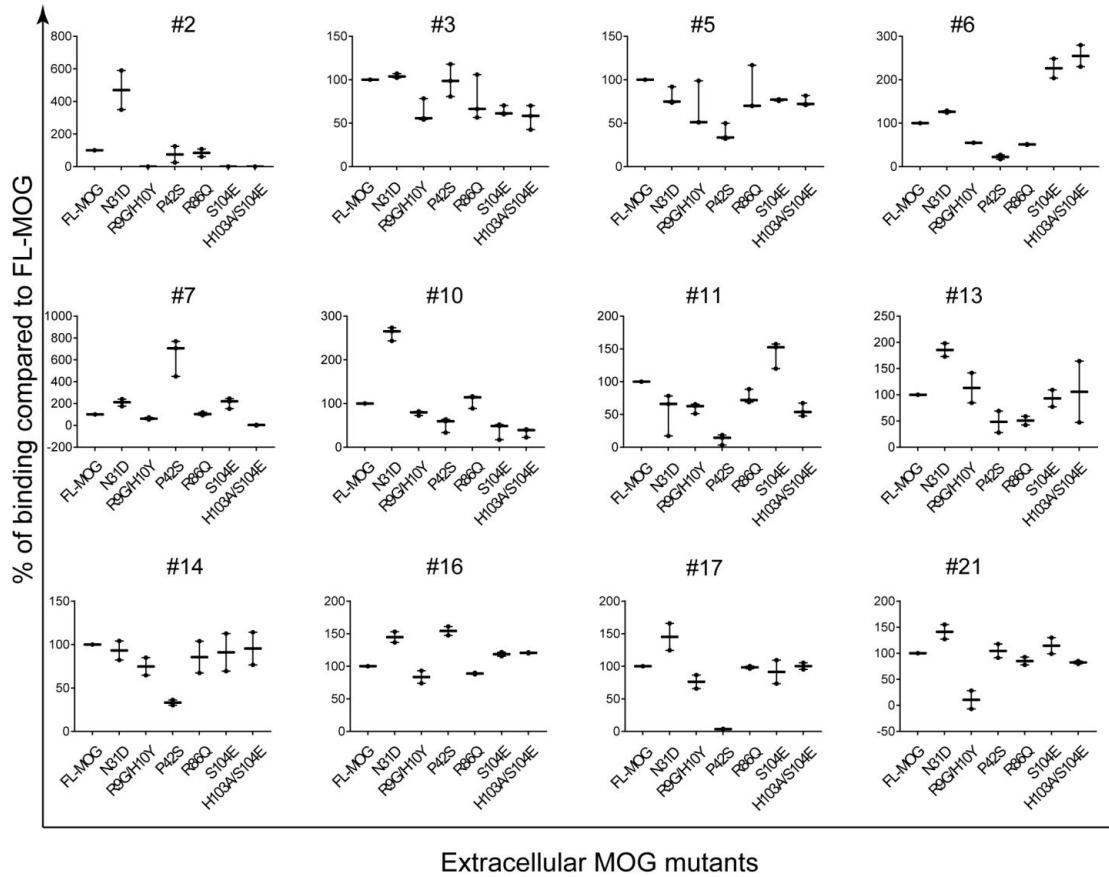
For Peer Review

Suppl. Figure 4



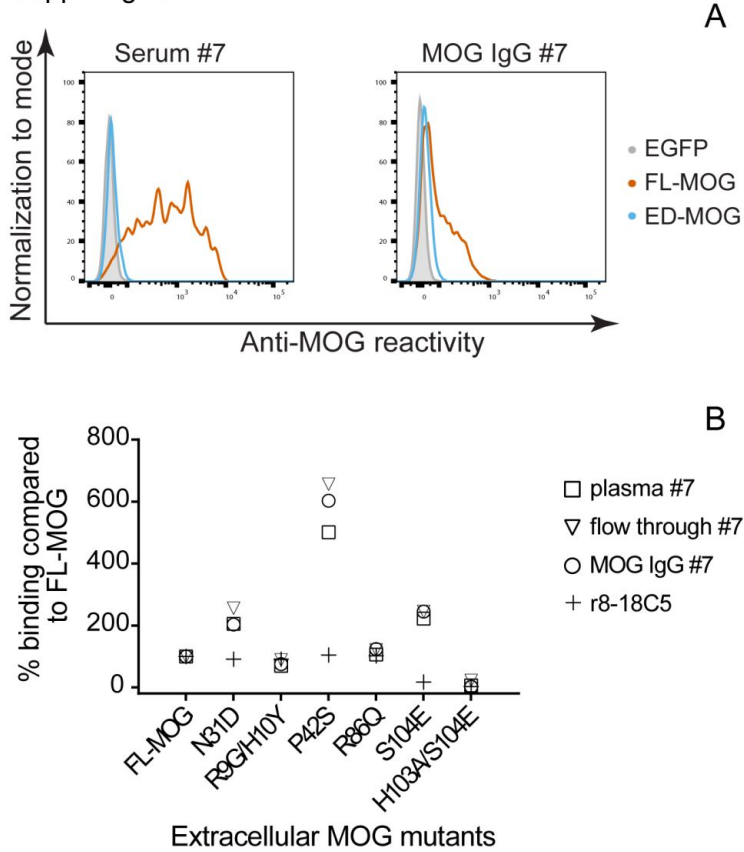
Suppl. Figure 4: Dose response of r8-18C5 on all the MOG variants. Increasing concentrations of r8-18C5 (0.01 $\mu\text{g/ml}$, 0.05 $\mu\text{g/ml}$ and 0.5 $\mu\text{g/ml}$) bound similarly to the applied MOG variants in this study. Cells with EGFP signal 100-500 were used in the analysis.

Suppl. Figure 5



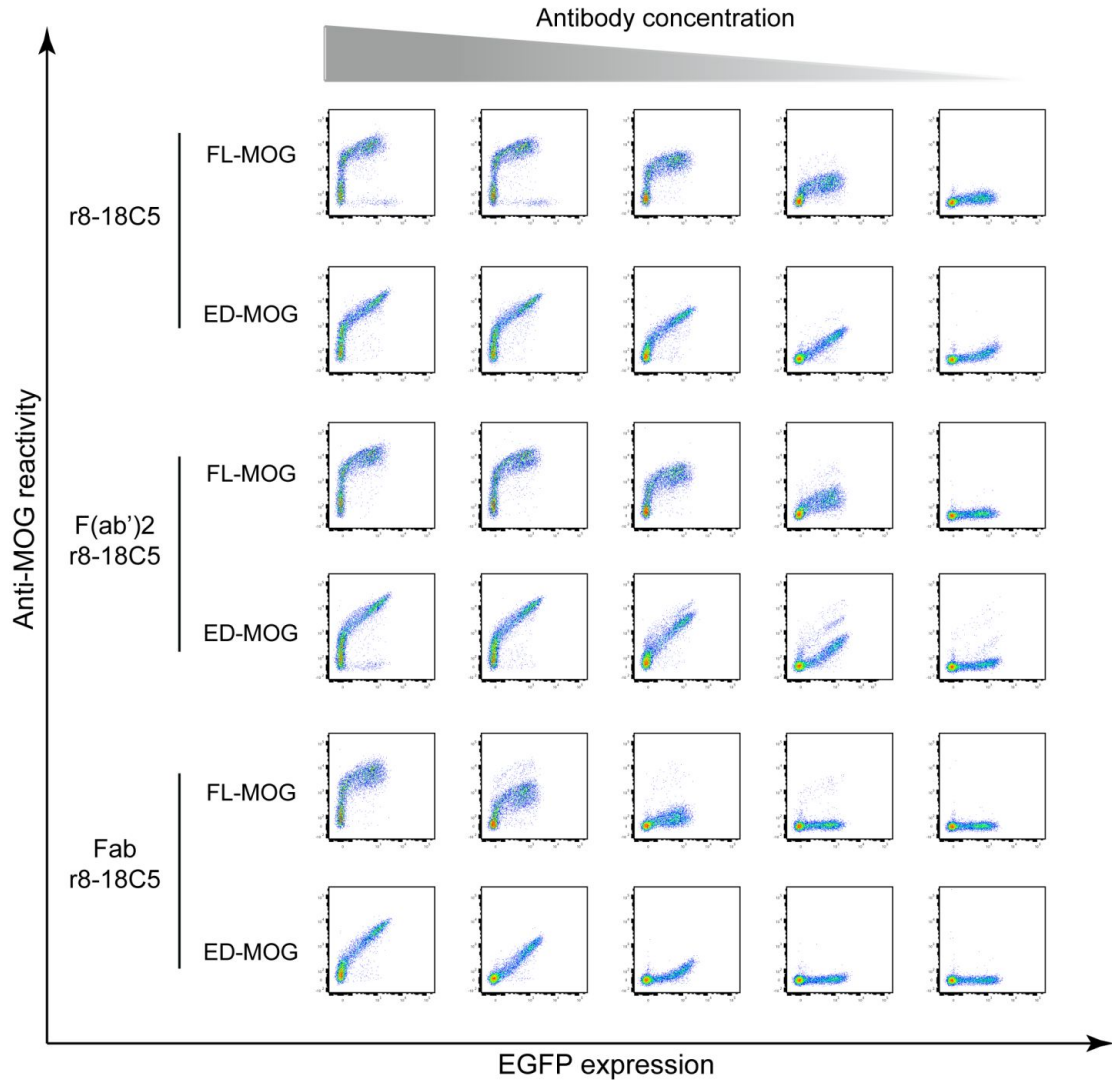
Suppl. Figure 5: Differential binding to mutants of the extracellular N-terminal part of MOG. The indicated MOG-variants were transiently transfected and the recognition by patients' sera in relation to wild type human MOG (described throughout the paper as FL-MOG) is given. Recognition of these mutants of patients #5 and #7 were also described in (Spadaro *et al.*, 2018), and of patient #24 in (Winklmeier *et al.*, 2019). Error bars indicate SEM of 2-3 experiments.

Suppl. Fig. 6



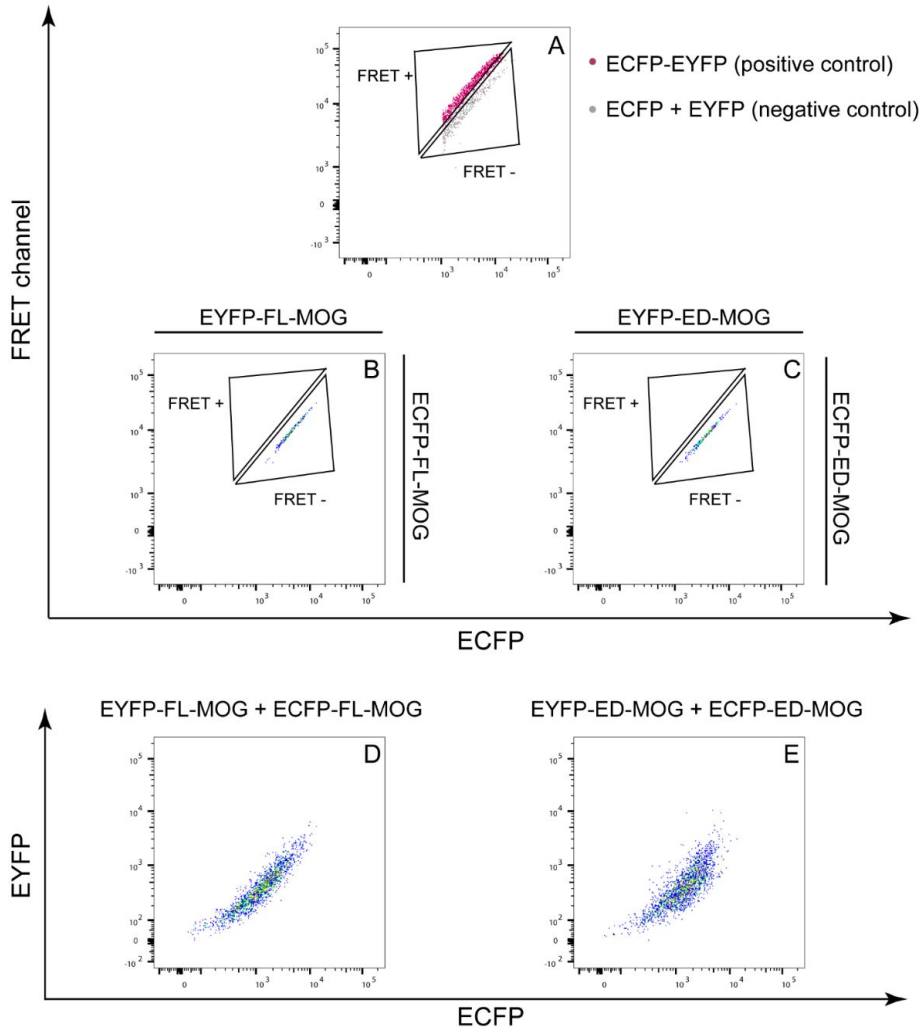
Suppl. Figure 6: MOG antibodies affinity-purified with MOG-1-125 compared with serum, plasma and flow-through. **A**) Serum (diluted 1:50) and MOG antibodies affinity-purified with MOG-1-125 (15 $\mu\text{g}/\text{ml}$), of patient #7 were tested for binding to cells transfected with FL-MOG or ED-MOG. **B**) Plasma (diluted 1:25), MOG antibodies affinity-purified with MOG-1-125 (15 $\mu\text{g}/\text{ml}$) and flow-through of patient #7 were tested also on cells transfected with extracellular mutants of MOG. The serum of this patient had a similar reactivity to the plasma towards the mutants (data not shown).

Suppl. Figure 7



Suppl. Figure 7: Recognition of FL-MOG and ED-MOG by F(ab')₂ and Fab of r8-18C5. HeLa cells transiently transfected with FL-MOG or ED-MOG were tested for MOG-recognition with different concentrations of r8-18C5 and its F(ab')₂ or Fab preparations at concentrations of 10 μg/ml, 1 μg/ml, 0.1 μg/ml, 10 ng/ml and 1 ng/ml.

Suppl. Figure 8



Suppl. Figure 8: Förster resonance energy transfer (FRET) shows no dimerization of MOG variants. **A)** The FRET+ control (ECFP-EYFP fusion construct in magenta) and the FRET- control (ECFP co-transfected with EYFP in grey) are shown. They define the FRET+ and FRET- gates. **B, D)** HEK-293T cells were co-transfected with ECFP-FL-MOG together with EYFP-FL-MOG. **B)** FRET-signal. The cells localized in the FRET- gate, indicating no dimerization between FL-MOG molecules. **C, E)** HEK-293T cells were co-transfected with ECFP-ED-MOG and with EYFP-ED-MOG. **C)** FRET-signal. The cells localized in the FRET- gate, indicating that dimerization also does not occur between ED-MOG molecules. **D) and E)** Dot-plots show the expression intensity of EYFP-FL-MOG + ECFP-FL-MOG and of EYFP-ED-MOG + ECFP-ED-MOG.

3.2 Publication 1.4: Marti Fernandez et al. (2019)



The Glycosylation Site of Myelin Oligodendrocyte Glycoprotein Affects Autoantibody Recognition in a Large Proportion of Patients

Iris Marti Fernandez¹, Caterina Macrini¹, Markus Krumbholz², Paul J. Hensbergen³, Agnes L. Hipgrave Ederveen³, Stephan Winklmeier¹, Atay Vural^{1,4}, Asli Kurne⁵, Dieter Jenne⁶, Frits Kamp⁷, Lisa Ann Gerdes¹, Reinhard Hohlfeld⁸, Manfred Wuhrer³, Tania Kümpfel¹ and Edgar Meinl^{1*}

¹ Biomedical Center and University Hospitals, Institute of Clinical Neuroimmunology, Ludwig-Maximilians-Universität München, Munich, Germany, ² Department of Neurology and Stroke, Hertie Institute for Clinical Brain Research, University of Tübingen, Tübingen, Germany, ³ Center for Proteomics and Metabolomics, Leiden University Medical Center, Leiden, Netherlands, ⁴ Koç University School of Medicine, Istanbul, Turkey, ⁵ Department of Neurology, Hacettepe University, Ankara, Turkey, ⁶ Comprehensive Pneumology Center (CPC), Institute of Lung Biology and Disease, Helmholtz Zentrum München, Munich, and Max Planck Institute of Neurobiology, Planegg, Germany, ⁷ Biomedical Center (BMC), Metabolic Biochemistry, LMU Munich, Munich, Germany, ⁸ Munich Cluster for Systems Neurology (SyNergy), Munich, Germany

OPEN ACCESS

Edited by:

Bert A. 'T Hart,
University Medical Center
Groningen, Netherlands

Reviewed by:

Juan J. Garcia-Vallejo,
VU University Medical
Center, Netherlands
Patrick Joseph Waters,
University of Oxford, United Kingdom

*Correspondence:

Edgar Meinl
edgar.meinl@med.uni-muenchen.de

Specialty section:

This article was submitted to
Multiple Sclerosis and
Neuroimmunology,
a section of the journal
Frontiers in Immunology

Received: 27 February 2019

Accepted: 10 May 2019

Published: 07 June 2019

Citation:

Marti Fernandez I, Macrini C,
Krumbholz M, Hensbergen PJ,
Hipgrave Ederveen AL, Winklmeier S,
Vural A, Kurne A, Jenne D, Kamp F,
Gerdes LA, Hohlfeld R, Wuhrer M,
Kümpfel T and Meinl E (2019) The
Glycosylation Site of Myelin
Oligodendrocyte Glycoprotein Affects
Autoantibody Recognition in a Large
Proportion of Patients.
Front. Immunol. 10:1189.
doi: 10.3389/fimmu.2019.01189

Autoantibodies to myelin oligodendrocytes glycoprotein (MOG) are found in a fraction of patients with inflammatory demyelination and are detected with MOG-transfected cells. While the prototype anti-MOG mAb 8-18C5 and polyclonal anti-MOG responses from different mouse strains largely recognize the FG loop of MOG, the human anti-MOG response is more heterogeneous and human MOG-Abs recognizing different epitopes were found to be pathogenic. The aim of this study was to get further insight into details of antigen-recognition by human MOG-Abs focusing on the impact of glycosylation. MOG has one known N-glycosylation site at N31 located in the BC loop linking two beta-sheets. We compared the reactivity to wild type MOG with that toward two different mutants in which the neutral asparagine of N31 was mutated to negatively charged aspartate or to the neutral alanine. We found that around 60% of all patients (16/27) showed an altered reactivity to one or both of the mutations. We noted seven different patterns of recognition of the two glycosylation-deficient mutants by different patients. The introduced negative charge at N31 enhanced recognition in some, but reduced recognition in other patients. In 7/27 patients the neutral glycosylation-deficient mutant was recognized stronger. The folding of the extracellular domain of MOG with the formation of beta-sheets did not depend on its glycosylation as seen by circular dichroism. We determined the glycan structure of MOG produced in HEK cells by mass spectrometry. The most abundant glycoforms of MOG expressed in HEK cells are diantennary, contain a core fucose, an antennary fucose, and are decorated with α 2,6 linked Neu5Ac, while details of the glycoforms of MOG in myelin remain to be identified. Together, we (1) increase the knowledge about heterogeneity of human autoantibodies to MOG, (2) show that the BC loop affects recognition in about 60% of the patients, (3) report that all patients recognized the unglycosylated protein backbone, while (4) in

about 20% of the patients the attached sugar reduces autoantibody binding presumably via steric hindrance. Thus, a neutral glycosylation-deficient mutant of MOG might enhance the sensitivity to identify MOG-Abs.

Keywords: myelin oligodendrocyte glycoprotein (MOG), glycosylation, autoantibody recognition, mass-spectrometry, demyelination

INTRODUCTION

Autoantibodies against myelin oligodendrocyte glycoprotein (MOG) detected in cell-based assays occur in a proportion of patients with inflammatory CNS diseases. High levels of such autoantibodies were initially detected in pediatric patients (1–3), then also in adults, and MOG-Abs are implicated in prognosis and therapy optimization (4–11). MOG-Abs are assumed to be pathogenic based on *in vitro* experiments (12–15) and injection of total IgG from anti-MOG positive patients into experimental animals (16–19). We have recently reported that affinity-purified MOG-Abs from two patients who show cross-reactivity to rodent MOG were pathogenic upon transfer into EAE animals by two different mechanisms, namely by enhancing T cell activation of cognate T cells and by inducing MS type II like demyelination when the blood-brain barrier is breached (20).

MOG is exposed on the outside of intermodal myelin; the crystal structure of the extracellular part of mouse (21) and rat MOG (22) allowed the modeling of human MOG (23). The antigen-binding fragment (Fab) of the prototype anti-MOG mAb 8-18C5 was crystallized together with the extracellular part of MOG and this revealed that the FG loop (aa101–108) of MOG, which constitutes an IgV-like fold, makes the dominant contribution to binding of this particular mAb (22). A subsequent study showed that the amino acids His103 and Ser104 are essential for binding of the mAb 8-18C5 and also for the polyclonal anti-MOG IgG induced upon MOG DNA-vaccination of BALB/c and SJL/J mice (24). In contrast to these rodent models, the anti-MOG Abs in human patients are more heterogeneous and most of the patients recognize epitopes that are different from that of the prototype mAb 8-18C5 (23). Also, the epitopes of MOG-Abs affinity-purified from two patients were found to be pathogenic upon transfer into rats and they differed in their fine-specificity from the mAb 8-18C5 (20).

The aim of this study was to get further insight into details of antigen recognition of human autoantibodies against MOG. Specifically, we analyzed here the impact of the glycosylation site of MOG on antibody binding. In principal, glycosylation of an antigen can have different, even opposing effects on antibody binding. For example, recognition of contactin by autoantibodies from 3/4 patients with chronic inflammatory demyelinating polyneuropathy depended on specific contactin N-glycosylation (25). In contrast, glycosylation of the Env-protein of the immunodeficiency viruses HIV and SIV at multiple sites blocks antibody binding and is an immune evasion strategy of these viruses in infected individuals (26, 27). Now broadly neutralizing Abs to HIV are a therapeutic perspective, but such Abs have to accommodate and avoid

glycans, while some of them recognize glycan-dependent epitopes (28).

MOG has one N-linked glycosylation site, N31 (23). It was previously observed that when this asparagine was mutated to aspartate (N31D), the MOG-recognition of some patients was altered (1, 23, 29). It was unclear, however, whether this altered binding is due to the introduction of the negatively charged aspartate or due to the abrogation of glycosylation. We addressed this issue here by generating a neutral glycosylation deficient mutant of MOG (N31A) and comparatively analyzed the anti-MOG reactivity in a total of 27 anti-MOG positive patients to wild type MOG and the different glycosylation-deficient variants of MOG. Thereby we found that the different mutations of the glycosylation site affect the antigen recognition in 15/27 patients and noted seven different patterns of antigen-recognition of variants of the glycosylation site. We applied mass spectrometry to determine the glycoforms of MOG in HEK cells, because HEK cells are the preferred expression system to analyse MOG-Abs in cell based-assays (12, 30–33). Our data extend our knowledge about the heterogeneity of human autoantibodies to MOG, indicate that the glycosylation site affects antigen-binding in a large proportion of patients and that the glycan attached to MOG is a steric hindrance for antigen recognition in some patients.

MATERIALS AND METHODS

Patients

This study included sera of 27 adult patients with different inflammatory CNS diseases and antibodies to cell-bound MOG (Table 1). We give the original diagnosis in Table 1. It is currently discussed whether patients with MOG-Abs constitute a separate disease entity. Some of our patients had got the initial diagnosis of MS, but typical MS patients do not have MOG-Abs (30). Nevertheless, in many studies patients have been described who met the diagnostic criteria of MS and were MOG-Ab positive (4, 7, 10). These may be atypical cases or patients fulfilling the criteria of MS, but with a specific phenotype (34), mostly with a low intensity of anti-MOG reactivity. Informed consent was obtained from each donor according to the Declaration of Helsinki and the ethical committee of the medical faculty of the LMU approved this study.

Molecular Cloning and Transfection

Full-length human MOG was subcloned into the pEGFP-N1 plasmid (CLONTECH Laboratories, Mountain View, CA, USA). This construct comprises a C-terminal enhanced GFP (EGFP)-tag. Using the QuickChange Site-Directed Mutagenesis Kit (Stratagene, Santa Clara, CA, USA), point mutations were induced into MOG. The oligonucleotides used were: 5'-CAT

TABLE 1 | Details of the anti-MOG positive patients.

Patient ID ^a	Diagnosis ^b	Treatment at the point of blood drawn
1	LETM	None
2	MS	Teriflunomide
3	MS/NMOSD	Steroids + Teriflunomide
4	ADEM	None
5	CIS	None
6	Relapsing ON	None
7	MS	Natalizumab
8	NMOSD	Cyclophosphamide
9	ON	None
10	RON	Rituximab
11	RON	Rituximab
12	ON	Azathioprine
13	NMOSD	Azathioprine
14	BON	Azathioprine
15	Relapsing encephalomyelitis	Steroids + Plasmapheresis
16	Relapsing ON	None
17	Relapsing encephalomyelitis	Azathioprine
18	Relapsing encephalomyelitis	Steroids
19	MS	Glatiramer acetate
20	NMOSD	Azathioprine
21	NMOSD	None
22	Relapsing ON	Azathioprine
23	NMOSD	Glatiramer acetate
24	Monophasic encephalitis	None
25	Relapsing ON	None
26	Relapsing ON	None
27	NMOSD	Steroids

^aSome patients have been previously described in more detail: Patient 17 in Spadaro et al. (29); patients 7 and 19 in Spadaro et al. (34), and patients 15, 16, 22, 23, 25, 26, and 27 in Spadaro et al. (20).

^bWe give the original diagnosis; It is currently discussed whether patients with MOG-Abs constitute a separate disease entity (8, 11, 35, 36). LETM, longitudinal extensive transverse myelitis; NMOSD, neuromyelitis optica spectrum disorder; ADEM, acute disseminated encephalomyelitis; CIS, clinically isolated syndrome; ON, optic neuritis; RON, recurrent optic neuritis; BON, bilateral optic neuritis.

ATC TCC TGG GAA GGA CGC TAC AGG CAT GGA GG-3' (N31D) (23), 5'-CAT ATC TCC TGG GAA GGC AGC TAC AGG CAT GGA GG-3' (N31A), and the corresponding reverse complementary oligonucleotides. The sequences of the purified plasmids were confirmed. HeLa cells were transfected transiently using jetPRIME (Polyplus, Illkirch, France) according to the instruction of the manufacturer, expressing MOG, N31D, or N31A fused C-terminally to EGFP. Surface expression of each of the MOG-constructs was confirmed by FACS-staining using a recombinant version of the anti-MOG mAbs 8-18C5 with a human IgG1 as Fc part (20, 37), which we call r8-18C5.

Determination of Reactivity to MOG Variants in a Cell-Based Assay

For detection of serum antibodies, HeLa cells transiently transfected with hMOG and its variants were suspended in

FACS buffer (1% FCS in PBS). The cells were incubated with a 1:50 serum dilution or mAb r8-18C5 (0.5 µg/ml) for 45 min at 4°C and washed three times in FACS buffer. The cells were then incubated with a 1:500 dilution of a biotin-SP conjugated goat anti-human IgG (Jackson ImmunoResearch, West Grove, PA, USA) for 30 min at 4°C, washed three times, and incubated with Alexa Fluor 647-conjugated streptavidin (Jackson ImmunoResearch) at a dilution of 1:2000. Finally, the cells were washed three times and suspended in a 1:2000 dilution of propidium iodide in PBS. Dead cells were excluded by positive propidium iodide staining. For the determination of anti-MOG reactivity, we gated on cells with a fluorescein isothiocyanate fluorescence (FITC) intensity above 500 and determined their mean channel fluorescence intensity (MFI) in the allophycocyanin channel (APC). Cells transfected with the mutants, wild type MOG, and with EGFP only were always measured together in the same experiment. To quantify the reactivity to the MOG variants, MFI ratio was calculated as (MFI to the MOG variant-EGFP)/(MFI to EGFP). This MFI ratio reflects properties of the autoantibodies, both amount and affinity.

Deglycosylation

HeLa cells transfected with MOG-EGFP constructs were lysed at 4°C for 1 h in RIPA buffer (150 mM NaCl, 1% NP-40, 0.5% sodium deoxycholate, 50 mM Tris pH8, 0.1% SDS) containing complete protease inhibitor mixture (Roche Applied Science, Penzberg, Germany). The lysate was then pelleted, and the supernatant was analyzed. For deglycosylation, the supernatant was digested with PNGaseF (New England Biolabs, Ipswich, MA) in Glycoprotein Denaturing Buffer (New England Biolabs), Glycobuffer 2 (New England Biolabs) and 1% NP40 (New England Biolabs) at 37°C overnight; Proteins (digested or undigested) were analyzed by SDS-PAGE. The proteins were electroblotted onto a PVDF membrane and detected by Western blot with an anti-GFP-HRP conjugated antibody (Genetex, Irvine, CA, USA) and developed using the Immobilon Western kit used (Millipore, Burlington, MA, USA) and the Odyssey Fc Imaging system (LI-COR, Bad Homburg, Germany).

Production of Recombinant MOG

We produced a recombinant version of the extracellular domain (ECD) of human MOG (20) in HEK293-EBNA cells and added at the C-terminus instead of the first transmembrane region a HisTag and an AviTag using the pTT5 vector (38). HEK293-EBNA cells were transfected, cultured under serum-free conditions with the FreeStyle293 Expression Medium (Thermo Fisher Scientific, Waltham, MA, USA). The secreted ECD of MOG was purified with a His Trap HP column (GE Healthcare, Uppsala, Sweden). With this expression system we produced the ECD of the wild type MOG and a glycosylation-deficient variant (T33N). Folding of the purified proteins (0.2 mg/ml) was analyzed by circular dichroism using a Jasco J-810 Spectropolarimeter (JASCO Corporation, Tokyo, Japan). Data were corrected for the spectrum of the buffer alone.

Preparation of Ethyl Esterified Released *N*-Glycans From Recombinant MOG

An SDS-PAGE gel band corresponding to HEK cell derived MOG (15–20 μ g, migrating at \sim 21 kDa) was reduced, alkylated and subsequently treated with *N*-glycosidase F (PNGase F; Roche Diagnostics, Mannheim, Germany) to release the *N*-glycans, as described previously (39). Additionally, 5 μ g of HEK derived MOG was denatured and incubated overnight with PNGaseF in-solution at 37°C (40, 41). Released *N*-glycans were subjected to the selective ethyl esterification of sialic acids, thereby introducing mass differences of +28.03 Da and –18.01 Da for α 2,6-linked *N*-acetylneuraminic and α 2,3 *N*-acetylneuraminic acid, respectively (40). Briefly, released glycans were incubated with the derivatization reagent (250 mM 1-ethyl-3-(3-(dimethylamino)propyl)carbodiimide and 250 mM 1-hydroxybenzotriazole in ethanol) and incubated for 60 min at 37°C. The derivatized glycans were enriched by cotton hydrophilic-interaction liquid chromatography (HILIC)–solid-phase extraction (SPE) as described before (42) and eluted in water.

MALDI-TOF(/TOF)-MS(/MS) Analysis of Released Glycans

MALDI-TOF-MS analysis was performed on an UltrafleXtreme (Bruker Daltonics) operated under flexControl 3.3 (Build 108; Bruker Daltonics). Two and 5 μ L of the enriched ethyl esterified glycans were spotted on a MALDI target (MTP AnchorChip 800/384 TF; Bruker Daltonics) together with 1 μ L of super-DHB (5 mg/mL in 50% ACN and 1 mM NaOH). The spots were dried by air at room temperature. For each spot, a mass spectrum was recorded in the range from m/z 1,000 to 5,000, combining 10,000 shots in a random walk pattern at 1,000 Hz and 200 shots per raster spot. Prior to the analysis of the samples, the instrument was calibrated using a peptide calibration standard (Bruker Daltonics). Tandem mass spectrometry (MALDI-TOF/TOF-MS/MS) was performed for the most abundant glycans using laser-induced dissociation, and compositions as well as structural features of *N*-glycans were assessed on the basis of the observed fragment ions.

Data Processing

For automated relative quantification of the released glycans, the MALDI-TOF-MS files were converted to text files and analyzed using MassTools (version 0.1.8.1.) (43). Spectra were internally calibrated using glycan peaks of known composition with a S/N above nine, covering the m/z range of the glycans. Integration was performed on selected peaks from all glycans that were observed. For this, at least 95% of the theoretical isotopic pattern was included. Several quality parameters were used to assess the actual presence of a glycan i.e., the mass accuracy (between –10 and 10 ppm), the deviation from the theoretical isotopic pattern (below 25%) and the S/N (above three) of an integrated signal. Analytes were included for relative quantification when present in at least half of the technical replicates (excluding poor quality spectra), resulting in a list of 58 glycans. Finally, only glycans with an intensity covering at least 1% of the

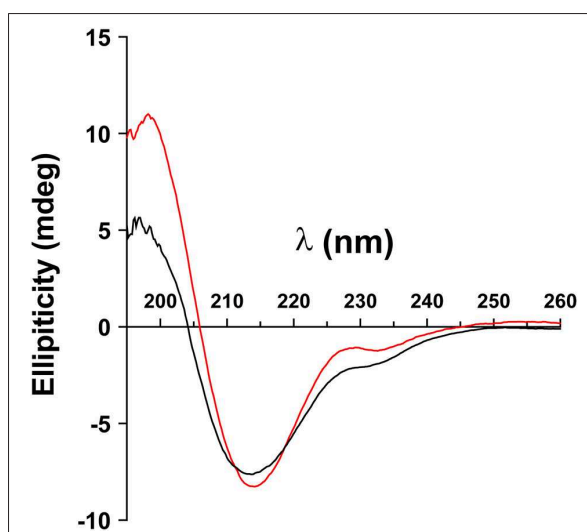


FIGURE 1 | Folding of MOG does not depend on its glycosylation. The extracellular domains of wild type MOG (black line) and an aglycosylated variant (T33N; red line) were analyzed by circular dichroism. Both spectra have a similar shape representing a predominant beta sheet conformation indicated by the negative band at 213 nm. The differences around 230 and 200 nm are probably due to the presence of the avi tag in the WT, which was absent in the mutant. Protein concentration of WT and N31D was 0.1 mg/ml.

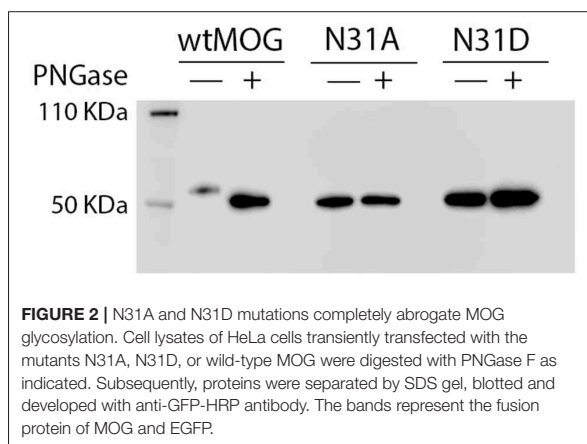
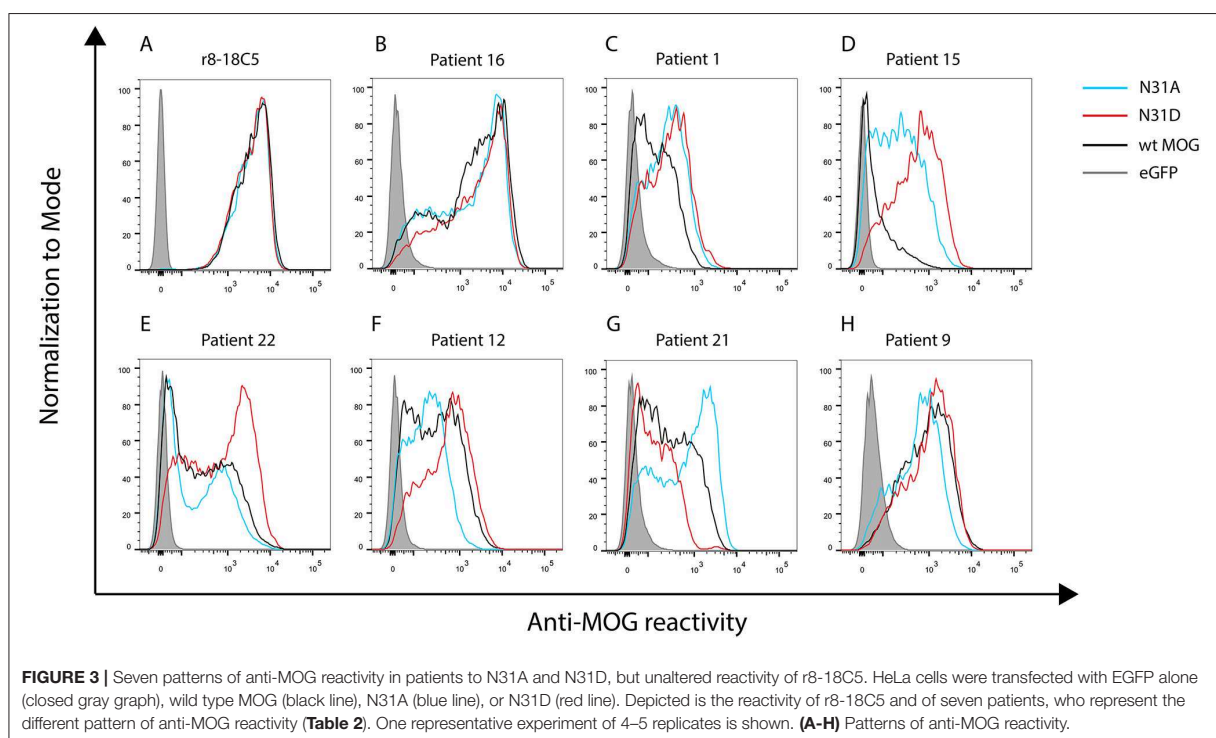


FIGURE 2 | N31A and N31D mutations completely abrogate MOG glycosylation. Cell lysates of HeLa cells transiently transfected with the mutants N31A, N31D, or wild-type MOG were digested with PNGase F as indicated. Subsequently, proteins were separated by SDS gel, blotted and developed with anti-GFP-HRP antibody. The bands represent the fusion protein of MOG and EGFP.

overall glycan abundance were selected, resulting in 28 glycans that were relatively quantified (as a fraction of the total glycan signal intensity).

Statistics

We tested 27 anti-MOG positive patients with wild-type MOG and two aglycosylated variants of MOG, N31A and N31D. Each serum was tested with each MOG variant 4–5 times. A difference between two MOG variants was considered significant if the p -value was <0.05 of both the Quade omnibus-test and *post-hoc* test and if the difference between the MFI ratios was >1 . Calculations were performed in R version 3.2.3. The Quade test



was chosen as non-parametric test for paired samples and more than two groups. This test is recommended for our sample size. The Friedman test gave almost identical results (data not shown).

RESULTS

Characterization of the Glycosylation Deficient Mutants

We analyzed whether the confirmation of the ECD of MOG depends on its glycosylation. To this end, we produced the ECD of wild type MOG and a mutated variant that lacks glycosylation recombinantly in HEK cells and analyzed these two proteins by circular dichroism. This showed a similar formation of beta-sheets indicating that the confirmation of MOG does not depend on its glycosylation (Figure 1).

Lysates of cells transfected with wild type MOG or with the mutants, N31A, and N31D, each fused to EGFP were treated with PNGaseF. Cell lysates were separated by SDS-PAGE, blotted and developed with anti-GFP mAb. Under the conditions chosen for our study, wild type MOG and also both deglycosylated forms of MOG appeared only as a monomer (Figure 2). PNGaseF treatment reduced the size of MOG while the sizes of the mutated variants N31A and N31D were not changed (Figure 2). This showed that N31A and N31D are not glycosylated and that N31 is the only N-linked glycosylation site used. To see, whether the introduced mutations induced a gross alteration of MOG, both mutants were analyzed for recognition by r8-18C5 using our cell-based assay. We observed a similar expression and binding to r8-18C5 (Figure 3A).

Heterogeneous Response to Two Glycosylation Deficient MOG Mutants

We tested 27 anti-MOG positive patients (Table 1) with wild-type MOG and two non-glycosylated variants of MOG, N31A, and N31D. About 60% of these patients (16/27) reacted to at least one of the two mutants differently than to the wild type MOG. The raw data of the reactivity of each patient to each mutant are given in Table 2 and FACS data for selected patients are shown Figure 3.

We noted seven different patterns of reactivity toward the different non-glycosylated variants of MOG (Table 2 and Figure 3). In 11/27 patients we saw no significant difference in recognition of these MOG mutants (example in Figure 3B). In 7/27 patients a higher reactivity to both non-glycosylated MOG variants was observed. A closer look at the reactivity of these seven patients showed a further diversity. Six of these seven patients responded to the two mutants similarly (Figure 3C), while another one had a higher reactivity to N31D than to N31A (#15) (Figure 3D). In five other patients we noted a higher reactivity to N31D than to wt MOG, while the reactivity to N31A was not higher than to wt (Figure 3E). Two patients (#12 and #13) showed an increased recognition of N31D, but had a reduced reactivity for the N31A (Figure 3F). An enhanced reactivity to N31A, but a reduced one to N31D was observed in one patient (#21) (Figure 3G). Patient #9 showed a reduced reactivity to N31A (Figure 3H). Together, the reactivity to N31A was higher in 8/27 and lower in 3/27 patients, while the reactivity to N31D was higher in 14/27 and lower in only 1/27 patients. Looking at individual patients, this study reveals an enormous

TABLE 2 | Heterogeneous response to two glycosylation deficient MOG mutants.

Patient ID	MFI ratio MOG	MFI ratio N31A	MFI ratio N31D	p-value WT vs. N31A	p-value WT vs. N31D	p-value N31A vs. N31D
WT = N31A = N31D						
2	6.0	7.4	5.6	0.506	0.506	1.000
4	29.0	34.2	32.9	0.506	0.506	1.000
6	211.2	164.3	199.9	0.297	1.000	0.297
10	142.4	138.3	168.5	0.574	0.083	0.188
16	187.2	225.0	211.1	0.622	0.203	0.399
18	3.7	3.9	4.6	0.390	0.060	0.214
20	5.7	7.7	7.7	0.049	0.058	0.910
23	3.7	3.6	4.4	0.064	0.039	0.003
25	97.5	114.4	117.6	0.058	0.049	0.910
26	132.5	103.9	133.7	0.161	0.781	0.108
27	77.5	86.7	121.2	0.897	0.227	0.190
WT < N31A = N31D						
1	9.1	16.8	18.9	0.022	0.008	0.500
7	2.6	6.0	5.3	0.002	0.034	0.034
8	44.3	70.5	90.1	0.047	0.017	0.473
11	93.2	124.7	117.4	0.008	0.022	0.500
17	27.9	89.9	56.5	0.002	0.025	0.112
19	5.9	7.5	8.2	0.024	0.005	0.337
WT < N31A < N31D						
15	9.8	13.9	47.4	0.034	0.002	0.034
WT = N31A < N31D						
3	28.5	28.0	36.6	0.325	0.022	0.005
5	80.6	77.0	108.3	0.894	0.013	0.017
14	28.9	30.6	40.7	0.500	0.008	0.022
22	45.8	42.0	102.8	0.112	0.025	0.002
24	14.5	14.4	18.9	0.337	0.024	0.005
N31A < WT < N31D						
12	38.8	31.4	70.1	0.034	0.034	0.002
13	94.2	65.7	102.1	0.034	0.034	0.002
WT < N31D < N31A						
21	15.1	45.5	7.7	0.034	0.034	0.002
WT = N31D > N31A						
9	26.1	20.9	27.5	0.042	0.625	0.019

Mean fluorescence intensity (MFI) ratios were calculated as described in materials and methods; values represent the arithmetic mean of 4–5 experiments. Highlighted in gray are values considered significant. Patients (#20 and #25) had a p-value <0.05, but the response to the mutants was overall considered not significant since they did not pass the Omnibus test. Also patients #7 and #23 had p-values <0.05, but also these responses were not considered significant, because their differences of the MFI ratios were <1.

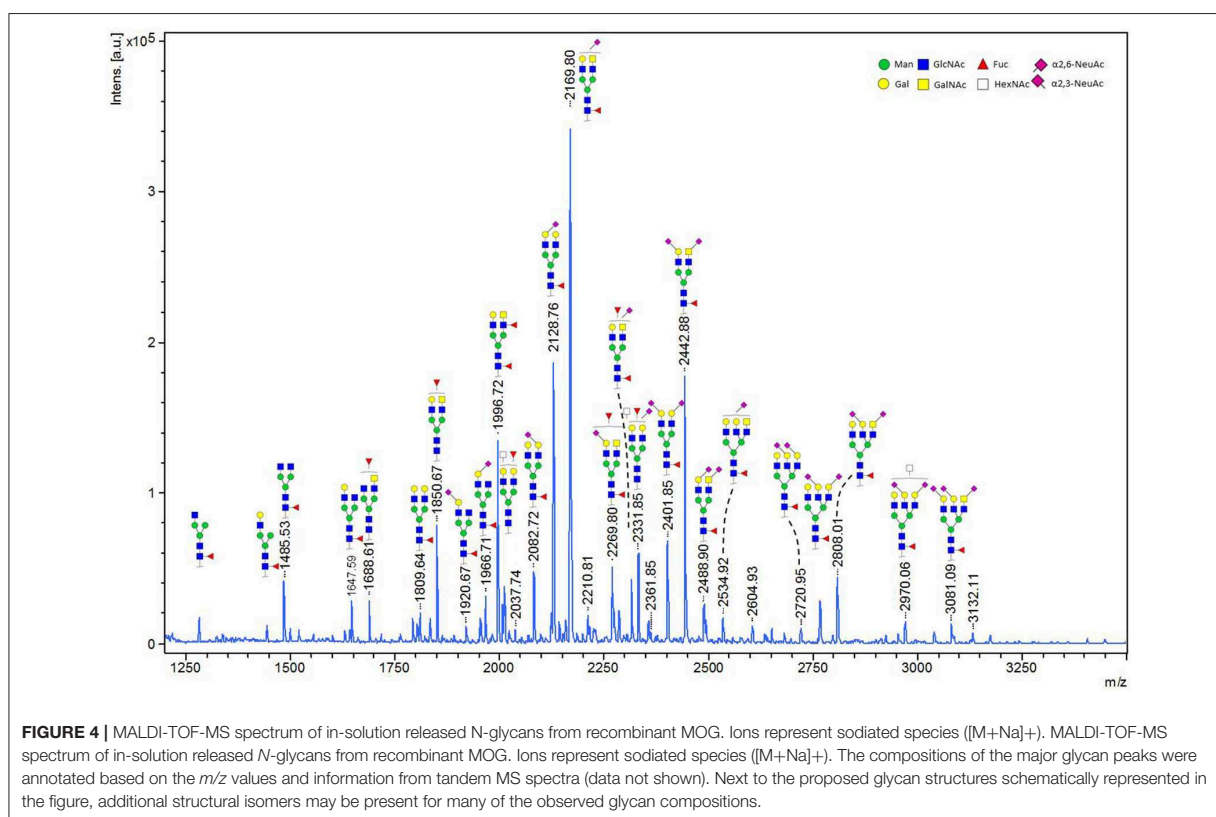
heterogeneity of human autoantibodies to MOG with seven different patterns of recognition uncovered by two mutations of the glycosylation site.

Glycoforms of MOG

We performed in-gel and in-solution enzymatic release of N-glycans from HEK derived MOG. The sialic acid stabilized N-glycans were analyzed with MALDI-TOF-MS. A representative MS spectrum is shown in **Figure 4**. To confirm our structural assignment, we subjected several *m/z* values to tandem mass spectrometry (MALDI-TOF/TOF-MS/MS, data not shown). For example, this proved informative with regard to antenna composition and fucosylation. Most spectra showed the presence of a core fucose, where the precursor showed a loss of the reducing end N-acetylglucosamine together with the fucose (367.2 Da). Antenna fucosylation was observed on both

LacDiNAc and LacNAc antennae, resulting in the loss of 552.1 and 511.1 Da, respectively. Additionally, the presence of LacDiNAc was confirmed by the specific fragment at *m/z* 429.3. The MS/MS spectrum of the most abundant peak at *m/z* 2169.8 showed signal losses of 725.1 Da (LacDiNAc antenna carrying an α 2,6-linked sialic acid) and 684.3 Da (LacNAc antenna carrying an α 2,6-linked sialic acid). This indicated a mixture of two isomers, with the sialic acid either on the LacDiNAc or LacNAc antenna. In general, the presence of bisection of glycans could not be excluded (indicated with the white squares in **Figures 4, 5**).

In total 28 glycans were selected for relative quantification (**Figure 5**). Most N-glycans were diantennary, with mainly LacNAc antennae as well as significant amounts of LacDiNAc antennae. The major glycans were sialylated species with predominantly 2,6-linked sialic acids. Most glycans showed core fucosylation, with some indications of additional antennary



fucosylation. The glycan profiles obtained from in-solution and in-gel glycan release were highly consistent and showed only minor differences.

DISCUSSION

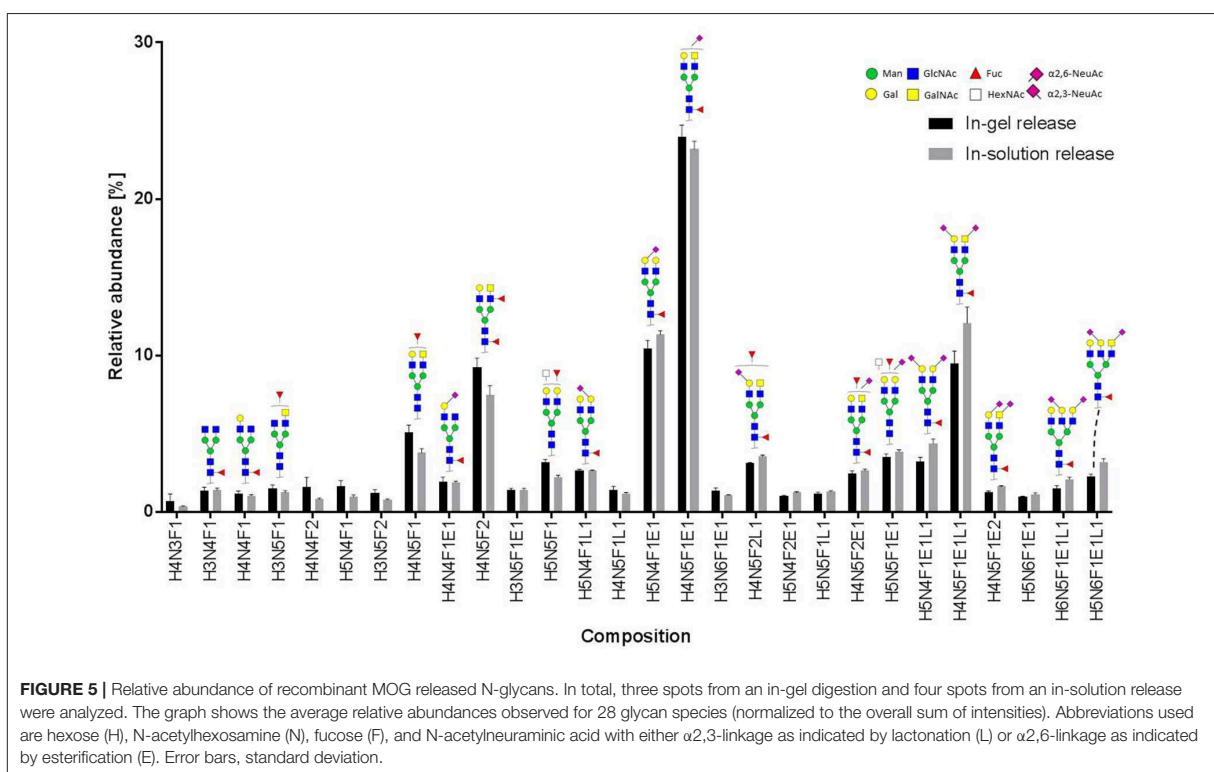
This study revealed that the glycosylation site of MOG influences its recognition by autoantibodies in about 60% of patients. We used two different glycosylation-deficient variants of MOG (N31D and N31A) and found seven different patterns of reactivity. While previous studies had noted that the N31D mutant was stronger recognized by some patients (1, 23, 29, 34), we now address the issue whether this is due to the introduced negative charge or due to the loss of the sugar part. Our study shows that both the negatively charged aspartate and the missing sugar can affect antigen recognition, in a different way in different patients.

Specifically, we noted that five patients showed a higher reactivity to N31D, while the reactivity to N31A was the same as to the wild type. In two other patients we observed a higher reactivity to N31D, but a lower one to N31A. We conclude that in these patients the introduced negative charge is responsible for the enhanced binding to MOG rather than the absence of the glycan.

In seven other patients, we observed a stronger reactivity to both N31D and N31A. Six of these patients showed a similarly

enhanced reactivity to both mutants, while one recognized N31D stronger than N31A. One further patient showed a higher reactivity to N31A, but even a lower one to N31D. We conclude that in these 7/27 patients with an enhanced reactivity to N31A the glycan on MOG provides a hindrance for antibody binding, reminding of the impact of the glycan shield of HIV and SIV (26, 27). We then determined the glycan structure of MOG produced in HEK cells by mass spectrometry and found that the most abundant glycoforms are diantennary, contain a core fucose, an antennary fucose and are decorated with α 2,6 linked Neu5Ac. Our findings indicate that this glycan structure can provide a steric hindrance for antibody binding; this might have implications for further improvement of cell-based assays to detect MOG antibodies suggesting that the use of a neutral glycosylation-deficient MOG mutant (like N31A) would enhance the sensitivity to detect autoantibodies to MOG. In none of the patients the reactivity to MOG depended on the glycan structure, clearly different than it was described for recognition of contactin (25).

Further, the MOG-reactivity of these patients is heterogeneous concerning the impact of the negatively charged N31D. One out of 27 patients showed a slightly lower reactivity to N31A, but still a clear reactivity to this glycosylation-deficient mutant. Thus, in this patient, the glycan on MOG might slightly enhance its binding to the protein-backbone. Our observation that the prototype anti-MOG r8-18C5 was not affected by any of



the glycosylation deficient mutants is in accordance with the previous reports (22, 23). Our identification of seven different patterns of reactivity just using different mutations of the glycosylation site extends the knowledge about heterogeneity of MOG-epitopes recognized by patient antibodies.

While our experiments revealed the importance of the glycosylation site for antibody recognition, details how the glycan structure impacts antibody recognition remain to be identified. This could be done by altering the glycan composition by inducing or suppressing key glycosyltransferases. This may tell whether tetra-antennary versus bi-antennary glycans or differences e.g., in sialic acid linkage or branch fucosylation have an impact on antibody recognition.

Those patients who show a different reactivity to N31D and/or N31A might directly recognize the BC-loop of MOG, where the N-linked glycosylation site is located (23), but we cannot exclude that mutations of N31 of MOG have far-reaching effects on other parts of MOG with an impact on antibody binding at a remote side. An example for an alteration of protein-protein bindings remote from the mutation site, is the recent observation that a variant of alpha-1 antitrypsin at one side (aa213) affects the interaction of a remote part of the molecule (aa143-153) with the enzyme it inhibits, neutrophil elastase (44).

While this study elaborated the importance of the glycosylation of MOG for antibody binding, also the glycosylation of antibodies has major impact on their biological activity, both on the effector functions and on

antigen-recognition. Glycosylation of the Fc-part of antibodies regulates complement activation and FcR binding (45, 46) and may serve as biomarker in autoimmunity (47). In multiple sclerosis, IgG-Fc glycosylation is altered in the CSF and indicates a pro-inflammatory pattern (48). Glycosylation of the Fab part of Ig may enhance or reduce antigen binding (49).

Glycans regulate protein-protein interactions. In an intriguing paper, glycosylation of MOG on myelin has been linked to binding to DC-SIGN and a role for myelin glycosylation in immune homeostasis of the healthy CNS was shown (50). That study further showed that removal of fucose from myelin reduced the DC-SIGN-dependent homeostatic control of myelin (50). The glycosylation in a cultured cell line may not reflect the native glycosylation of MOG in myelin. The identification of the glycoforms of MOG in myelin may help to identify binding partners of MOG. Whether MOG also interacts with sialic acid binding proteins such as Siglecs (sialic acid-binding immunoglobulin like lectins) (51) remains to be analyzed.

Together, this study shows the importance of the glycosylation site of MOG for binding of autoantibodies. Our finding that the glycan provides a hindrance for antibody binding in a proportion of patients has implications for development of assays to enhance the sensitivity to detect antibodies to MOG. Our observation of seven different patterns of MOG-binding to glycosylation-deficient variants provides further insight into details of antigen-recognition and

extends the known heterogeneity of human autoantibodies against MOG.

DATA AVAILABILITY

All datasets generated for this study are included in the Manuscript.

ETHICS STATEMENT

Informed consent was obtained from each donor according to the Declaration of Helsinki and the ethical committee of the medical faculty of the LMU approved this study.

AUTHOR CONTRIBUTIONS

IME, CM, PH, AH, SW, AV, and FK performed experiments and analyzed data. DJ, RH, MW, TK, and EM designed the study and analyzed data. AK, LG, and TK provided clinical data and analyzed data. MK performed statistical analysis. All authors contributed to drafting of the manuscript.

REFERENCES

- O'Connor KC., McLaughlin KA., De Jager PL., Chitnis T, Bettelli E, Xu C, et al. Wucherpennig: Self-antigen tetramers discriminate between myelin autoantibodies to native or denatured protein. *Nat Med.* (2007) 13:211–7. doi: 10.1038/nm1488
- Brilot F, Dale RC, Selter RC, Grummel V, Kalluri SR, Aslam M, et al. Antibodies to native myelin oligodendrocyte glycoprotein in children with inflammatory demyelinating central nervous system disease. *Ann Neurol.* (2009) 66:833–42. doi: 10.1002/ana.21916
- Pröbstel AK, Dornmair K, Bittner R, Sperl P, Jenne D, Magalhães S, et al. Antibodies to MOG are transient in childhood acute disseminated encephalomyelitis. *Neurology.* (2011) 77:580–8. doi: 10.1212/WNL.0b013e318228c0b1
- Peschl P, Bradl M, Hoffberger R, Berger T, Reindl M. Myelin oligodendrocyte glycoprotein: deciphering a target in inflammatory demyelinating diseases. *Front Immunol.* (2017) 8:529. doi: 10.3389/fimmu.2017.00529
- Jarius S, Ruprecht K, Kleiter I, Borisow N, Asgari N, Pitarokoili K, et al. MOG-IgG in NMO and related disorders: a multicenter study of 50 patients. Part 2: epidemiology, clinical presentation, radiological and laboratory features, treatment responses, and long-term outcome. *J Neuroinflammation.* (2016) 13:280. doi: 10.1186/s12974-016-0718-0
- Ramanathan S, Dale RC, Brilot F. Anti-MOG antibody: the history, clinical phenotype, and pathogenicity of a serum biomarker for demyelination. *Autoimmun Rev.* (2016) 15:307–24. doi: 10.1016/j.autrev.2015.12.004
- Hohlfeld R, Dornmair K, Meinl E, Wekerle H. The search for the target antigens of multiple sclerosis, part 2: CD8+ T cells, B cells, and antibodies in the focus of reverse-translational research. *Lancet Neurol.* (2016) 15:317–31. doi: 10.1016/S1474-4422(15)00313-0
- Jurczyk M, Messina S, Woodhall MR, Raza N, Everett R, Roca-Fernandez A, et al. Clinical presentation and prognosis in MOG-antibody disease: a UK study. *Brain.* (2017) 140:3128–38. doi: 10.1093/brain/awx276
- Mayer MC, Meinl E. Glycoproteins as targets of autoantibodies in CNS inflammation: MOG and more. *Ther Adv Neurol Disord.* (2012) 5:147–59. doi: 10.1177/1756285611433772
- Reindl M, Waters P. Myelin oligodendrocyte glycoprotein antibodies in neurological disease. *Nat Rev Neurol.* (2018) 15:89–102. doi: 10.1038/s41582-018-0112-x
- Di Pauli F, Berger T. Myelin oligodendrocyte glycoprotein antibody-associated disorders: toward a new spectrum of inflammatory demyelinating

FUNDING

This work was supported by the DFG (SFB TR128), the Munich Cluster for Systems Neurology (ExC 1010 SyNergy), the Clinical Competence Network for Multiple Sclerosis, the Werner Reichenberger Stiftung, and the Verein zur Therapieforschung für Multiple Sklerose-Kranke and by grants (to DJ) from the European Union's Horizon 2020 Research and Innovation Program (668036, RELENT). Responsibility for the information and views set out in this article lies entirely with the authors. AV was supported by post-doctoral fellowships from European Academy of Neurology, TÜBİTAK-BİDEB 2219 program and Alexander von Humboldt Foundation Georg Forster Research Fellowship Program during this project.

ACKNOWLEDGMENTS

We are grateful to Heike Rübsamen for expert technical assistance and to Drs. Stefanie Hauck and Klaus Dornmair for valuable support. We thank Drs. Anneli Peters and Naoto Kawakami for comments on the manuscript.

- CNS disorders? *Front Immunol.* (2018) 9:2753. doi: 10.3389/fimmu.2018.02753
- Mader S, Gredler V, Schanda K, Rostasy K, Dujmovic I, Pfaller K, et al. Complement activating antibodies to myelin oligodendrocyte glycoprotein in neuromyelitis optica and related disorders. *J Neuroinflammation.* (2011) 8:184. doi: 10.1186/1742-2094-8-184
- Dale RC, Tantsis EM, Merheb V, Kumaran RY, Sinmaz N, Pathmanandavel K, et al. Antibodies to MOG have a demyelination phenotype and affect oligodendrocyte cytoskeleton. *Neurol Neuroimmunol Neuroinflamm.* (2014) 1:e12. doi: 10.1212/NXI.0000000000000012
- Peschl P, Schanda K, Zeka B, Given K, Böhm D, Ruprecht K, et al. Human antibodies against the myelin oligodendrocyte glycoprotein can cause complement-dependent demyelination. *J Neuroinflammation.* (2017) 14:208. doi: 10.1186/s12974-017-0984-5
- Kinzel S, Lehmann-Horn K, Torke S, Hausler D, Winkler A, Stadelmann C, et al. Myelin-reactive antibodies initiate T cell-mediated CNS autoimmune disease by opsonization of endogenous antigen. *Acta Neuropathol.* (2016) 132:43–58. doi: 10.1007/s00401-016-1559-8
- Zhou D, Srivastava R, Nessler S, Grummel V, Sommer N, Bruck W, et al. Identification of a pathogenic antibody response to native myelin oligodendrocyte glycoprotein in multiple sclerosis. *Proc Natl Acad Sci USA.* (2006) 103:19057–62. doi: 10.1073/pnas.0607242103
- Saadoun S, Waters P, Owens GP, Bennett JL, Vincent A, Papadopoulos MC. Neuromyelitis optica MOG-IgG causes reversible lesions in mouse brain. *Acta Neuropathol Commun.* (2014) 2:35. doi: 10.1186/2051-5960-2-35
- Flach AC, Litke T, Strauss J, Haberl M, Gomez CC, Reindl M, et al. Autoantibody-boosted T-cell reactivation in the target organ triggers manifestation of autoimmune CNS disease. *Proc Natl Acad Sci USA.* (2016) 113:3323–28. doi: 10.1073/pnas.1519608113
- Khare P, Challa DK, Devanaboyina SC, Velmurugan R, Hughes S, Greenberg BM, et al. Myelin oligodendrocyte glycoprotein-specific antibodies from multiple sclerosis patients exacerbate disease in a humanized mouse model. *J Autoimmun.* (2018) 86:104–15. doi: 10.1016/j.jaut.2017.09.002
- Spadaro M, Winklmeier S, Beltran E, Macrini C, Hoffberger R, Schuh E, et al. Pathogenicity of human antibodies against myelin oligodendrocyte glycoprotein. *Ann Neurol.* (2018) 84:315–28. doi: 10.1002/ana.25291
- Clements CS, Reid HH, Beddoe T, Tynan FE, Perugini MA, Johns TG, et al. The crystal structure of myelin oligodendrocyte glycoprotein, a key autoantigen in multiple sclerosis. *Proc Natl Acad Sci USA.* (2003) 100:11059–64. doi: 10.1073/pnas.1833158100

22. Breithaupt C, Schubart A, Zander H, Skerra A, Huber R, Linington C, et al. Structural insights into the antigenicity of myelin oligodendrocyte glycoprotein. *Proc Natl Acad Sci USA*. (2003) 100:9446–51. doi: 10.1073/pnas.1133443100
23. Mayer MC, Breithaupt C, Reindl M, Schanda K, Rostasy K, Berger T, et al. Distinction and temporal stability of conformational epitopes on myelin oligodendrocyte glycoprotein recognized by patients with different inflammatory central nervous system diseases. *J Immunol*. (2013) 191:3594–604. doi: 10.4049/jimmunol.1301296
24. Breithaupt C, Schafer B, Pellkofer H, Huber R, Linington C, Jacob U. Demyelinating myelin oligodendrocyte glycoprotein-specific autoantibody response is focused on one dominant conformational epitope region in rodents. *J Immunol*. (2008) 181:1255–63. doi: 10.4049/jimmunol.181.2.1255
25. Labasque M, Hivert B, Nogales-Gadea G, Querol L, Illa I, Favre-Sarrailh C. Specific contactin N-glycans are implicated in neurofascin binding and autoimmune targeting in peripheral neuropathies. *J Biol Chem*. (2014) 289:7907–18. doi: 10.1074/jbc.M113.528489
26. Reitter JN, Means RE, Desrosiers RC. A role for carbohydrates in immune evasion in AIDS. *Nat Med*. (1998) 4:679–84. doi: 10.1038/nm0698-679
27. Wei X, Decker JM, Wang S, Hui H, Kappes JC, Wu X, et al. Antibody neutralization and escape by HIV-1. *Nature*. (2003) 422:307–12. doi: 10.1038/nature01470
28. Falkowska E, Le KM, Ramos A, Doores KJ, Lee JH, Blattner C, et al. Broadly neutralizing HIV antibodies define a glycan-dependent epitope on the prefusion conformation of gp41 on cleaved envelope trimers. *Immunity*. (2014) 40:657–68. doi: 10.1016/j.immuni.2014.04.009
29. Spadaro M, Gerdes LA, Mayer MC, Ertl-Wagner B, Laurent S, Krumbholz M, et al. Histopathology and clinical course of MOG-antibody associated encephalomyelitis. *Ann Clin Transl Neurol*. (2015) 2:295–301. doi: 10.1002/acn3.164
30. Waters P, Woodhall M, O'Connor KC, Reindl M, Lang B, Sato DK, et al. MOG cell-based assay detects non-MS patients with inflammatory neurologic disease. *Neurol Neuroimmunol Neuroinflamm*. (2015) 2:e89. doi: 10.1212/NXI.0000000000000089
31. Lopez-Chiriboga AS, Majed M, Fryer J, Dubey D, McKeon A, Flanagan EP, et al. Association of MOG-IgG serostatus with relapse after acute disseminated encephalomyelitis and proposed diagnostic criteria for MOG-IgG-associated disorders. *JAMA Neurol*. (2018) 75:1355–63. doi: 10.1001/jamaneurol.2018.1814
32. Ramanathan S, Reddel SW, Henderson A, Parratt JD, Barnett M, Gatt PN, et al. Antibodies to myelin oligodendrocyte glycoprotein in bilateral and recurrent optic neuritis. *Neurol Neuroimmunol Neuroinflamm*. (2014) 1:e40. doi: 10.1212/NXI.0000000000000040
33. Kaneko K, Sato DK, Nakashima I, Ogawa R, Akaishi T, Takai Y, et al. CSF cytokine profile in MOG-IgG+ neurological disease is similar to AQP4-IgG+ NMOSD but distinct from MS: a cross-sectional study and potential therapeutic implications. *J Neurol Neurosurg Psychiatry*. (2018) 89:927–36. doi: 10.1136/jnnp-2018-317969
34. Spadaro M, Gerdes LA, Krumbholz M, Ertl-Wagner B, Thaler FS, Schuh E, et al. Autoantibodies to MOG in a distinct subgroup of adult multiple sclerosis. *Neurol Neuroimmunol Neuroinflamm*. (2016) 3:e257. doi: 10.1212/NXI.0000000000000257
35. Zamvil SS, Slavin AJ. Does MOG Ig-positive AQP4-seronegative opticospinal inflammatory disease justify a diagnosis of NMO spectrum disorder? *Neurol Neuroimmunol Neuroinflamm*. (2015) 2:e62. doi: 10.1212/NXI.0000000000000062
36. Jarius S, Paul F, Aktas O, Asgari N, Dale RC, de Seze J, et al. MOG encephalomyelitis: international recommendations on diagnosis and antibody testing. *J Neuroinflammation*. (2018) 15:134. doi: 10.1186/s12974-018-1144-2
37. Brändle SM, Obermeier B, Senel M, Bruder J, Mentele R, Khademi M, et al. Distinct oligoclonal band antibodies in multiple sclerosis recognize ubiquitous self-proteins. *Proc Natl Acad Sci USA*. (2016) 113:7864–9. doi: 10.1073/pnas.1522730113
38. Perera NC, Wiesmuller KH, Larsen MT, Schacher B, Eickholz P, Borregaard N, et al. NSP4 is stored in azurophilic granules and released by activated neutrophils as active endoprotease with restricted specificity. *J Immunol*. (2013) 191:2700–7. doi: 10.4049/jimmunol.1301293
39. Royle L, Radcliffe CM, Dwek RA, Rudd PM. Detailed structural analysis of N-glycans released from glycoproteins in SDS-PAGE gel bands using HPLC combined with exoglycosidase array digestions. *Methods Mol Biol*. (2006) 347:125–43. doi: 10.1385/1-59745-167-3:125
40. Reiding KR, Blank D, Kuijper DM, Deelder AM, Wuhrer M. High-throughput profiling of protein N-glycosylation by MALDI-TOF-MS employing linkage-specific sialic acid esterification. *Anal Chem*. (2014) 86:5784–93. doi: 10.1021/ac500335t
41. Ruhaak LR, Huhn C, Waterreus WJ, de Boer AR, Neuss C, Hokke CH, et al. Hydrophilic interaction chromatography-based high-throughput sample preparation method for N-glycan analysis from total human plasma glycoproteins. *Anal Chem*. (2008) 80:6119–26. doi: 10.1021/ac800630x
42. Selman MH, Hemayatkar M, Deelder AM, Wuhrer M. Cotton HILIC SPE microtips for microscale purification and enrichment of glycans and glycopeptides. *Anal Chem*. (2011) 83:2492–9. doi: 10.1021/ac1027116
43. Jansen BC, Reiding KR, Bondt A, Hipgrave Ederveen AL, Palmblad M, Falck D, et al. Massy tools: a high-throughput targeted data processing tool for relative quantitation and quality control developed for glycomic and glycoproteomic MALDI-MS. *J Proteome Res*. (2015) 14:5088–98. doi: 10.1021/acs.jproteome.5b00658
44. Malik R, Dau T, Gonik M, Sivakumar A, Deredge DJ, Edeleva EV, et al. Common coding variant in SERPINA1 increases the risk for large artery stroke. *Proc Natl Acad Sci USA*. (2017) 114:3613–8. doi: 10.1073/pnas.1616301114
45. Bournazos S, Wang TT, Dahan R, Maamary J, Ravetch JV. Signaling by antibodies: recent progress. *Annu Rev Immunol*. (2017) 35:285–311. doi: 10.1146/annurev-immunol-051116-052433
46. Dekkers G, Treffers L, Plomp R, Bentlage AEH, de Boer M, Koeleman CAM, et al. Decoding the human immunoglobulin G-glycan repertoire reveals a spectrum of Fc-receptor- and complement-mediated-effector activities. *Front Immunol*. (2017) 8:877. doi: 10.3389/fimmu.2017.00877
47. Seeling M, Bruckner C, Nimmerjahn F. Differential antibody glycosylation in autoimmunity: sweet biomarker or modulator of disease activity? *Nat Rev Rheumatol*. (2017) 13:621–30. doi: 10.1038/nrrheum.2017.146
48. Wuhrer M, Selman MH, McDonnell LA, Kumpfel T, Derfuss T, Khademi M, et al. Pro-inflammatory pattern of IgG1 Fc glycosylation in multiple sclerosis cerebrospinal fluid. *J Neuroinflammation*. (2015) 12:235. doi: 10.1186/s12974-015-0450-1
49. van de Bovenkamp FS, Hafkenscheid L, Rispens T, Rombouts Y. The emerging importance of IgG fab glycosylation in immunity. *J Immunol*. (2016) 196:1435–41. doi: 10.4049/jimmunol.1502136
50. Garcia-Vallejo JJ, Ilarregui JM, Kalay H, Chamorro S, Koning N, Unger WW, et al. CNS myelin induces regulatory functions of DC-SIGN-expressing, antigen-presenting cells via cognate interaction with MOG. *J Exp Med*. (2014) 211:1465–83. doi: 10.1084/jem.20122192
51. Macauley MS, Crocker PR, Paulson JC. Siglec-mediated regulation of immune cell function in disease. *Nat Rev Immunol*. (2014) 14:653–66. doi: 10.1038/nri3737

Conflict of Interest Statement: The authors declare that the research was conducted in the absence of any commercial or financial relationships that could be construed as a potential conflict of interest.

Copyright © 2019 Marti Fernandez, Macrini, Krumbholz, Hensbergen, Hipgrave Ederveen, Winklmeier, Vural, Kurne, Jenne, Kamp, Gerdes, Hohlfeld, Wuhrer, Kumpfel and Meinel. This is an open-access article distributed under the terms of the Creative Commons Attribution License (CC BY). The use, distribution or reproduction in other forums is permitted, provided the original author(s) and the copyright owner(s) are credited and that the original publication in this journal is cited, in accordance with accepted academic practice. No use, distribution or reproduction is permitted which does not comply with these terms.

3.3 Publication 1.6: Spadaro et al. (2018)



Pathogenicity of Human Antibodies against Myelin Oligodendrocyte Glycoprotein

Melania Spadaro, PhD,¹ Stephan Winklmeier, MSc,¹ Eduardo Beltrán, PhD,¹ Caterina Macrini, MSc,¹ Romana Höftberger, MD,² Elisabeth Schuh, MD, PhD,¹ Franziska S. Thaler, MD,¹ Lisa Ann Gerdes, MD,¹ Sarah Laurent, MD, PhD,¹ Ramona Gerhards, MSc,¹ Simone Brändle, PhD,¹ Klaus Dornmair, PhD,¹ Constanze Breithaupt, PhD,³ Markus Krumbholz, MD,⁴ Markus Moser, PhD,⁵ Gurumoorthy Krishnamoorthy, PhD,⁵ Frits Kamp, PhD,⁶ Dieter Jenne, MD,⁷ Reinhard Hohlfeld, MD,^{1,8} Tania Kümpfel, MD,¹ Hans Lassmann, MD,⁹ Naoto Kawakami, PhD,^{1*} and Edgar Meinl, MD^{1*}

Objective: Autoantibodies against myelin oligodendrocyte glycoprotein (MOG) occur in a proportion of patients with inflammatory demyelinating diseases of the central nervous system (CNS). We analyzed their pathogenic activity by affinity-purifying these antibodies (Abs) from patients and transferring them to experimental animals.

Methods: Patients with Abs to MOG were identified by cell-based assay. We determined the cross-reactivity to rodent MOG and the recognized MOG epitopes. We produced the correctly folded extracellular domain of MOG and affinity-purified MOG-specific Abs from the blood of patients. These purified Abs were used to stain CNS tissue and transferred in 2 models of experimental autoimmune encephalomyelitis. Animals were analyzed histopathologically.

Results: We identified 17 patients with MOG Abs from our outpatient clinic and selected 2 with a cross-reactivity to rodent MOG; both had recurrent optic neuritis. Affinity-purified Abs recognized MOG on transfected cells and stained myelin in tissue sections. The Abs from the 2 patients recognized different epitopes on MOG, the CC' and the FG loop. In both patients, these Abs persisted during our observation period of 2 to 3 years. The anti-MOG Abs from both patients were pathogenic upon intrathecal injection in 2 different rat models. Together with cognate MOG-specific T cells, these Abs enhanced T-cell infiltration; together with myelin basic protein-specific T cells, they induced demyelination associated with deposition of C9neo, resembling a multiple sclerosis type II pathology.

Interpretation: MOG-specific Abs affinity purified from patients with inflammatory demyelinating disease induce pathological changes in vivo upon cotransfer with myelin-reactive T cells, suggesting that these Abs are similarly pathogenic in patients. ANN NEUROL 2018;00:000–000

ANN NEUROL 2018;84:315–328

High levels of antibodies (Abs) to conformationally intact myelin oligodendrocyte glycoprotein (MOG) have initially been detected in pediatric patients,¹ then also in a proportion of patients with different

View this article online at wileyonlinelibrary.com. DOI: 10.1002/ana.25291

Received Feb 28, 2018, and in revised form May 15, 2018. Accepted for publication Jul 1, 2018.

Address correspondence to: Dr Meinl, Institute of Clinical Neuroimmunology, Biomedical Center and University Hospitals, Ludwig-Maximilians-Universität München, Großhaderner Str 9, 82152 Planegg-Martinsried, Germany. E-mail: edgar.meinl@med.uni-muenchen.de

*Naoto Kawakami and Edgar Meinl contributed equally

From the ¹Institute of Clinical Neuroimmunology, Biomedical Center and University Hospitals, Ludwig-Maximilians-Universität München, Munich, Germany; ²Institute of Neurology, Medical University of Vienna, Vienna, Austria; ³Department of Physical Biotechnology, Martin Luther University of Halle-Wittenberg, Halle, Germany; ⁴Department of Neurology and Hertie Institute for Clinical Brain Research, Eberhard Karl University, Tübingen, Germany; ⁵Max Planck Institute of Biochemistry, Martinsried, Germany; ⁶Department of Biophysics, Biomedical Center, Ludwig Maximilian University of Munich, Munich, Germany; ⁷Comprehensive Pneumology Center (CPC), Institute of Lung Biology and Disease, Helmholtz Zentrum München, Munich, and Max Planck Institute of Neurobiology, Planegg-Martinsried, Germany; ⁸Munich Cluster for Systems Neurology, Munich, Germany; and ⁹Center for Brain Research, Medical University of Vienna, Austria.

demyelinating diseases such as optic neuritis, myelitis, encephalomyelitis, brainstem encephalitis, acute disseminated encephalomyelitis (ADEM), and anti-N-methyl-D-aspartate receptor (NMDAR) encephalitis, and in a few patients with multiple sclerosis (MS).²⁻⁶ Patients with autoantibodies to MOG have distinct brain magnetic resonance imaging (MRI) characteristics.^{7,8} It is debated whether anti-MOG disease constitutes a separate entity.⁹

In animal models, some monoclonal Abs (mAbs) to MOG induce demyelination provided the blood-brain barrier is breached giving the Abs access to the CNS (reviewed in Hohlfeld et al,⁵ Mayer and Meinl¹⁰). Only a proportion of anti-MOG Abs are able to induce demyelination in vivo, related to complement activation¹¹ and recognition of conformationally correct MOG.^{12,13} In rodents, pathogenic MOG-specific Abs mainly recognize the FG loop of MOG as the prototype mAb 8-18C5,¹⁴ whereas patients with Abs to MOG recognize different loops of MOG, most frequently the CC' loop around the amino acid P42.¹⁵

Previous experiments to test the potential pathogenic activity of human anti-MOG Abs in vitro reported that sera of patients with Abs to MOG activated complement,¹⁶ stimulated natural killer cell mediated toxicity,¹⁷ induced cytoskeletal changes in oligodendroglial cells,¹⁸ mediated myelin destruction in slice cultures,¹⁹ and facilitated MOG uptake by macrophages.²⁰ Peripheral injection of concentrated serum from MS patients in rats with experimental autoimmune encephalomyelitis (EAE) slightly enhanced demyelination and axonal loss.²¹ Total IgG preparations pooled from 5 neuromyelitis optica (NMO) patients were injected intracerebrally and induced myelin changes independent of complement, but no inflammation.²² Intrathecal injection of IgG from a patient with MOG Abs accelerated EAE in mice.²³ Peripheral injection of IgG from MS patients with Abs to MOG exacerbated EAE in mice.²⁴ Thus, there is evidence that human Abs to MOG are pathogenic, but one has to consider that patients with neuroinflammation may have multiple autoantibodies,²⁵⁻²⁷ which complicates the interpretation of transfer experiments with whole IgG preparations. Transfer experiments with human affinity-purified Abs to MOG have not yet been done, and therefore detailed pathogenic mechanisms of human Abs to MOG remain to be elaborated.

Patients with Abs to MOG have a pathology described as MS pattern II,²⁸⁻³¹ characterized by active demyelination along with deposition of C9neo, suggesting an Ab-mediated demyelination.^{32,33} Transfer experiments with autoantibodies to MOG from these patients were hampered because only a proportion of MOG Abs from patients cross-react with rodent MOG^{15,28}; therefore, the

linkage of human MOG Abs to a certain neuropathology is still speculative.

The aim of this study was to analyze which human Abs to MOG are pathogenic, to identify recognized epitopes of pathogenic autoantibodies, to test whether they can mediate MS type II pathology, and to explore their pathogenic mechanisms. To this end, we combined affinity purification of Abs that recognize cell-based MOG, epitope identification with mutants of MOG, staining of tissue sections, and transfer experiments in 2 EAE models. This showed that Abs to MOG were pathogenic by 2 mechanisms; in synergy with myelin basic protein (MBP)-specific T cells they mediate MS type II pathology, and together with MOG-specific T cells they enhance T-cell infiltration.

Patients and Methods

Standard Protocol Approvals, Registrations, and Patient Consents

We analyzed sera from 260 patients with inflammatory CNS diseases for anti-MOG reactivity. The clinical characteristics of patients who scored positive in our cell-based assay detecting Abs to MOG are summarized in the Table. All MOG Ab-positive patients were followed longitudinally. Informed consent was obtained from each donor according to the Declaration of Helsinki and the ethical committee of the medical faculty of Ludwig-Maximilians-Universität München approved this study.

Determination of anti-MOG Reactivity and Epitope Recognition

Patients positive for Abs to MOG were identified with a cell-based flow cytometry assay using viable cells and a serum dilution of 1:50, as described.^{28,34} Isotype-specific secondary Abs were obtained from Southern Biotech (Birmingham, AL). To identify the recognized epitopes, mutant variants of MOG were applied and the percentage binding compared to human MOG was calculated as described.¹⁵ In some experiments, we used a recombinant variant of the mAb 8-18C5 (designated r8-18C5), which has the same antigen recognition site, but a human IgG1 Fc part.³⁵

Production and Validation of Recombinant Human MOG

We aimed to produce a recombinant version of the extracellular domain (ECD) of human MOG that comes as close as possible to the conformation of MOG displayed in transfected cells. To this end, we produced the ECD of human MOG in HEK293-EBNA cells and added at the C-terminus instead of the first transmembranous region a HisTag and an AviTag using the pTT5 vector.³⁶ MOG

was biotinylated by using the BirA biotin ligase Kit (Avidity, Aurora, CO). Folding of the purified protein (0.2mg/ml) was analyzed by circular dichroism using a Jasco J-810 spectropolarimeter (JASCO Corporation, Tokyo, Japan). To further validate the anti-MOG binding activity of our recombinant MOG, we tested whether this MOG was bound by B cells from mice with a knock-in of the heavy chain of the anti-MOG 8-18C5.³⁷ To this end, we formed MOG tetramers with our biotinylated MOG and fluorescently labeled streptavidin (Jackson ImmunoResearch, West Grove, PA).

Affinity Purification of Anti-MOG Abs

Biotinylated MOG was bound to a HiTrap Streptavidin HP column (GE Healthcare, Munich, Germany). Ig from plasma (obtained from ethylenediaminetetraacetic acid [EDTA]–blood) was first enriched by ammonium sulfate precipitation and then loaded on this column. Bound Ig was eluted (100mM glycine, 150mM NaCl, pH 2.5) and immediately neutralized with 1M Tris-HCl, pH 8.8. The eluates from both patients were separated by reducing and nonreducing sodium dodecyl sulfate gel electrophoresis and stained by Coomassie. The excised gel bands were in-gel digested essentially as described.³⁵ Peptides were analyzed by matrix-assisted laser desorption/ionization time of flight/time of flight using a 4800 Analyzer (Applied Biosystems, Foster City, CA). The eluates were tested by enzyme-linked immunosorbent assay (ELISA) for streptavidin reactivity using streptavidin-coated plates.

Staining of Tissue with Patient Abs

Rat brains were fixed in 4% paraformaldehyde (PFA) for 1 hour, cryoprotected with 40% sucrose, and snap frozen. Seven-micrometer-thick sagittal sections were incubated with 0.3% hydrogen peroxide for 20 minutes and with 10% donkey serum in phosphate-buffered saline (PBS) for 1 hour, and then labeled with the Abs at 4°C overnight. The next day, sections were labeled with a donkey–antihuman IgG (H+L) secondary Ab (Jackson ImmunoResearch) and visualized with an avidin–biotin–diaminobenzidine reaction.

Transfer EAE and Rat T-Cell Lines

Antigen specific T cells were established from Lewis rats immunized with antigen emulsified in complete Freund adjuvant as described previously.³⁸ The following antigens were used: recombinant MOG (amino acid 1–125), MBP purified from guinea pig brain, and ovalbumin (OVA) purchased from Sigma-Aldrich (St Louis, MO). To induce mild EAE, freshly restimulated 15×10^6 MOG-specific T cells or 1.2×10^6 MBP-specific T cells were injected intravenously in Lewis rats. Clinical scores were evaluated as follows: 0 = normal; 0.5 = loss of tail tonus; 1 = tail

paralysis; 2 = gait disturbance; 3 = hindlimb paralysis. Two days after injection of T cells, 100 µg of the indicated Ab preparations was injected intrathecally into the cisterna magna to animals anesthetized by fentanyl/midazolam/medetomidine. For the monitoring of clinical score, animals were followed until full recovery and were then sacrificed. For histopathological analysis, 72 hours after Ab injection, animals were perfused with PBS and 4% PFA in PBS under terminal anesthesia with fentanyl/midazolam/medetomidine; the spinal cord and brain were then postfixed with 4% PFA in PBS at 4°C. The procedures are approved by the government of Upper Bavaria.

Histological Examination of the EAE Rats

Brain, spinal cord, and optic nerves were dissected and embedded in paraffin. Serial sections of all tissues were stained with hematoxylin/eosin, Luxol fast blue (LFB) myelin stain, and Bielschowsky silver impregnation for axons. Immunocytochemistry was performed on paraffin sections after antigen retrieval in a food steamer with EDTA buffer, pH 8.5. Primary Abs against the following targets were used in the following dilutions: CD3 (T cells; rabbit monoclonal; Neomarkers, Fremont, CA; RM-9107-5; 1:2,000), ED1 (phagocytic macrophages and microglia; mouse monoclonal; Serotec, Raleigh, NC; MCA341R, 1:10,000), Iba 1 (pan microglia and macrophages; rabbit polyclonal; Wako, Osaka, Japan; 019-19741; 1:3,000), cyclic nucleotide phosphodiesterase (oligodendrocytes; mouse monoclonal; Sternberger Monoclonals, Lutherville, MD/BioLegend, San Diego, CA; SMI 91; 1:2,000), glial fibrillary acidic protein (astrocytes; rabbit polyclonal; Dako, Santa Clara, CA; Z0334; 1:3,000), human Ig (biotinylated species specific antihuman Ig; donkey polyclonal, Jackson ImmunoResearch, 709-065-149; 1:1,000) and activated complement (C9neo antigen, rabbit polyclonal; 1:2,000).¹¹ Bound primary Abs were visualized with a biotin/avidin/peroxidase system. To quantify the inflammation, CD3⁺ T cells/mm² were counted in a zone of 200 µm spanning from the ventral subpial surface into the tissue of the pons. To quantify demyelination, the distance of subpial demyelination from the ventral surface of the pons was measured. To this end, macrophages were stained with ED1 and the distance from the pial surface on which could be seen classical macrophages with degradation products was measured. This also represents the area of macrophages in LFB staining that contain myelin degradation products.

Results

Anti-MOG Reactivity in Patients with Inflammatory CNS Diseases and Cross-Reactivity to Rodent MOG

We tested sera from 260 patients with different inflammatory CNS diseases; 17 of them had autoantibodies to

MOG (clinical details in the Table). The highest anti-MOG reactivity was seen in patients with relapsing optic neuritis and NMO phenotype. The vast majority of patients with MS do not have Abs to MOG, but Abs to MOG are detected in special cases with MS.³⁴ The 5 patients with MOG Abs included in the Table fulfill the diagnostic criteria of MS, including MS-typical cerebrospinal fluid (CSF) and radiological features, but had a clinical phenotype that overlaps with NMO (severe myelitis, brainstem involvement, and optic neuritis). These patients did not have Abs to NMDAR or AQP4. Details of their clinical picture, their MRI, and their anti-MOG reactivity have been described in a previous paper.³⁴ We determined the cross-reactivity to rodent MOG of these patients. Further analysis of the pathogenic features of Abs to MOG was performed with Patients 7 and 5, who showed a high reactivity toward MOG and cross-reactivity to rodent MOG (Fig 1). Both patients had a recurrent optic neuritis, one of the diseases associated with MOG Abs.^{39,40} These patients were followed for periods of about 26 and 35 months and kept recognizing MOG. Their anti-MOG reactivity was so high that a reactivity could still be detected at serum dilutions of 1:3,000 to 1:10,000. Both patients had anti-MOG of isotype IgG1. Patient 5 had in addition to IgG also persisting IgM to MOG.

The applications of mutant variants of MOG showed that the 2 patients recognized different epitopes on MOG (see Fig 1C, D). The binding to MOG of Patient 5 was reduced by the mutation P42S, indicating that this patient's Abs recognize the CC' loop on MOG; the MOG Abs of IgG and IgM isotype showed similar reactivity to MOG mutants. Patient 7 showed a stronger reactivity to mouse MOG than to human MOG. Such a feature we had previously noted in 12 of 111 patients analyzed.¹⁵ Consistent with the better recognition of mouse MOG, this patient also showed a stronger reactivity to the MOG mutant P42S, in which the serine present in murine MOG replaces the proline of human MOG. Another mutation at the EF loop (H103A, S104E) greatly reduces the MOG binding of this patient. MOG residues important for binding of Abs from Patients 5 and 7 are visualized in Figure 1E.

From Patient 5, we could also analyze CSF and this showed that anti-MOG IgG were present in this compartment, but there was no evidence that the anti-MOG IgG present in the CSF was produced intrathecally; after adjustment to equal IgG concentrations, similar anti-MOG reactivity was seen in CSF and serum (see Fig 1F).

Specificity of Affinity-Purified Abs to MOG

We produced the ECD of human MOG in HEK cells with an AviTag at the C-terminus replacing the transmembranous and intracellular part. Then MOG was enzymatically biotinylated

at the AviTag and bound to a streptavidin column, which puts the extracellular part of MOG on the beads in the same orientation as in the membrane. The confirmation with beta-sheet formation was seen by circular dichroism (Fig 2A). To further validate this MOG preparation, we formed MOG tetramers and tested the binding to B cells from mice with a knock-in of the heavy chain of the anti-MOG mAb 8-18C5 and found that this stained about one-third of the B cells from these mice, which is in line with their published MOG-binding activity (data not shown).³⁷ With this protein, we could affinity purify MOG-specific Abs from both patients (see Fig 2). Starting from > 600ml blood, we eluted from the MOG-column 471 µg of IgG and 55 µg of IgM from Patient 5 and 571 µg IgG but no IgM from Patient 7. Mass spectrometry showed that the eluates from Patient 5 contained IgG, IgM, α-2 macroglobulin, fibrinogen, and albumin, and from Patient 7 IgG and fibrinogen. Importantly, no MOG was detected in the eluates. The eluates did not bind to streptavidin as seen by ELISA using streptavidin-coated plates. We could not obtain Abs that recognize MOG on transfected cells from donors who did not have a strong anti-MOG reactivity in their blood. This excludes that the anti-MOG reactivity we observed in the purified fraction is an artifact due to the purification procedure.

These affinity-purified Abs showed a highly enriched reactivity to human MOG in a cell-based assay; when plasma and affinity-purified Abs were adjusted to the same concentration of 12 µg/ml, we noted the following mean channel fluorescence (MCF) ratios, which were calculated as described above: Patient 5: plasma 14.9, purified 190.3, flow through 8.1; Patient 7: plasma 8.6, purified 207.5, flow through 3.5 (see Fig 2). We noted that in both patients the reactivity to our mutated variants was the same in the anti-MOG Abs from the starting material and the eluates. We also compared the affinity-purified MOG Abs from both patients with the prototype anti-MOG 8-18C5. For this comparison we used a recombinant variant of 8-18C5 with a human Fc-IgG1, so the same detection Ab could be used. Our dose responses show that these purified MOG Abs recognized MOG in a cell-based assay still in the ng/ml range and came quite close to the intensity of MOG binding of the 8-18C5. The isotype of the anti-MOG response of the affinity-purified Abs of both patients was IgG1. We also analyzed the cross-reactivity of the patient-derived MOG Abs to rat MOG, because their pathogenicity will be tested in a rat model (see below). We noted that Patient 7 recognized rat MOG more strongly than human MOG, which is consistent with our observation that this patient also recognizes mouse MOG more strongly than human MOG (see Fig 1D); mouse and rat MOG are very similar although not identical.

The flow through of the column used for affinity purification of MOG Abs from these 2 patients still contained

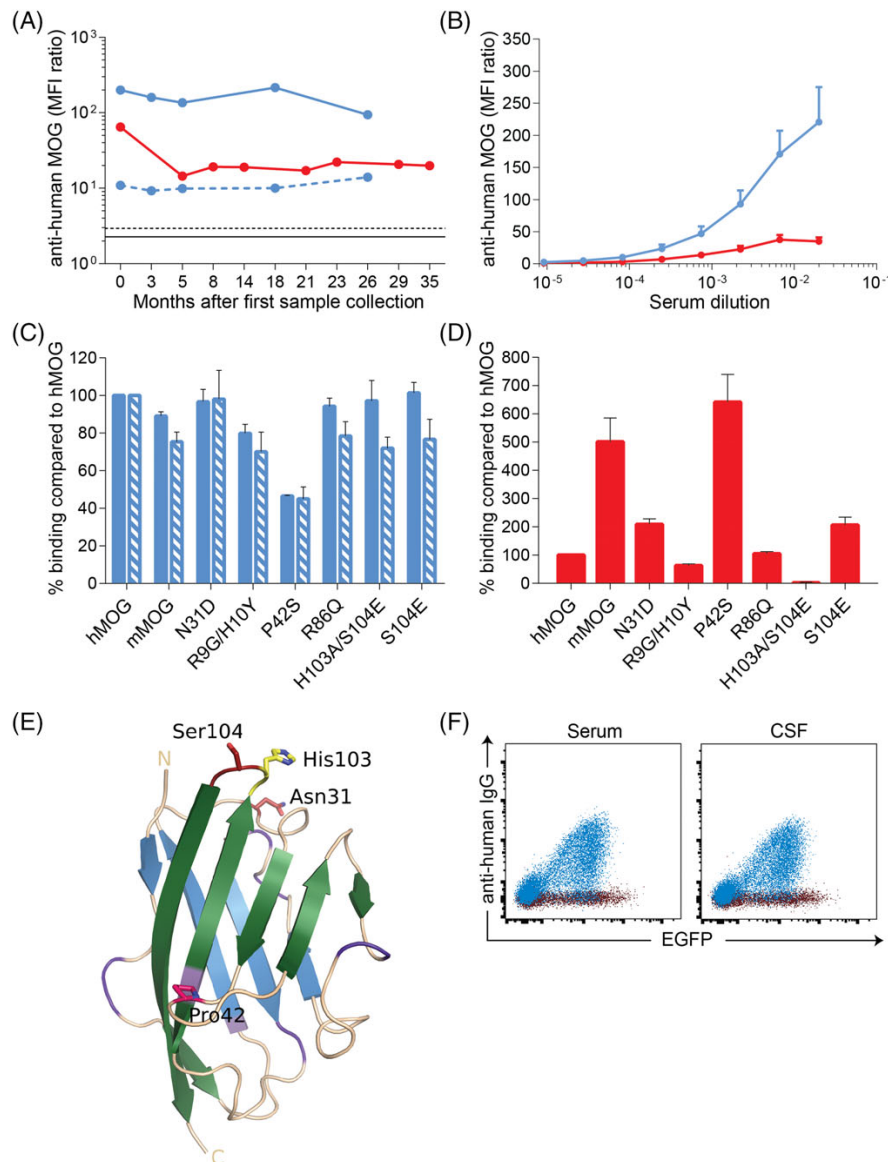


FIGURE 1: Anti-myelin oligodendrocyte glycoprotein (MOG) reactivity in the 2 patients selected for transfer experiments. The anti-MOG reactivity in serum and plasma of Patient 5 (blue) and Patient 7 (red) was determined with transfected cells as described in Patients and Methods. (A) Longitudinal analysis. Solid lines indicate anti-MOG IgG; the dotted bluish line shows persisting anti-MOG IgM in Patient 5. The solid black line shows the cutoff for anti-MOG IgG, the dotted black line the cutoff for anti-MOG IgM. (B) Anti-MOG reactivity in serum dilutions. (C, D) Reactivity to human MOG (hMOG), mouse MOG (mMOG), and the indicated mutations of MOG. The IgG responses are indicated in solid bars, the anti-MOG IgM response from Patient 5 in hatched bars. (E) The structure of the human MOG model¹⁵ is shown as a ribbon representation with residues influencing antibody binding depicted as stick models. In addition, residues that differ between mouse and human MOG are colored pink (Pro 42), light violet (2 conservatively mutated interior 13-strand residues), and violet (remaining nonidentical residues). N and C indicate the N-terminal and C-terminal part of the extracellular domain of MOG. (F) Anti-MOG in cerebrospinal fluid (CSF) of Patient 5. CSF (IgG 0.022g/l) was used undiluted and serum was diluted 1:377 to obtain the same IgG concentration as in the CSF. The calculated mean fluorescence intensity (MFI) ratio (MOG-enhanced green fluorescent protein [EGFP]/EGFP) of the CSF was 72.44, whereas that of the serum sample was 86.34. Control EGFP transfectants are shown in gray, the MOG-EGFP transfectants in blue. Error bars indicate the standard error of the mean of 2 to 3 experiments.

anti-MOG reactivity as seen with MOG transfectants. This was not due to a limited capacity of the column, as it could still bind the mAb 8-18C5. Along this line, from another

patient (Patient 14), we could obtain only a small amount of anti-MOG IgG with this column and the flow through still contained a similar reactivity to MOG as the starting

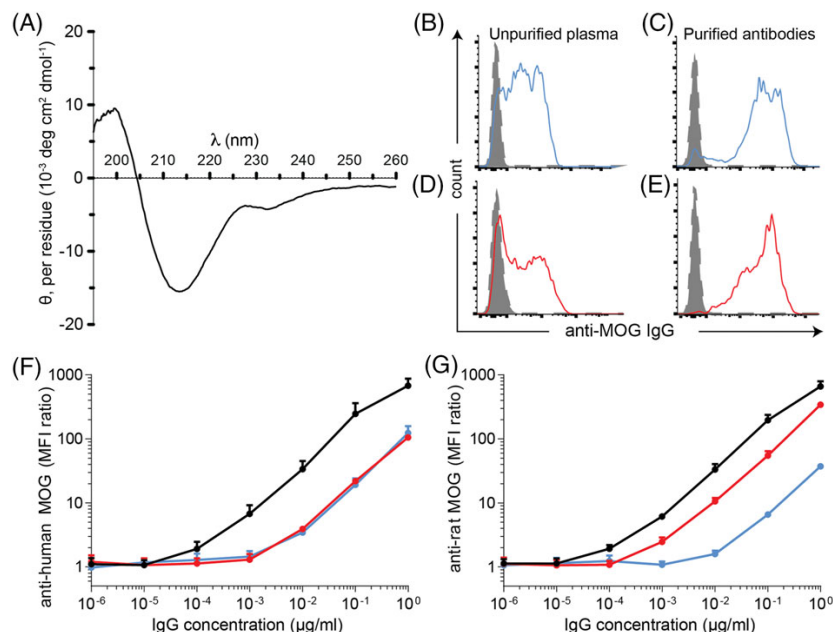


FIGURE 2: Affinity-purified antibodies (Abs) to myelin oligodendrocyte glycoprotein (MOG). (A) Circular dichroism spectrum of MOG (0.2mg/ml). The beta-sheet formation is indicated by the negative band at 213nm. (B–E) Comparative analysis of plasma and affinity-purified MOG Abs to cells transfected with MOG of Patient 5 (blue) and Patient 7 (red). Plasma and purified Abs were used at an IgG concentration of 12 $\mu\text{g/ml}$. Closed graphs indicate the recognition of enhanced green fluorescent protein (EGFP)-transfected cells, open graphs of MOG-EGFP transfectants. (F, G) MOG recognition of the affinity-purified Abs from Patients 5 (blue) and 7 (red) in comparison with the recombinant humanized mAb 8-18C5 (black) on transfected cells. Error bars indicate standard error of the mean of 2 to 3 experiments. MFI = mean fluorescence intensity.

material. Thus, the ECD of human MOG produced in HEK cells binds only a fraction of Abs to MOG.

Staining of Brain Tissue with Affinity-Purified Abs to MOG

The affinity-purified Abs from both patients bound to myelin in tissue sections from the rat; r8-18C5 was used as a positive control (Fig 3). We noted a stronger binding of the Abs from Patient 7 (see Fig 3C, D) than from Patient 5, which is consistent with the dose response of these preparations to rat MOG on the surface of rat transfectants (see Fig 2G). Because the MOG reactivity of these patients was established by using native cells, while the tissue was fixed with PFA, we compared the recognition of live and PFA-fixed cells after MOG transfection. This showed that Patients 5 and 7 recognized MOG also after PFA fixation of the transfected cells, but the background was much higher with fixed cells (data not shown).

Pathogenicity and Histopathological Changes Induced by Patient-Derived Abs to MOG

We analyzed the pathogenic potential of patient-derived MOG-specific Abs in 2 models of T-cell-mediated EAE in the Lewis rat. In both models, we injected the MOG Abs intrathecally 2 days after the injection of either MOG-specific T cells or MBP-specific T cells. Because

the amount of purified Abs from patients was limited, we first established the details of the transfer models with 8-18C5 and the humanized r8-18C5. These experiments showed that EAE can be enhanced, when 8-18C5 or r8-18C5 were injected 2 days later than the T cells. Under these conditions, the peak of disease was reached at day 5; the animals recovered largely until day 10. Therefore, we sacrificed the EAE rats after injection with the patient-derived Abs at day 5.

The MOG-specific T cells alone did not induce a clinical effect in our Lewis rat model. However, when affinity-purified Abs from both Patients 5 and 7 were injected, a clinical disease was induced (Fig 4). As control, we used human ivIg and Ig obtained from a protein G column. This control human Ig did not induce disease, whereas the positive control 8-18C5 enhanced disease. In contrast to the MOG-specific T cells, the MBP-specific T cells induced a clinical disease on their own in the absence of any added Ab, consistent with previous observations with MBP-specific T cells in this rat model.⁴¹ One day after injection of r8-18C5 and the Abs from Patient 7 the clinical disease was enhanced.

All animals shown in Figure 4 were perfused at day 5 and analyzed by histopathology. A quantitative analysis of the T-cell infiltration and of demyelination in all

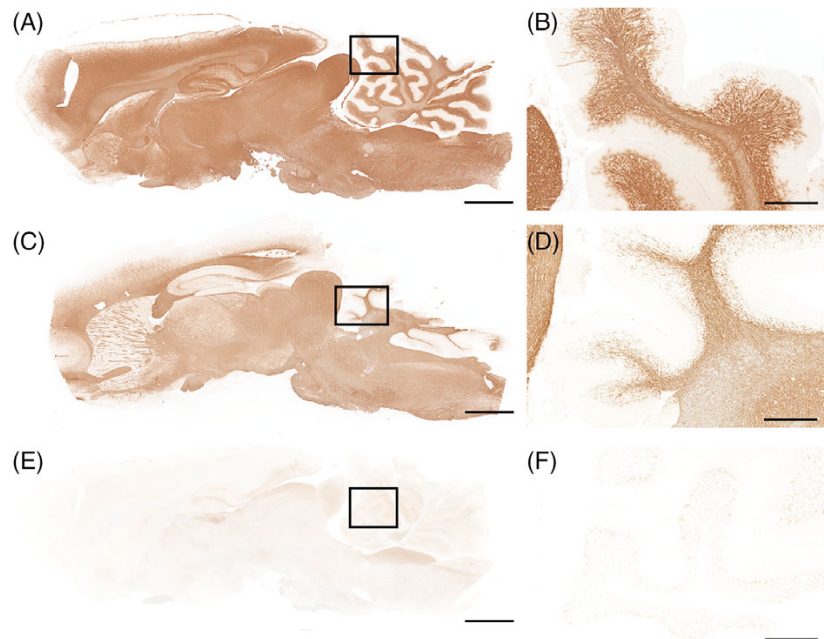


FIGURE 3: Myelin staining of affinity-purified myelin oligodendrocyte glycoprotein (MOG)-specific antibodies (Abs). Samples were stained on sagittal rat brain sections. The humanized r8-18C5 was used as positive control (A) and showed a specific myelin staining throughout the cerebrum and cerebellum (B; rectangle in A enlarged). The affinity-purified MOG-specific Ab from Patient 7 (C, D) showed a strong binding to myelin; a recombinant human IgG that does not bind MOG on transfected cells (r#7_D7) was negative (E, F). All Abs were used at a concentration of 3 μ g/ml. Scale bars = 2mm (A, C, E), 300 μ m (B, D, F).

17 animals revealed the following. The patient-derived MOG-specific Abs massively enhanced the T-cell infiltration in the subpial area of the pons when given together with cognate MOG-specific T cells, but not together with MBP-specific T cells (see Fig 4). Pathological analysis of animals injected with MOG-specific T cells alone or together with control Abs displayed a moderate inflammatory reaction in the spinal cord and less obviously in the brain and optic nerve, consisting of T-cell infiltrates in the meninges and CNS tissue and of ED1⁺ macrophages, being restricted to the meninges (Fig 5, middle panels).

In combination with the injection of the MOG-specific Abs from Patients 5 and 7, a massively enhanced T-cell and macrophage infiltration in the meninges and the subpial CNS tissue was observed, and this was similar to the pathology observed after injection of the 8-18C5 Ab (see Figs 4 and 5). The enormous enhancement of the infiltration of T cells is already visible at a low magnification displaying cross sections of the whole spinal cord (see Fig 5, first and third rows). Human immunoglobulin reactivity was seen on subpial myelin, but only traces of activated complement (C9neo antigen) and a slight perivascular demyelination were present (data not shown).

Following transfer of MBP-specific T cells alone (which induced with the applied cell number a mild EAE

on their own) or in combination with control Abs, a different pathology was seen. It consisted of mild to moderate T-cell infiltration together with the dispersion of ED1⁺ macrophages throughout the tissue (Fig 6). In combination with patient-derived MOG-specific Abs, human Ig was also seen on subpial myelin, but this was associated with complement C9neo activation. This was accompanied by subpial demyelination (see Fig 4D), which was seen by LFB staining and by immunostaining for cyclic nucleotide phosphodiesterase. Demyelination and complement activation were massive with the Abs from Patient 7, less intense but detectable with the Abs from Patient 5, and absent after control Ab injection (see Figs 4D and 6). Due to injection into the cisterna cerebelli magna, the Abs hardly reached the optic nerve.

Thus, in this model, we see an impressive effect of the MOG Abs on the histopathology, but only a slight enhancement of the clinical disease. There are 2 reasons for this. First, the sensitivity to detect an enhanced clinical disease is lower if the control group is already sick (see Fig 4B) as compared to a model in which the control group is not sick at all (see Fig 4A). Second, the clinical score in this EAE model detects only motor functions. We have quantified the amount of lipopolysaccharide (LPS) in the samples used for in vivo experiments and found that the

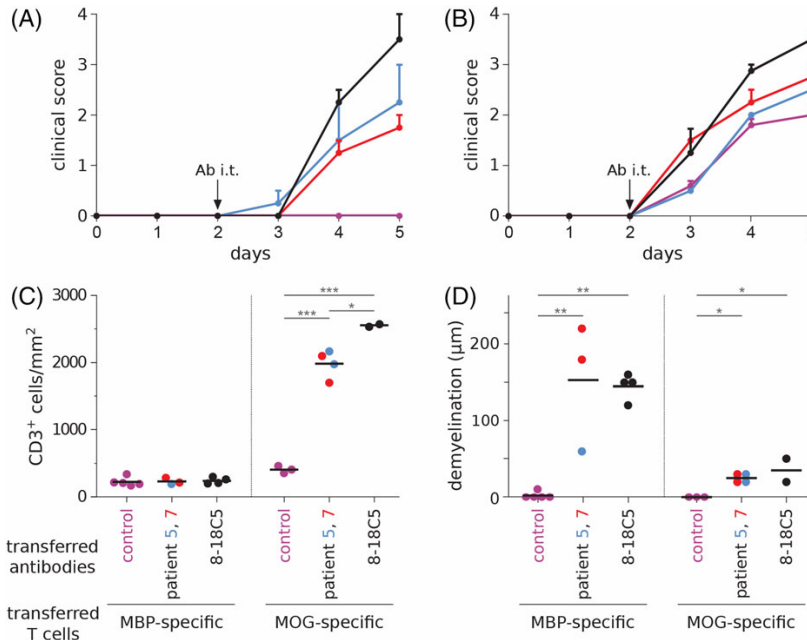


FIGURE 4: Pathogenicity of affinity-purified patient-derived myelin oligodendrocyte glycoprotein (MOG)-specific antibodies (Abs). Lewis rats were injected with MOG-specific (A) or myelin basic protein (MBP)-specific T cells (B). Two days later, 100 µg of affinity-purified MOG-specific Abs from Patient 5 (blue), Patient 7 (red), control IgG (purple), or 8-18C5 (black) were injected intrathecally (i.t.) into the spinal fluid (cisterna magna). (A) Three animals received human control IgG, 2 Abs from Patient 7 and 2 from Patient 5. Because the animals with the control IgG did not show any clinical disease, the induction of the clinical EAE with MOG-specific Abs from patients (data from the patients pooled) reached statistical significance at day 4 ($p < 0.05$) and day 5 ($p = 0.005$) using the unpaired 2-tailed t test. (B) Together with MBP-specific T cells, 1 animal received Abs from Patient 5, 2 animals Abs from Patient 7, 5 control IgG. As positive controls, r8-18C5 (A, B) and 8-18C5 (A) were used. Error bars indicate standard error of the mean. All animals were perfused at the end of the observation period and analyzed for histopathology. (C, D) Quantification of inflammation and demyelination of animals shown in A and B. (C) The T-cell infiltrates in the subpial region at the basis of the pons were counted with a 40 × objective, and the number of CD3⁺ T cells/mm² was calculated. (D) The distance of subpial demyelination at the basis of the pons was measured. (C, D) We performed analysis of variance testing followed by Tukey honest significant difference test. * < 0.05 ; ** < 0.01 ; *** < 0.001 .

contaminating amount of LPS was similar in control Ig and patient preparations; $< 10\text{ng}$ were injected per animal. The same Ig preparations had different effects depending on the antigen specificity of the coinjected T cells; the patient Abs enhanced microglia activation and T-cell infiltration only together with MOG-specific T cells, but not in the context of MBP-specific T cells; a strong activation of terminal complement complex C9neo, conversely, was seen in the context of MBP-specific T cells, but little activation was seen in the context of MOG-specific T cells. We conclude from all this that the effects we describe were induced by the patient-derived Ig and not by LPS.

In this project, we had tested 3 different human Ig control preparations, namely ivIg, human IgG not specific for MOG obtained from a protein G column, and recombinant IgG with human Fc part. None of these human Ig variants recognized MOG, and none of them had any effect on enhancement of the disease. As a further control experiment, we injected OVA-specific T cells in the absence or presence of an intrathecal injection of r8-18C5. In this context, no

induction of clinical disease and no demyelination or complement activation was present (data not shown).

Discussion

Our study shows that Abs to MOG affinity-purified from the blood of patients with inflammatory demyelination are pathogenic in transfer experiments to rodents. We found that these patient-derived MOG-specific Abs mediate damage to the CNS by different mechanisms. In synergy with T cells that induce clinical EAE, associated with profound blood–brain barrier damage and activation of macrophages (MBP-specific T cells in the Lewis rat in our model), human Abs to MOG mediate MS type II–like pathology, characterized by active demyelination (phagocytes containing myelin in the lesion) and local activation of the terminal complement complex, visible as deposition of C9neo.^{32,33} We show here that these features are induced by the patient-derived MOG-specific Abs. This suggests that in patients with MOG Abs and MS type II pathology,^{28–31} MOG Abs are responsible for this part of the pathology.

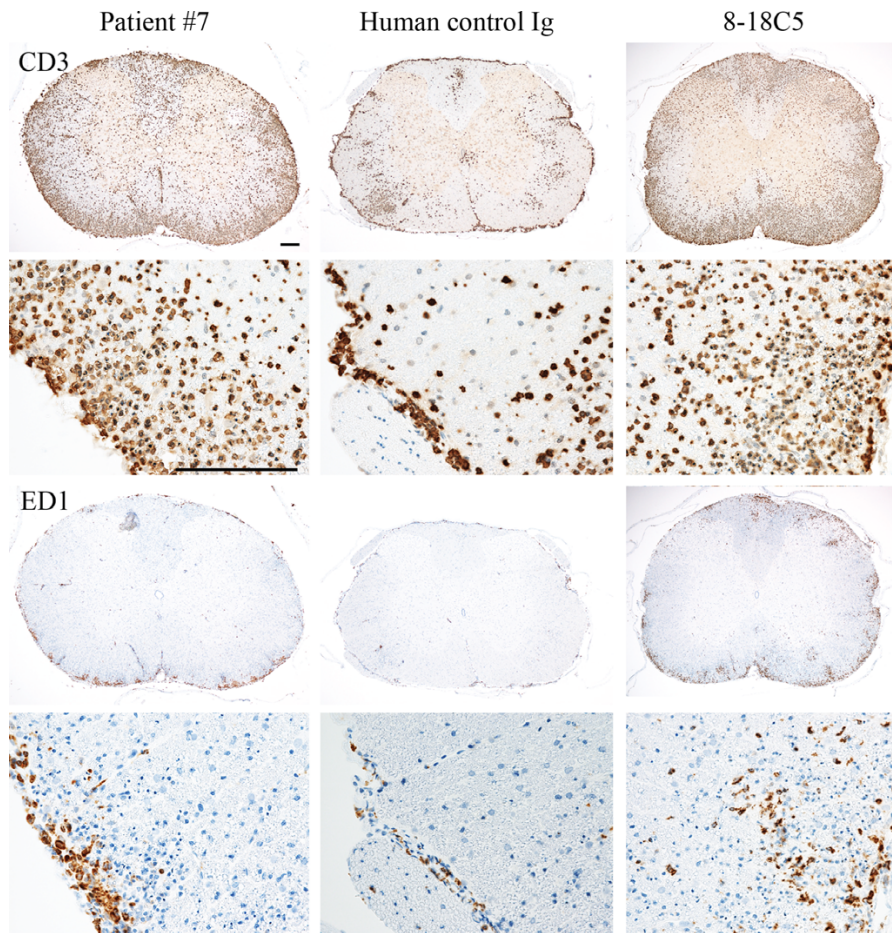


FIGURE 5: Affinity-purified antibodies (Abs) to myelin oligodendrocyte glycoprotein (MOG) enhance T-cell activation and promote microglia activation in the subpial parenchyma together with MOG-specific T cells. Spinal cord pathology is shown following passive cotransfer of MOG-specific T-cells with control IgG or anti-MOG Abs. Experimental autoimmune encephalomyelitis after injection of control Abs is characterized by T-cell infiltration in the meninges and diffusely in the spinal cord parenchyma, but ED1⁺ macrophages are largely restricted to the meningeal space (middle panels). After injection of Patient 7 Ab (left panels) or 8-18C5 (right panels), there is a massive enhancement of subpial T-cell infiltration and ED1⁺ macrophages pass the astrocytic glia limitans and infiltrate the central nervous system parenchyma. Scale bars = 100 μ m.

Remarkably, most patients with MOG Abs and an MS type II pathology described so far do not have a typical MS,⁴² but rather an encephalomyelitis overlapping with MS and NMO spectrum disorder. It is discussed whether this should be grouped as MOG Ab disease. Conversely, most patients with clinical MS and an MS type II pathology do not have Abs to MOG,^{30,34} suggesting that these patients recognize other not yet identified autoantigens.

In our second model, in synergy with cognate MOG-specific T cells, which by themselves do not induce clinical disease, but only mild, predominantly meningeal inflammation in our rat model, the same affinity-purified Ab preparations induced clinical disease with other pathological features, namely a massively enhanced T-cell infiltration. An enhancement of T-cell activation by mAbs to

MOG has been shown in 2 recent studies and suggested to be mediated by opsonization of the antigen.^{20,23} We found that the patient-derived anti-MOG Abs not only enhanced T-cell infiltration induced by MOG-specific T cells, but also stimulated microglia/macrophage infiltration in the subpial gray matter. This indicates that human anti-MOG Abs in the CSF might also participate in the development of gray matter pathology together with MOG-specific T cells. MOG-specific T cells have been observed in patients with demyelination, and their recognized epitopes were identified.⁴³ Further studies are needed to analyze MOG-specific T cells in patients with Abs to MOG.

Our 2 EAE transfer models show that the human Abs to MOG mediate tissue destruction via 2 different

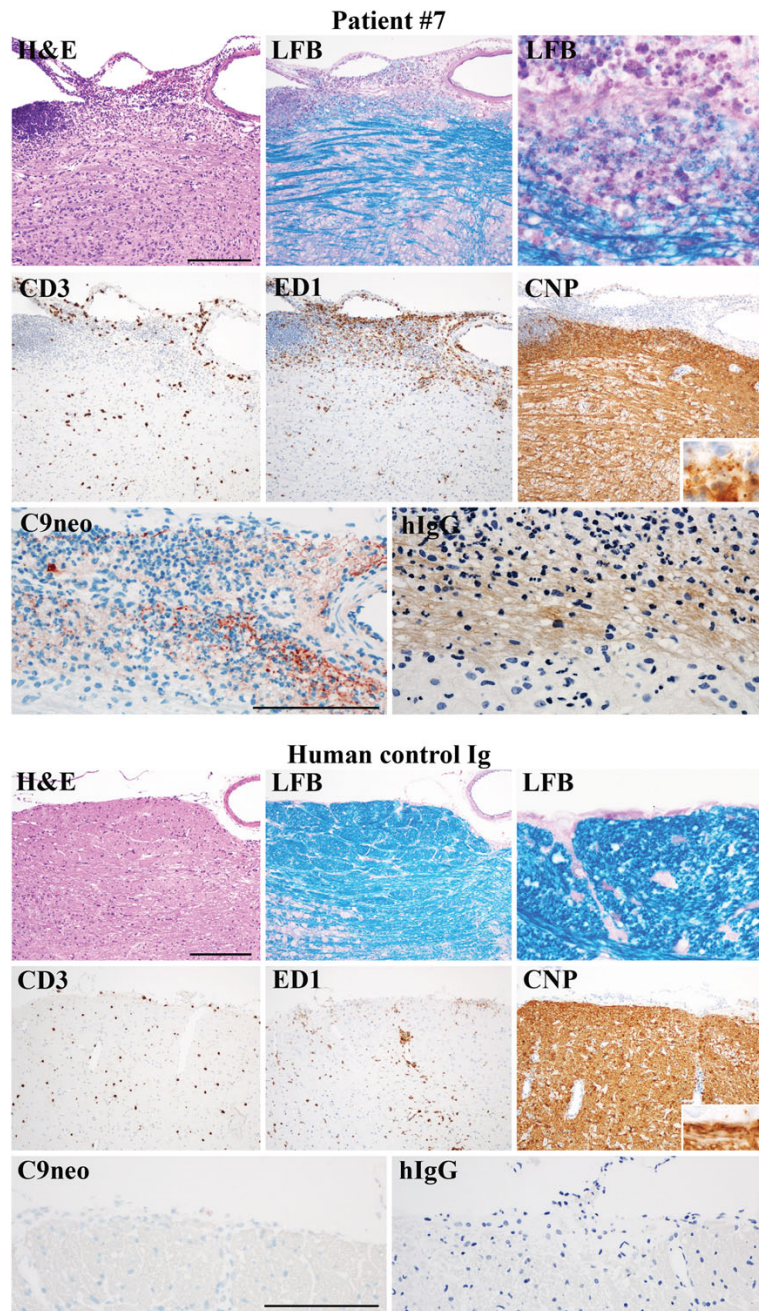


FIGURE 6: Affinity-purified antibodies (Abs) to myelin oligodendrocyte glycoprotein (MOG) induce complement activation and demyelination together with myelin basic protein (MBP)-specific T cells. Experimental autoimmune encephalomyelitis was induced with MBP-specific T cells. After 2 days, either MOG-specific affinity-purified Abs from Patient 7 (upper panels) or human control Ig (lower panels) was injected. When human control Ig was injected, there is a diffuse infiltration of the tissue by CD3⁺ T cells and ED1⁺ macrophages, but there is no deposition of human IgG on myelin or activation of complement (C9neo; lower panels). However, when anti-MOG Ig from Patient 7 was cotransferred, inflammation is massively enhanced and ED1⁺ macrophages are concentrated at sites of active myelin destruction, associated with immunoglobulin deposition on myelin and complement activation (C9neo antigen deposition; lower left of upper panels). Scale bars = 100 μ m. CNP, cyclic nucleotide phosphodiesterase; H&E = hematoxylin and eosin; LFB = Luxol fast blue.

TABLE 1. Features of Patients with Anti-MOG Reactivity

ID	Current Diagnosis	Gender	Age at First MOG ⁺ Sample, yr	Reactivity to Human MOG, MFI Ratio	Reactivity to Mouse MOG, MFI Ratio
5	Relapsing bilateral ON	F	42	220.7	212.9
14	Relapsing bilateral ON	M	54	44.9	20.6
8	NMOSD	M	37	38.3	3.0
7	Relapsing unilateral ON	M	46	34.7	216.8
16	NMOSD	M	30	18.6	5.6
17	Relapsing bilateral ON	F	31	18.2	2.1
6	Monophasic encephalitis	F	31	17.7	2.3
10	RRMS	F	37	11.9	8.3
13	Relapsing encephalomyelitis	M	34	8.6	5.5
1	NMOSD	M	40	6.1	1.7
3	Relapsing encephalomyelitis	M	26	5.4	1.8
4	RRMS	F	55	4.6	7.1
11	RRMS	F	50	4.1	1.5
2	Relapsing encephalomyelitis	F	66	4.0	0.9
9	RRMS	M	32	3.9	3.1
12	RRMS	F	23	2.9	3.9
21	NMOSD	F	33	2.7	1.8

Details about Patients 4, 9, 10, 11, and 12 are reported in Spadaro et al.³⁴ and about Patient 2 in Spadaro et al.²⁸ Patients with MOG antibodies might constitute a condition called MOG antibody disease. The cutoff for recognition of human MOG was 2.27 (mean + 3 standard deviation of controls). The MFI ratio was calculated as the mean of 2 to 5 experiments.
F = female; M = male; MFI = mean fluorescence intensity; MOG = myelin oligodendrocyte glycoprotein; NMOSD = neuromyelitis optica spectrum disorders; ON = optic neuritis; RRMS = relapsing–remitting multiple sclerosis.

mechanisms. This could be revealed because in our models the 2 different T-cell lines showed different intensities of T-cell reactivation in the CNS.^{41,44} In the model with MBP-specific T cells, strong T-cell activation in the CNS was associated with blood–brain barrier disruption and the diffuse infiltration of the CNS tissue by recruited ED1⁺ macrophages. Therefore, the incoming Abs find a good environment to mediate demyelination via Ab-dependent cell-mediated cytotoxicity and complement activation, which results in a pathology similar to MS type II. In the model with MOG-specific T cells, T-cell activation in the CNS is not optimal and recruitment of ED1⁺ macrophages is sparse and largely restricted to the meninges. Here, the entering MOG-specific Abs massively enhance the T-cell recruitment and activation, because they recognize the same antigen; this then promotes infiltration of ED1⁺ macrophages, which is associated with clinical disease but may be too low to effectively induce

demyelination. Our observation that the patient-derived Abs perform tissue destruction by 2 different mechanisms, demyelination and enhanced inflammation, is consistent with a previous study transferring sera from immunized nonhuman primates.⁴⁵

Our EAE experiments indicate further that the anti-MOG Abs are not pathogenic on their own, as together with irrelevant T cells no pathology was induced. This is consistent with previous observations in other EAE models³⁷ or after intrathecal injection of the 8-18C5 Ab⁴⁶ and supports the concept that the anti-MOG Abs perform a second hit to enhance pathology. Thus, human MOG Abs are pathogenic, but the precise pathological effects depend on their interactions with T cells; the human anti-MOG Abs can mediate MS type II pathology and gray matter injury upon transfer.

Experiences with mAbs in animals have shown that recognition of conformational MOG is required for

pathogenicity.^{12,14} The secondary structure of MOG is characterized by 2 antiparallel beta-sheets that form an immunoglobulinlike beta-sandwich fold.⁴⁷ In rodents, pathogenic MOG-specific Abs mainly recognize the FG loop of MOG as the prototype mAb 8-18C5.¹⁴ Although the epitope specificity of human anti-MOG Abs was previously dissected by ELISA⁴⁸ and transfection of mutated variants of MOG,¹⁵ epitope specificity of pathogenic Abs from patients was unknown. The pathogenic MOG-specific autoantibodies from the 2 patients recognize different epitopes, and both are different from the one recognized by 8-18C5. Patient 5 recognized the CC' loop, as its binding was reduced by the mutation P42S; this is the most frequently recognized part of human MOG.¹⁵ This patient nevertheless strongly recognized mouse MOG, although the mouse MOG contains P42S. These 2 characteristics of MOG recognition (reduced reactivity to P42S, but strong recognition of mouse MOG) we had observed before in 5 of 111 patients.¹⁵ Patient 7 recognized the FG loop of MOG, as its binding was completely abrogated by the mutation H103A+S104E. This resembles the recognition of 8-18C5, which is also abrogated by the double mutation H103A+S104E. A closer look at the reactivity of Patient 7 to other mutants of MOG points to epitopes that are discontinuous like the one recognized by the mAb 8-18C5,⁴⁷ but that differ from the 8-18C5 epitope as they are influenced by P42 positioned in the CC' loop and/or the glycosylation site at N31 in addition to binding to the FG loop. The observed binding pattern of Patient 7 would therefore be consistent with the recognition of an ensemble of epitopes that include the FG loop and are located at the top, membrane-distal part and/or at the 5-stranded front β -sheet of MOG (see Fig 1E).

Together, this part of our analysis shows that pathogenic MOG Abs from patients recognize different loops on MOG.

The anti-MOG response of the patients with recurrent optic neuritis persisted for the observation periods of 26 and 35 months. This extends our knowledge of kinetic of MOG Abs. In children with ADEM, the Abs to MOG appeared only transiently and were rapidly lost, whereas in children with MS the MOG Abs persisted for years.⁴⁹ One of our analyzed patients had the unusual feature of having both an anti-MOG IgG and an anti-MOG IgM response. Both reactivities were directed against the same epitope of MOG. The co-occurrence of anti-IgG and anti-IgM to MOG is rare but was noted in a previous study in 3 of 19 children with ADEM and Abs to MOG.¹⁷ The long-term persistence of an anti-MOG IgM response might be surprising, but it is consistent with recently described human IgM memory B cells that have passed the germinal center.⁵⁰ Our study shows that rarely an IgM response to MOG may also persist.

Our study has the following limitations. First, we injected the patient-derived Abs intrathecally, not systemically, although MOG Abs are typically detected in the blood. In pilot experiments with mAbs, we noted that EAE can be enhanced both by peripheral and by intrathecal injection, but that higher amounts of Abs were needed when the Abs were injected systemically. Because the amount of patient-derived Abs was limited, we chose intrathecal injection. We feel this is justified, as we found MOG Abs also in the CSF. From Patient 5, we could analyze CSF and found strong anti-MOG reactivity without evidence for intrathecal production of Abs to MOG. Second, we analyzed the pathology only at 1 time point after injection because we could inject only a limited number of animals with precious patient-derived Ig material. Compared to recombinant Abs, however, patient-derived Abs more closely reflect the human *in vivo* situation. This is important when evaluating the pathogenic potential of the MOG Abs present in the blood of patients, as the effector function of IgG is regulated by its glycosylation⁵¹ and there is evidence that IgG glycosylation is altered in MS patients.⁵² Third, we show that human MOG Abs identified in a cell-based assay include pathogenic Abs, but it remains unclear whether all of the MOG Abs are pathogenic and which features of the human Abs would allow predicting their pathogenicity. Our approach displaying the correctly folded extracellular part of MOG on a column purified only a proportion of MOG Abs. To affinity-purify and subsequently test the pathogenic activity of the other MOG Abs, MOG might have to be displayed in a membrane-bound environment. Our observation that the extracellular part of MOG purifies only part of the MOG Abs is consistent with the previous observation that in a cell-based assay a short construct of MOG lacking the intracellular part is less sensitive to detect anti-MOG Abs than full-length MOG.⁵³ Possible reasons for the differential reactivity to the 2 MOG variants with the same ECD include oligomerization or yet unidentified effects of the intracellular part of MOG on the conformation of the extracellular part. Furthermore, human MOG Abs are heterogeneous with respect to cross-reactivity to rodents. To address the pathogenicity of MOG Abs not cross-reactive with rodent MOG, mice with a knock-in of human MOG or even transfers to nonhuman primates might have to be used.

Together, we show here that Abs to MOG, which were affinity purified from the blood of patients and recognize different epitopes on MOG, synergize with T cells in transfer experiments to rodents; they induce MS type II pathology and trigger T-cell infiltration with microglia/macrophage activation in the subpial parenchyma. We conclude that MOG Abs contribute to the pathology of

patients with inflammatory demyelinating diseases by these mechanisms.

Acknowledgment

This work was supported by the German Research Foundation (SFB TR128, KA2651/2-1, KA2651/3-1), the Munich Cluster for Systems Neurology (ExC 1010 SyNergy), the Clinical Competence Network for Multiple Sclerosis, the Nonprofit Hertie Foundation, the Novartis Foundation for Therapeutic Research, the European Union's Horizon 2020 Research and Innovation Program (No. 668036, "RELENT"). Responsibility for the information and views set out in this article lies entirely with the authors, the Werner Reichenberger Foundation, and the Verein Therapieforschung für Multiple Sklerose-Kranke.

We thank H. Rübsamen, V. Pichler, and R. Mentele for expert technical assistance and Drs S. Liebscher and J. Havla for comments on the manuscript. Part of the Flow Cytometry analysis was supported by Dr. L. Richter, Core Facility Flow Cytometry at the Biomedical Center, Ludwig-Maximilians-Universität München.

Author Contributions

M.S., S.W., E.B., C.M., R.Hö., R.G., M.M., F.K., H.L., and N.K. conducted experiments, and acquired and analyzed data. E.S., F.S.T., L.-A.G., S.L., G.K., D.J., S.B., K.D., M.K., R.Hö., T.K., S.W., and C.B. analyzed data and contributed to manuscript preparation. M.S., H.L., T.K., R.Hö., N.K., and E.M. designed the study and wrote the manuscript.

Potential Conflicts of Interest

Nothing to report.

References

- O'Connor KC, Chitnis T, Griffin DE, et al. Myelin basic protein-reactive autoantibodies in the serum and cerebrospinal fluid of multiple sclerosis patients are characterized by low-affinity interactions. *J Neuroimmunol* 2003;136:140–148.
- Sinmaz N, Nguyen T, Tea F, et al. Mapping autoantigen epitopes: molecular insights into autoantibody-associated disorders of the nervous system. *J Neuroinflammation* 2016;13:219.
- Ramanathan S, Dale RC, Brilot F. Anti-MOG antibody: the history, clinical phenotype, and pathogenicity of a serum biomarker for demyelination. *Autoimmun Rev* 2016;15:307–324.
- Peschl P, Bradl M, Hofberger R, et al. Myelin oligodendrocyte glycoprotein: deciphering a target in inflammatory demyelinating diseases. *Front Immunol* 2017;8:529.
- Hohlfeld R, Dormair K, Meinl E, Wekerle H. The search for the target antigens of multiple sclerosis, part 2: CD8 + T cells, B cells, and antibodies in the focus of reverse-translational research. *Lancet Neurol* 2016;15:317–331.
- Reindl M, Di Pauli F, Rostasy K, Berger T. The spectrum of MOG autoantibody-associated demyelinating diseases. *Nat Rev Neurol* 2013;9:455–461.
- Jarius S, Ruprecht K, Kleiter I, et al. MOG-IgG in NMO and related disorders: a multicenter study of 50 patients. Part 2: Epidemiology, clinical presentation, radiological and laboratory features, treatment responses, and long-term outcome. *J Neuroinflammation* 2016;13:280.
- Jurynczyk M, Gerales R, Probert F, et al. Distinct brain imaging characteristics of autoantibody-mediated CNS conditions and multiple sclerosis. *Brain* 2017;140:617–627.
- Zamvil SS, Slavin AJ. Does MOG Ig-positive AQP4-seronegative opticospinal inflammatory disease justify a diagnosis of NMO spectrum disorder? *Neurol Neuroimmunol Neuroinflamm* 2015;2:e62.
- Mayer MC, Meinl E. Glycoproteins as targets of autoantibodies in CNS inflammation: MOG and more. *Ther Adv Neurol Disord* 2012;5:147–159.
- Piddlesden SJ, Lassmann H, Zimprich F, et al. The demyelinating potential of antibodies to myelin oligodendrocyte glycoprotein is related to their ability to fix complement. *Am J Pathol* 1993;143:555–564.
- Brehm U, Piddlesden SJ, Gardinier MV, Linington C. Epitope specificity of demyelinating monoclonal autoantibodies directed against the human myelin oligodendrocyte glycoprotein (MOG). *J Neuroimmunol* 1999;97:9–15.
- von Budingen HC, Hauser SL, Fuhrmann A, et al. Molecular characterization of antibody specificities against myelin/oligodendrocyte glycoprotein in autoimmune demyelination. *Proc Natl Acad Sci U S A* 2002;99:8207–8212.
- Breithaupt C, Schafer B, Pellkofer H, et al. Demyelinating myelin oligodendrocyte glycoprotein-specific autoantibody response is focused on one dominant conformational epitope region in rodents. *J Immunol* 2008;181:1255–1263.
- Mayer MC, Breithaupt C, Reindl M, et al. Distinction and temporal stability of conformational epitopes on myelin oligodendrocyte glycoprotein recognized by patients with different inflammatory central nervous system diseases. *J Immunol* 2013;191:3594–3604.
- Mader S, Gredler V, Schanda K, et al. Complement activating antibodies to myelin oligodendrocyte glycoprotein in neuromyelitis optica and related disorders. *J Neuroinflammation* 2011;8:184.
- Brilot F, Dale RC, Selter RC, et al. Antibodies to native myelin oligodendrocyte glycoprotein in children with inflammatory demyelinating central nervous system disease. *Ann Neurol* 2009;66:833–842.
- Dale RC, Tantsis EM, Merheb V, et al. Antibodies to MOG have a demyelination phenotype and affect oligodendrocyte cytoskeleton. *Neurol Neuroimmunol Neuroinflamm* 2014;1:e12.
- Peschl P, Schanda K, Zeka B, et al. Human antibodies against the myelin oligodendrocyte glycoprotein can cause complement-dependent demyelination. *J Neuroinflammation* 2017;14:208.
- Kinzel S, Lehmann-Horn K, Torke S, et al. Myelin-reactive antibodies initiate T cell-mediated CNS autoimmune disease by opsonization of endogenous antigen. *Acta Neuropathol* 2016;132:43–58.
- Zhou D, Srivastava R, Nessler S, et al. Identification of a pathogenic antibody response to native myelin oligodendrocyte glycoprotein in multiple sclerosis. *Proc Natl Acad Sci U S A* 2006;103:19057–19062.
- Saadoun S, Waters P, Owens GP, et al. Neuromyelitis optica MOG-IgG causes reversible lesions in mouse brain. *Acta Neuropathol Commun* 2014;2:35.
- Flach AC, Litke T, Strauss J, et al. Autoantibody-boosted T-cell reactivation in the target organ triggers manifestation of autoimmune CNS disease. *Proc Natl Acad Sci U S A* 2016;113:3323–3328.
- Khare P, Challa DK, Devanaboyina SC, et al. Myelin oligodendrocyte glycoprotein-specific antibodies from multiple sclerosis patients

- exacerbate disease in a humanized mouse model. *J Autoimmun* 2018;86:104–115.
25. Pitttock SJ, Lennon VA, de Seze J, et al. Neuromyelitis optica and non organ-specific autoimmunity. *Arch Neurol* 2008;65:78–83.
 26. Titulaer MJ, Höftberger R, Iizuka T, et al. Overlapping demyelinating syndromes and anti-N-methyl-D-aspartate receptor encephalitis. *Ann Neurol* 2014;75:411–428.
 27. Shimizu F, Schaller KL, Owens GP, et al. Glucose-regulated protein 78 autoantibody associates with blood-brain barrier disruption in neuromyelitis optica. *Sci Transl Med* 2017;9(397).
 28. Spadaro M, Gerdes LA, Mayer MC, et al. Histopathology and clinical course of MOG-antibody associated encephalomyelitis. *Ann Clin Transl Neurol* 2015;2:295–301.
 29. Di Pauli F, Höftberger R, Reindl M, et al. Fulminant demyelinating encephalomyelitis: Insights from antibody studies and neuropathology. *Neurol Neuroimmunol Neuroinflamm* 2015;2:e175.
 30. Jarius S, Metz I, König FB, et al. Screening for MOG-IgG and 27 other anti-gliar and anti-neuronal autoantibodies in 'pattern II multiple sclerosis' and brain biopsy findings in a MOG-IgG-positive case. *Mult Scler* 2016;22:1541–1549.
 31. Kortvelyessy P, Breu M, Pawlitzki M, et al. ADEM-like presentation, anti-MOG antibodies, and MS pathology: TWO case reports. *Neurol Neuroimmunol Neuroinflamm* 2017;4:e335.
 32. Lucchinetti C, Brück W, Parisi J, et al. Heterogeneity of multiple sclerosis lesions: implications for the pathogenesis of demyelination. *Ann Neurol* 2000;47:707–717.
 33. Kuhlmann T, Ludwin S, Prat A, et al. An updated histological classification system for multiple sclerosis lesions. *Acta Neuropathol* 2017;133:13–24.
 34. Spadaro M, Gerdes LA, Krumbholz M, et al. Autoantibodies to MOG in a distinct subgroup of adult multiple sclerosis. *Neurol Neuroimmunol Neuroinflamm* 2016;3:e257.
 35. Brändle SM, Obermeier B, Senel M, et al. Distinct oligoclonal band antibodies in multiple sclerosis recognize ubiquitous self-proteins. *Proc Natl Acad Sci U S A* 2016;113:7864–7869.
 36. Perera NC, Wiesmuller KH, Larsen MT, et al. NSP4 is stored in azurophil granules and released by activated neutrophils as active endoprotease with restricted specificity. *J Immunol* 2013;191:2700–2707.
 37. Litzenburger T, Fässler R, Bauer J, et al. B lymphocytes producing demyelinating autoantibodies: development and function in gene-targeted transgenic mice. *J Exp Med* 1998;188:169–180.
 38. Flügel A, Willem M, Berkowicz T, Wekerle H. Gene transfer into CD4 + T lymphocytes: green fluorescent protein-engineered, encephalitogenic T cells illuminate brain autoimmune responses. *Nat Med* 1999;5:843–847.
 39. Ramanathan S, Reddel SW, Henderson A, et al. Antibodies to myelin oligodendrocyte glycoprotein in bilateral and recurrent optic neuritis. *Neurol Neuroimmunol Neuroinflamm* 2014;1:e40.
 40. Chang T, Waters P, Woodhall M, Vincent A. Recurrent optic neuritis associated with MOG antibody seropositivity. *Neurologist* 2017;22:101–102.
 41. Kawakami N, Lassmann S, Li Z, et al. The activation status of neuroantigen-specific T cells in the target organ determines the clinical outcome of autoimmune encephalomyelitis. *J Exp Med* 2004;199:185–197.
 42. Reich DS, Lucchinetti CF, Calabresi PA. Multiple sclerosis. *N Engl J Med* 2018;378:169–180.
 43. Varrin-Doyer M, Shetty A, Spencer CM, et al. MOG transmembrane and cytoplasmic domains contain highly stimulatory T-cell epitopes in MS. *Neurol Neuroimmunol Neuroinflamm* 2014;1:e20.
 44. Berger T, Weerth S, Kojima K, et al. Experimental autoimmune encephalomyelitis: the antigen specificity of T lymphocytes determines the topography of lesions in the central and peripheral nervous system. *Lab Invest* 1997;76:355–364.
 45. von Budingen HC, Hauser SL, Ouallet JC, et al. Frontline: epitope recognition on the myelin/oligodendrocyte glycoprotein differentially influences disease phenotype and antibody effector functions in autoimmune demyelination. *Eur J Immunol* 2004;34:2072–2083.
 46. Vass K, Heining K, Schafer B, et al. Interferon-gamma potentiates antibody-mediated demyelination in vivo. *Ann Neurol* 1992;32:198–206.
 47. Breithaupt C, Schubart A, Zander H, et al. Structural insights into the antigenicity of myelin oligodendrocyte glycoprotein. *Proc Natl Acad Sci U S A* 2003;100:9446–9451.
 48. Menge T, Lalive PH, von Budingen HC, Genain CP. Conformational epitopes of myelin oligodendrocyte glycoprotein are targets of potentially pathogenic antibody responses in multiple sclerosis. *J Neuroinflamm* 2011;8:161.
 49. Pröbstel AK, Dornmair K, Bittner R, et al. Antibodies to MOG are transient in childhood acute disseminated encephalomyelitis. *Neurology* 2011;77:580–588.
 50. Weisel F, Shlomchik M. Memory B cells of mice and humans. *Annu Rev Immunol* 2017;35:255–284.
 51. Seeling M, Bruckner C, Nimmerjahn F. Differential antibody glycosylation in autoimmunity: sweet biomarker or modulator of disease activity? *Nat Rev Rheumatol* 2017;13:621–630.
 52. Wuhrer M, Selman MH, McDonnell LA, et al. Pro-inflammatory pattern of IgG1 Fc glycosylation in multiple sclerosis cerebrospinal fluid. *J Neuroinflammation* 2015;12:235.
 53. Waters P, Woodhall M, O'Connor KC, et al. MOG cell-based assay detects non-MS patients with inflammatory neurologic disease. *Neurol Neuroimmunol Neuroinflamm* 2015;2:e89.

4 DISCUSSION

4.1 Details of antigen recognition of MOG-Abs

With this thesis, we further characterized the binding of MOG antibodies present in serum of MOGAD patients to the target protein MOG.

Firstly, with my contribution to (Marti Fernandez *et al.*, 2019) I illustrated that mutations in the glycosylation site of MOG highlighted the heterogeneity of MOG antibodies, since several patterns of antibody recognition were detected. The Asn31 was substituted with aspartate (negatively charged), or with alanine (neutrally charged). We observed that all the patients' antibodies recognized the protein backbone lacking the glycosylation; secondly, 20% of the patients of the cohort used in the study had lower binding to the protein when the glycosylation was in place, an effect probably due to steric hindrance.

Secondly, we report that the intracellular portion of MOG, in particular the second hydrophobic domain is essential for the recognition of the extracellular domain. The external domain has been used to detect MOG antibodies with ELISA assay, however, several studies together with ours showed that this method does not have a good diagnostic value, even though, the external portion of MOG contains all the epitopes detected by the human antibodies (Mayer *et al.*, 2013).

Therefore, we tried to explain what is required for MOG antibodies derived from patients in order to bind to the MOG protein and to be detected. We firstly designed a MOG variant, called ED-MOG, which comprehended the external domain, the first hydrophobic domain and few amino acids of the cytosolic internal part. We then compared the reactivity of the sera of 14 MOG+ patients, of one MOG- serum (#C) and the humanized recombinant 8-18C5 towards the FL-MOG and ED-MOG in the CBA. Intriguingly, we found that ED-MOG has a slightly higher expression than FL-MOG; however, of the 14 MOG+ patients, only five could be detected by ED-MOG. All the 14 sera bound preferentially to FL-MOG compared to ED-MOG. The obtained result showed that even when the external domain of MOG is displayed on the cell surface, it is still not capable to properly detect MOG autoantibodies, similarly

to the outcome of the ELISA assay. Furthermore, our CBA results are also in line with previous work from Waters and colleagues. They showed already in 2015 that ED-MOG in cells was not capable to perform as well as FL-MOG. However, no further investigation or explanation of this observation was given (Waters *et al.*, 2015).

Subsequently, with the design of two other truncated variants of MOG, we could prove that the intracellular part of MOG, in particular the second hydrophobic domain, is essential for binding of the MOG-Abs from patients. The variant MOG-Cyt behaved similarly as ED-MOG, it could also detect only five of the 14 MOG+ sera (the same also detected by ED-MOG). Instead, MOG-2TMD, a longer variant, which includes in its structure the second hydrophobic domain and lacks the C-terminus, completely restored the antibody binding. Likewise, FL-MOG, all the MOG+ sera bound to MOG-2TMD.

We demonstrated that this different recognition of FL-MOG, MOG-2TMD and ED-MOG was not due to the incapacity of the selected sera to bind to the pivotal epitopes in the external region of the protein. From the 14 patients we investigated 12 patients' antibodies detected different epitopes on MOG, meaning, that most likely the presence of the second hydrophobic domain induces a change in the structure that facilitates the antibody binding. We also showed that the C-terminus of MOG is intracellular and thus cannot be recognized in living cells by MOG-Abs. With an antibody that targets the last 12 amino acids of the MOG protein, it was possible to see that the antibody was only able to detect the C-terminus when the cells displaying the protein were permeabilized. Importantly, the second hydrophobic domain is monotopic, meaning that it is inserted only in one side of the membrane. This monotopic localization is due to two prolines in the hydrophobic domain; proline is known as helix breaker and induces a kink (von Heijne, 1991; Nilsson *et al.*, 1998). Furthermore, another indication for the intracellular localization of the C terminus comes also from the amino acids at the end of the second hydrophobic domain. There are two arginines, which are positively charged amino acids, therefore more likely to bind to the negatively charged lipids facing the intracellular side of the cell (Figure 2). These amino acids

explain the monotopic localization of the second hydrophobic domain and they are conserved from opossum to human (Suppl. Fig. 9 of (Macrini *et al.*, 2021) shown in 3.1). The presence of two hydrophobic domains and the fact that one of the two is monotopic and characterized by two prolines kinks make MOG similar in the display to another protein, PEN-2, which is one of the subunits of γ -secretase, a protease connected to the Notch signaling pathway (Zhang *et al.*, 2015).

We further analysed whether the restored binding observed with MOG-2TMD was due to a specific sequence of MOG or due to the overall MOG structure. Therefore, we used a MOG protein deriving from opossum to test the same sera. The decision to use the opossum is connected to the fact that even though myelin is present in all vertebrates, MOG is only present in mammals. In particular, the opossum was the most distant animal from which we could get a MOG protein sequence from the NCBI database. The opossum MOG (including the signal peptide) has just 77% of identity to the human MOG. Whereas, mouse MOG, for example, has 89% of identity (see Suppl. Fig. 9 of the publication in 3.1). As expected, the opossum MOG bound the antibodies in the sera used for the other MOG variants weakly or not at all. This was predictable, since many patients do not present cross-reactivity even to rodent MOG, due to the different amino acids at the level of known important epitopes (Mayer *et al.*, 2013; Spadaro *et al.*, 2018). However, when we used a chimeric MOG construct (human MOG until glycine 155 plus opossum MOG until the whole second hydrophobic domain), all the MOG+ sera were again capable to detect it. This was the final proof, which clearly indicated that the second hydrophobic domain induces a change in the structure of MOG that facilitates the binding of the autoantibodies, and this improvement in the detection is not connected to a better exposure of defined essential epitopes. Since, as previously mentioned sera included in this study recognize different epitopes on the extracellular part. Therefore, for all future diagnostic tests the presence of the second hydrophobic domain is essential when using MOG-transfected cells.

There is a consensus that indicates the CBA on live cells as the only reliable method for MOG antibodies detection. The results we described above

explain why a CBA is needed. Furthermore, proper antigen conformation seems to be a pivotal matter concerning MOG antibody detection. In fact, it is also the reason why a CBA with fixed cells is not a successful MOG-Abs detection method (Tea *et al.*, 2019). It is known that formaldehyde distorts β -sheet strands and rigidifies the protein structure. Besides, the extracellular portion of MOG contains lysines, which are major sites for crosslinking (Sutherland *et al.*, 2008; Toews *et al.*, 2010). This, together with the subsequent distortion of the β -sheet and the loss of flexibility could have a huge impact on the antigen antibody interaction. Alternatively, another effect of the formaldehyde could be a major exposure of other portions of the protein, which are usually not essential in the binding (Tea *et al.*, 2019; Reindl *et al.*, 2020). A study conducted by different laboratories in parallel proved that the use of a CBA with fixed cells makes the method less reproducible and lastly, it tends to miss around 15% of MOG IgG positive patients (Reindl *et al.*, 2020).

In our study, we also performed two different variants of MOG ELISA, we used the external domain of MOG (MOG-1-125), correctly folded, confirmed by circular dichroism spectroscopy (Spadaro *et al.*, 2018). In the first variant, MOG-1-125 was randomly bound to a MaxiSorp plate. Similarly to the results shown by Tea and colleagues, this type of ELISA was capable to detect only four of the 18 MOG positive patients we analysed. In the second variant, MOG-1-125 was biotinylated at the Avi-tag positioned in the C-terminus. In this way, the antigen was site bound with the same orientation to streptavidin plates. Even though this type of assay managed to test positivity in 50% of the samples showing therefore a superiority compared to the other ELISA assay, it is still a mediocre method incapable to detect all MOG+ sera. Even with improvements on the front of the type of antigen to utilize, our results confirmed that the ELISA assay is not a suitable technique for diagnosing MOGAD. However, some researchers believe that the ELISA assay could still be a useful tool to quantify the titre of MOG antibodies of positive MOGAD patients for instance for longitudinal studies (Tea *et al.*, 2019). From our side we tried to find a reason for the failure of the site-directed ELISA assay, which could be connected to the fact that in this methodology the MOG-1-125 is not capable to move freely as it happens when MOG is displayed on the cellular surface. Therefore, we embedded MOG-1-125 in a fluid lipid environment, by

coating glass beads of similar cell size with a lipid mixture mimicking the cell membrane. Nonetheless, even this new methodology did not show a superiority compared to a “normal” ELISA assay. It actually even had a lower sensitivity for the detection of MOG-binding of 8-18C5 and of five sera from patients with MOGAD. This indicated that in general the MOG-1-125 is not sufficient to detect autoantibodies, independent from the environment. This is also in line with the results, which we obtained with ED-MOG displayed on cells.

In this thesis, we addressed the issue whether autoantibodies from patients with MOGAD recognize MOG also monovalently or whether they require bivalent binding. By generating Fab and F(ab)[']₂ fragments from patients' MOG antibodies, we demonstrated that these autoantibodies bind to MOG only bivalently. Humanized 8-18C5, instead, binds also monovalently. In 2019, the spacing required for bivalent binding of IgG1 has been identified, and it is around 13 nm (Shaw *et al.*, 2019). In our case, we found that, upon transfection, molecules of MOG (FL-MOG or ED-MOG) did not interact so closely to induce a Förster resonance energy transfer (FRET) signal, indicating that they are more than 6 nm apart (Macrini *et al.*, 2021). However, we cannot exclude that dimerization is occurring in the myelin or under other experimental conditions. For instance, Clements and colleague in their crystallography manuscript showed that the external portion of MOG could dimerize in vitro in a head-to-tail manner (Clements *et al.*, 2003).

We believe that the reason for the high sensitivity of the CBA is connected to the protein localization within the cell membrane, which could favour the bivalent binding (see Figure 2). MOG has been associated with the detergent insoluble fractions of the cell membrane (or also known as lipid rafts) (Kim and Pfeiffer, 1999). Interestingly, Kim and Pfeiffer in their study discovered that only around 40% of MOG was partitioning in the detergent insoluble cholesterol enriched domains. They hypothesized that the non-active protein is associated with the soluble part of the membrane, whereas, when the MOG molecules cluster together in the lipid rafts, they are activated and might activate themselves and other proteins of a signal transduction pathway (Kim and Pfeiffer, 1999). In this context, we believe that all the MOG variants

containing the second hydrophobic domain cluster preferentially in the lipid raft portions of the cell membrane and this clustering of the MOG molecules at a defined distance (~13-16 nm) which favours the bivalent binding of the patients antibodies (see Figure 2). Whereas, the MOG variants ED-MOG and MOG-Cyt, which do not efficiently detect MOG antibodies, might tend to cluster much less in the cholesterol enriched domain. The ED-MOG/MOG-Cyt molecules will be too close or too far from each other to allow a strong and bivalent binding of the autoantibodies (see Figure 2). This, however, remains to be analysed in future studies.

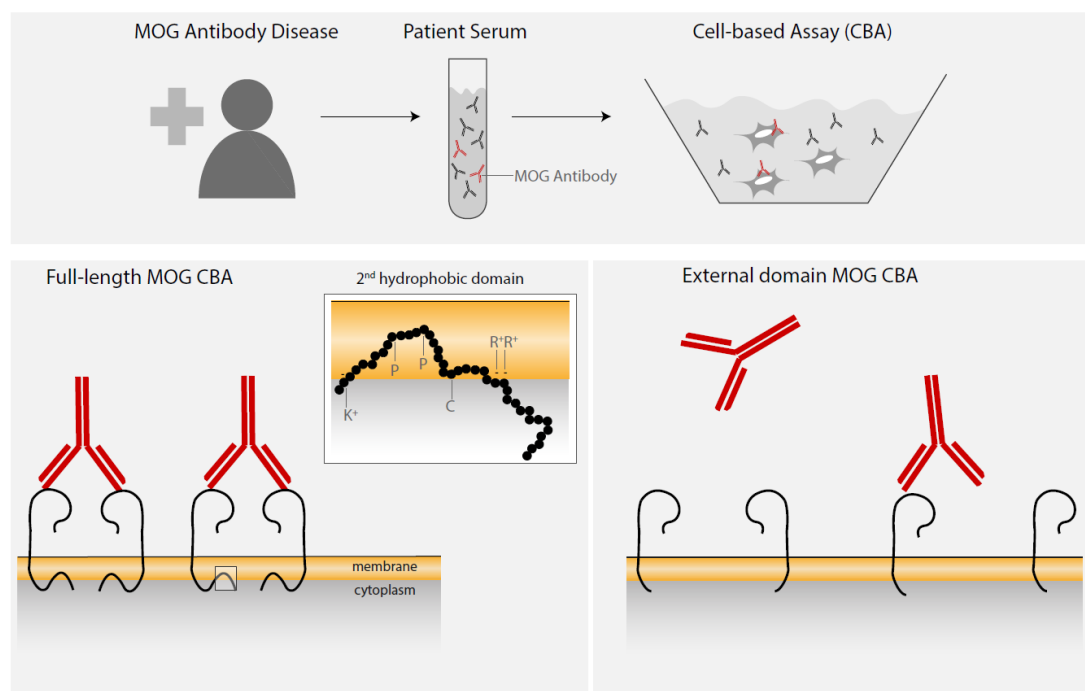


Figure 2: Schematic representation of the testing for MOG antibodies. Subjects showing clinical symptoms attributable to MOGAD, get tested to detect possible MOG antibodies. The serum derived from withdrawn blood, is incubated on cells transfected with FL-MOG. The CBA performed with FL-MOG is superior to the one performed with ED-MOG, because of the presence in the FL-MOG of the second hydrophobic domain. This domain has a monotopic localization and it keeps the FL-MOG molecules at a defined distance (~13-16 nm), which favors the bivalent binding of the human antibodies. The lack of this domain, instead, induces the ED-MOG molecules at different distances, which decrease the chances for a bivalent binding of the human MOG IgGs. (Adapted from Macrini *et al.*, 2021)

Our data give a more in depth explanation on why CBA works on these antibodies (Figure 2). However, we believe that there can be some aspects that can still be improved in order to have a more reliable, more reproducible and efficient testing. For instance, we observed that the MOG variant MOG-2TMD is significantly higher expressed than FL-MOG. As it is illustrated in the

suppl. Figure 2B of (Macrini *et al.*, 2021) there is a higher percentage of cells that present an EGFP (mean fluorescence signal) MFI >1000 when they are transfected with MOG-2TMD or with human-opossum-MOG. In both those constructs, the C-terminus was substituted with an SG linker of 13 amino acids. The higher expression of these variants over the full-length version of MOG could indicate that actually the normal C-terminus of MOG has an influence on the expression of the protein on the surface. Since we showed that the C-terminus is not an epitope and cannot be bound by the patients' antibodies, we would therefore suggest to transfect the cells with MOG-2TMD for the CBA instead of FL-MOG. Furthermore, if we gate the live cells for an EGFP signal >100, MOG-2TMD yields a slightly higher antibody detection than wild-type MOG, meaning we could gain a more intense detection signal. The use of the MOG-2TMD construct could actually be very handy in the case of low positive patients (see suppl. Fig 3 in (Macrini *et al.*, 2021)). In particular, the signal of the antibodies in the sera of patients #22 and #24 coming from MOG-2TMD binding to MOG-2TMD is higher than the one coming from the cells transfected with FL-MOG. However, as Reindl and colleagues argue in their multicentre study (Reindl *et al.*, 2020), low positive patients would need a more careful clinical evaluation, in order to rule out other possible inflammatory diseases of the CNS. Furthermore, one of the reasons why the MOG titre is low could depend on the fact that probably the sample was not taken at the disease onset or that it was taken after an immunosuppressive therapy (Reindl *et al.*, 2020).

Another point we want to stress is the differences we encountered between human MOG antibodies and the humanized monoclonal antibody 8-18C5 in the CBA we performed. Over the years of MOG research, 8-18C5 has been an extremely powerful tool in the field of CNS autoimmunity, because of its high affinity binding towards MOG. Throughout all the conducted experiments, we realized that 8-18C5 binds to all the different types of MOG variants we produced, without having any effect on its binding. Whereas, the patients' antibodies strongly bound only to the MOG variants that include the second hydrophobic domain. Furthermore, we could show that 8-18C5 can bind also monovalently to FL-MOG and ED-MOG with high affinity. In contrast, the human antibodies deriving from patients, mostly bind bivalently. We believe

that in future research of MOG-IgG in MOGAD, the use of 8-18C5 should be applied moderately because of the profound differences compared to the human antibodies, and the generation of recombinant antibodies from patient material would be desirable.

4.2 Pathogenic activity of MOG-Abs from patients

With our work, we contributed to the manuscript of (Spadaro *et al.*, 2018), which gave a more in depth understanding of the pathomechanisms that MOG antibodies exert in the CNS. Antibodies were affinity purified from plasma of patients with high MOG antibody levels and which were capable to react with rodent MOG. These patient-derived Abs were intrathecally injected in rats with EAE. This revealed two pathomechanisms, which are illustrated in Figure 3.

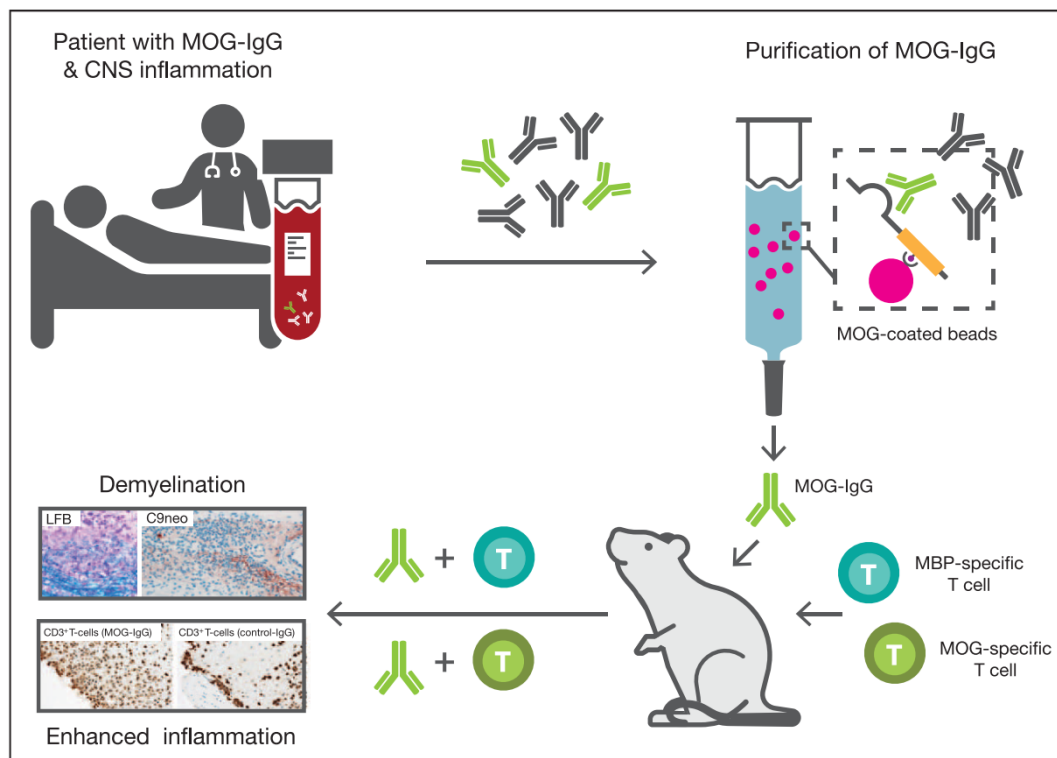


Figure 3: Pathogenic mechanisms of affinity-purified MOG antibodies deriving from patients. From the plasma of patients with MOGAD, MOG antibodies reacting with rodent MOG, were affinity purified. The purified antibodies were then concentrated and injected in rats together with MBP specific T cells or together with MOG specific T cells. The T cells caused EAE in the animals, and the MOG IgGs worsened the disease with two different mechanisms. When MOG IgGs were injected with MBP T cells, which breached the BBB, they induced demyelination (luxol fast blue (LFB) staining) accompanied with complement deposition (C9neo). In the second mechanisms, MOG antibodies together with cognate MOG T cells, increased T cell infiltration, in comparison to MOG T cells together with control IgGs. The figure was adapted from (Mader *et al.*, 2020).

First, when the purified IgGs were administered together with MBP specific T cells, which breach the BBB, a strong demyelination with C9neo deposition (similar to MS type II pattern) was observed. Second, together with cognate MOG specific T cells, there was an increased T cell infiltration.

In (Macrini *et al.*, 2021), we showed that MOG patients' antibodies mostly bind their target bivalently. This has major implications in the pathological mechanism that MOG antibodies exert, and it is in line with the mechanisms highlighted with the transfer experiments. In fact, it is known that the complement is better activated by the IgGs with monovalent binding; this means that MOG antibodies can still bind C1q, however, in a less efficient manner (Diebolder *et al.*, 2014). Furthermore, the transfer experiment indicated that MOG antibodies could induce pathogenicity in combination with MOG specific T cells. In fact, the presence of the autoantibodies were enhancing the recruitment and the action of the cognate T cells. We hypothesize that the recruitment and subsequent enhanced activation of the T cells could be a consequence of FcR-dependent opsonisation of MOG (Kinzel *et al.*, 2016).

These findings on the diverse mechanisms of antibody-mediated pathogenicity corroborate the statement that indicates MOGAD and AQP4+ NMOSD as two different diseases (Mader *et al.*, 2020). Histological stainings of brain lesions from subjects affected by AQP4+ NMOSD clearly showed astrocyte destruction with GFAP loss and abundant perivascular complement deposition (Bruck *et al.*, 2012; Bradl *et al.*, 2018; Weber *et al.*, 2018). Furthermore, it has been demonstrated that AQP4 antibodies bind strongly and monovalently to the M23 isoform of AQP4 (the one that forms OAPs) (Crane *et al.*, 2011). As previously stated, the ability of IgGs to bind monovalently increases the capacity of binding C1q and to activate complement, more than bivalent binding would do (Crane *et al.*, 2011; Diebolder *et al.*, 2014; Soltys *et al.*, 2019). Therefore, CDC is one of the mechanisms used by AQP4 antibodies to exert damage in the CNS. Ratelade and colleagues showed *in vivo* that antibodies binding to AQP4 that are capable of performing only CDC but not ADCC were exerting much less pathology in mice (Ratelade *et al.*, 2013). Moreover, the pathological effects

were greatly reduced even when compounds were used to block the FC gamma receptors usually involved in the activation of effector cells during ADCC (Ratelade *et al.*, 2013). To sum up, AQP4 antibodies cause astrocyte damage mostly with a combination of CDC and ADCC. MOGAD brain lesions, instead, are mostly characterized by demyelination, CD4+ T cell infiltration, relative axons and complete astrocytes preservation. In contrast to AQP4 antibodies, MOG antibodies need to be affinity purified and concentrated in order to exert a pathogenic effect in the CNS of rodents (Spadaro *et al.*, 2018). Instead, IgG samples from patients with AQP4+ NMOSD are enough to show strong pathogenicity in transfer experiments and exert tissue damage (Bradl *et al.*, 2009; Mader *et al.*, 2020). Furthermore, the histological analysis of samples coming from MOGAD patients or the results obtained in rodents from the transfer of the affinity purified MOG antibodies illustrated that the complement deposition is less pronounced than in AQP4+ NMOSD patients. (Spadaro *et al.*, 2015; Jarius *et al.*, 2016; Spadaro *et al.*, 2018; Weber *et al.*, 2018; Hoftberger *et al.*, 2020). The fact that CDC might not be one of the key mechanisms in the MOGAD pathogenicity could have consequences also in the treatment options. In fact, for AQP4+ NMOSD eculizumab (an inhibitor of C5) has been approved (Pittock *et al.*, 2019). Based on our data, this therapy might not be so effective for MOGAD patients.

4.3 Conclusions

In conclusion, with these studies we increased the knowledge of the underlying mechanisms that govern the interaction between MOG antibodies and their target. We found that the second hydrophobic domain of MOG enhances recognition of the extracellular part of MOG by autoantibodies from patients with MOGAD. This explains now why a CBA is the gold standard for the detection of these antibodies. Furthermore, we demonstrated that MOG antibodies coming from patients with MOGAD require bivalent binding to recognize MOG. The bivalent binding of MOG antibodies shows also a clear difference to AQP4 antibodies. Consequently, the role of complement and CDC in MOGAD is resized. Furthermore, this implies that MOGAD and AQP4+ NMOSD, do share some clinical phenotypes, however, they do not

overlap completely especially at the immunopathogenic level, meaning that it is correct to categorize MOGAD as a separate disease belonging to the group of inflammatory demyelinating diseases of the CNS. The difference between AQP4+ NMOSD and MOGAD could also be extended in the treatment options. Complement inhibitors like eculizumab are emerging as treatment option for NMOSD. Based on our findings on the lower complement activation, MOGAD patients might not benefit from this type of medicament leading in the future to more investigations to define the best treatment options for these subjects.

5 REFERENCE LIST

Amor S, Groome N, Linington C, Morris MM, Dornmair K, Gardinier MV, *et al.* Identification of epitopes of myelin oligodendrocyte glycoprotein for the induction of experimental allergic encephalomyelitis in SJL and Biozzi AB/H mice. *J Immunol* 1994; 153(10): 4349-56.

Anlar B, Basaran C, Kose G, Guven A, Haspolat S, Yakut A, *et al.* Acute disseminated encephalomyelitis in children: outcome and prognosis. *Neuropediatrics* 2003; 34(4): 194-9.

Baecher-Allan C, Kaskow BJ, Weiner HL. Multiple Sclerosis: Mechanisms and Immunotherapy. *Neuron* 2018; 97(4): 742-68.

Baumann M, Sahin K, Lechner C, Hennes EM, Schanda K, Mader S, *et al.* Clinical and neuroradiological differences of paediatric acute disseminating encephalomyelitis with and without antibodies to the myelin oligodendrocyte glycoprotein. *J Neurol Neurosurg Psychiatry* 2015; 86(3): 265-72.

Ben-Nun A, Wekerle H, Cohen IR. Vaccination against autoimmune encephalomyelitis with T-lymphocyte line cells reactive against myelin basic protein. *Nature* 1981; 292(5818): 60-1.

Bennett JL, Lam C, Kalluri SR, Saikali P, Bautista K, Dupree C, *et al.* Intrathecal pathogenic anti-aquaporin-4 antibodies in early neuromyelitis optica. *Ann Neurol* 2009; 66(5): 617-29.

Berger T, Rubner P, Schautzer F, Egg R, Ulmer H, Mayringer I, *et al.* Antimyelin antibodies as a predictor of clinically definite multiple sclerosis after a first demyelinating event. *N Engl J Med* 2003; 349(2): 139-45.

Binder DK, Yao X, Verkman AS, Manley GT. Increased seizure duration in mice lacking aquaporin-4 water channels. *Acta Neurochir Suppl* 2006; 96: 389-92.

Bloch O, Auguste KI, Manley GT, Verkman AS. Accelerated progression of kaolin-induced hydrocephalus in aquaporin-4-deficient mice. *J Cereb Blood Flow Metab* 2006; 26(12): 1527-37.

Boyle LH, Traherne JA, Plotnek G, Ward R, Trowsdale J. Splice variation in the cytoplasmic domains of myelin oligodendrocyte glycoprotein affects its cellular localisation and transport. *J Neurochem* 2007; 102(6): 1853-62.

Bratl M, Misu T, Takahashi T, Watanabe M, Mader S, Reindl M, *et al.* Neuromyelitis optica: Pathogenicity of patient immunoglobulin in vivo. *Annals of Neurology* 2009; 66 630-43.

Bratl M, Reindl M, Lassmann H. Mechanisms for lesion localization in neuromyelitis optica spectrum disorders. *Curr Opin Neurol* 2018; 31(3): 325-33.

Breithaupt C, Schafer B, Pellkofer H, Huber R, Lington C, Jacob U. Demyelinating myelin oligodendrocyte glycoprotein-specific autoantibody response is focused on one dominant conformational epitope region in rodents. *J Immunol* 2008; 181(2): 1255-63.

Breithaupt C, Schubart A, Zander H, Skerra A, Huber R, Lington C, *et al.* Structural insights into the antigenicity of myelin oligodendrocyte glycoprotein. *Proceedings of the National Academy of Sciences of the United States of America* 2003; 100(16): 9446-51.

Brilot F, Dale RC, Selter RC, Grummel V, Kalluri SR, Aslam M, *et al.* Antibodies to native myelin oligodendrocyte glycoprotein in children with inflammatory demyelinating central nervous system disease. *Ann Neurol* 2009; 66(6): 833-42.

Brimberg L, Mader S, Fujieda Y, Arinuma Y, Kowal C, Volpe BT, *et al.* Antibodies as Mediators of Brain Pathology. *Trends in immunology* 2015; 36(11): 709-24.

Bruck W, Popescu B, Lucchinetti CF, Markovic-Plese S, Gold R, Thal DR, *et al.* Neuromyelitis optica lesions may inform multiple sclerosis heterogeneity debate. *Ann Neurol* 2012; 72(3): 385-94.

Brunner C, Lassmann H, Waehnel TV, Matthieu JM, Lington C. Differential ultrastructural localization of myelin basic protein, myelin/oligodendroglial glycoprotein, and 2',3'-cyclic nucleotide 3'-phosphodiesterase in the CNS of adult rats. *J Neurochem* 1989; 52(1): 296-304.

Carbrey JM, Agre P. Discovery of the aquaporins and development of the field. *Handb Exp Pharmacol* 2009(190): 3-28.

Clements CS, Reid HH, Beddoe T, Tynan FE, Perugini MA, Johns TG, *et al.* The crystal structure of myelin oligodendrocyte glycoprotein, a key autoantigen in multiple sclerosis. *Proc Natl Acad Sci U S A* 2003; 100(19): 11059-64.

Compston A, Coles A. Multiple sclerosis. *Lancet* 2008; 372(9648): 1502-17.

Cong H, Jiang Y, Tien P. Identification of the myelin oligodendrocyte glycoprotein as a cellular receptor for rubella virus. *J Virol* 2011; 85(21): 11038-47.

Crane JM, Lam C, Rossi A, Gupta T, Bennett JL, Verkman AS. Binding affinity and specificity of neuromyelitis optica autoantibodies to aquaporin-4 M1/M23 isoforms and orthogonal arrays. *J Biol Chem* 2011; 286(18): 16516-24.

Dale RC, Tantsis EM, Merheb V, Kumaran RY, Sinmaz N, Pathmanandavel K, *et al.* Antibodies to MOG have a demyelination phenotype and affect oligodendrocyte cytoskeleton. *Neurol Neuroimmunol Neuroinflamm* 2014; 1(1): e12.

Delarasse C, Daubas P, Mars LT, Vizler C, Litzemberger T, Iglesias A, *et al.* Myelin/oligodendrocyte glycoprotein-deficient (MOG-deficient) mice reveal lack of immune tolerance to MOG in wild-type mice. *J Clin Invest* 2003; 112(4): 544-53.

Delarasse C, Della Gaspera B, Lu CW, Lachapelle F, Gelot A, Rodriguez D, *et al.* Complex alternative splicing of the myelin oligodendrocyte glycoprotein gene is unique to human and non-human primates. *J Neurochem* 2006; 98(6): 1707-17.

Dendrou CA, Fugger L, Friese MA. Immunopathology of multiple sclerosis. *Nat Rev Immunol* 2015; 15(9): 545-58.

Di Pauli F, Berger T. Myelin Oligodendrocyte Glycoprotein Antibody-Associated Disorders: Toward a New Spectrum of Inflammatory Demyelinating CNS Disorders? *Front Immunol* 2018; 9: 2753.

Diebold CA, Beurskens FJ, de Jong RN, Koning RI, Strumane K, Lindorfer MA, *et al.* Complement is activated by IgG hexamers assembled at the cell surface. *Science* 2014; 343(6176): 1260-3.

Dyer CA, Matthieu JM. Antibodies to myelin/oligodendrocyte-specific protein and myelin/oligodendrocyte glycoprotein signal distinct changes in the organization of cultured oligodendroglial membrane sheets. *J Neurochem* 1994; 62(2): 777-87.

Feinstein A, Freeman J, Lo AC. Treatment of progressive multiple sclerosis: what works, what does not, and what is needed. *Lancet Neurol* 2015; 14(2): 194-207.

Flach AC, Litke T, Strauss J, Haberl M, Gomez CC, Reindl M, *et al.* Autoantibody-boosted T-cell reactivation in the target organ triggers manifestation of autoimmune CNS disease. *Proc Natl Acad Sci U S A* 2016; 113(12): 3323-8.

Frigeri A, Gropper MA, Turck CW, Verkman AS. Immunolocalization of the mercurial-insensitive water channel and glycerol intrinsic protein in epithelial cell plasma membranes. *Proc Natl Acad Sci U S A* 1995a; 92(10): 4328-31.

Frigeri A, Gropper MA, Umenishi F, Kawashima M, Brown D, Verkman AS. Localization of MIWC and GLIP water channel homologs in neuromuscular, epithelial and glandular tissues. *J Cell Sci* 1995b; 108 (Pt 9): 2993-3002.

Furman CS, Gorelick-Feldman DA, Davidson KG, Yasumura T, Neely JD, Agre P, *et al.* Aquaporin-4 square array assembly: opposing actions of M1 and M23 isoforms. *Proc Natl Acad Sci U S A* 2003; 100(23): 13609-14.

Garcia-Vallejo JJ, Ilarregui JM, Kalay H, Chamorro S, Koning N, Unger WW, *et al.* CNS myelin induces regulatory functions of DC-SIGN-expressing, antigen-presenting cells via cognate interaction with MOG. *J Exp Med* 2014; 211(7): 1465-83.

Gold R, Lington C, Lassmann H. Understanding pathogenesis and therapy of multiple sclerosis via animal models: 70 years of merits and culprits in experimental autoimmune encephalomyelitis research. *Brain* 2006; 129(Pt 8): 1953-71.

Gough SC, Simmonds MJ. The HLA Region and Autoimmune Disease: Associations and Mechanisms of Action. *Curr Genomics* 2007; 8(7): 453-65.

Greer JM, McCombe PA. Role of gender in multiple sclerosis: clinical effects and potential molecular mechanisms. *J Neuroimmunol* 2011; 234(1-2): 7-18.

Gregory SG, Schmidt S, Seth P, Oksenberg JR, Hart J, Prokop A, *et al.* Interleukin 7 receptor alpha chain (IL7R) shows allelic and functional association with multiple sclerosis. *Nat Genet* 2007; 39(9): 1083-91.

Haase CG, Guggenmos J, Brehm U, Andersson M, Olsson T, Reindl M, *et al.* The fine specificity of the myelin oligodendrocyte glycoprotein autoantibody response in patients with multiple sclerosis and normal healthy controls. *J Neuroimmunol* 2001; 114(1-2): 220-5.

Hamid SHM, Whittam D, Mutch K, Linaker S, Solomon T, Das K, *et al.* What proportion of AQP4-IgG-negative NMO spectrum disorder patients are MOG-IgG positive? A cross sectional study of 132 patients. *J Neurol* 2017; 264(10): 2088-94.

Hartmann FJ, Khademi M, Aram J, Ammann S, Kockum I, Constantinescu C, *et al.* Multiple sclerosis-associated IL2RA polymorphism controls GM-CSF production in human TH cells. *Nat Commun* 2014; 5: 5056.

Hauser SL. The Charcot Lecture | beating MS: a story of B cells, with twists and turns. *Mult Scler* 2015; 21(1): 8-21.

Hemmer B, Archelos JJ, Hartung HP. New concepts in the immunopathogenesis of multiple sclerosis. *Nat Rev Neurosci* 2002; 3(4): 291-301.

Hemmer B, Kerschensteiner M, Korn T. Role of the innate and adaptive immune responses in the course of multiple sclerosis. *Lancet Neurol* 2015; 14(4): 406-19.

Hillebrand S, Schanda K, Nigritinou M, Tsymala I, Bohm D, Peschl P, *et al.* Circulating AQP4-specific auto-antibodies alone can induce neuromyelitis optica spectrum disorder in the rat. *Acta Neuropathol* 2019; 137(3): 467-85.

Hillert J, Olerup O. HLA and MS. *Neurology* 1993; 43(11): 2426-7.

Hinson SR, McKeon A, Fryer JP, Apiwattanakul M, Lennon VA, Pittock SJ. Prediction of neuromyelitis optica attack severity by quantitation of complement-mediated injury to aquaporin-4-expressing cells. *Arch Neurol* 2009; 66(9): 1164-7.

Ho JD, Yeh R, Sandstrom A, Chorny I, Harries WE, Robbins RA, *et al.* Crystal structure of human aquaporin 4 at 1.8 Å and its mechanism of conductance. *Proc Natl Acad Sci U S A* 2009; 106(18): 7437-42.

Hoftberger R, Guo Y, Flanagan EP, Lopez-Chiriboga AS, Endmayr V, Hochmeister S, *et al.* The pathology of central nervous system inflammatory demyelinating disease accompanying myelin oligodendrocyte glycoprotein autoantibody. *Acta Neuropathol* 2020.

Hohlfeld R, Dornmair K, Meinl E, Wekerle H. The search for the target antigens of multiple sclerosis, part 1: autoreactive CD4+ T lymphocytes as pathogenic effectors and therapeutic targets. *Lancet Neurol* 2016a; 15(2): 198-209.

Hohlfeld R, Dornmair K, Meinl E, Wekerle H. The search for the target antigens of multiple sclerosis, part 2: CD8+ T cells, B cells, and antibodies in the focus of reverse-translational research. *Lancet Neurol* 2016b; 15(3): 317-31.

Hollenbach JA, Oksenberg JR. The immunogenetics of multiple sclerosis: A comprehensive review. *J Autoimmun* 2015; 64: 13-25.

Iglesias A, Bauer J, Litznerburger T, Schubart A, Linington C. T- and B-cell responses to myelin oligodendrocyte glycoprotein in experimental autoimmune encephalomyelitis and multiple sclerosis. *Glia* 2001; 36(2): 220-34.

Jarius S, Metz I, König FB, Ruprecht K, Reindl M, Paul F, *et al.* Screening for MOG-IgG and 27 other anti-glial and anti-neuronal autoantibodies in 'pattern II multiple sclerosis' and brain biopsy findings in a MOG-IgG-positive case. *Mult Scler* 2016; 22: 1541-9.

Jarius S, Wildemann B. AQP4 antibodies in neuromyelitis optica: diagnostic and pathogenetic relevance. *Nat Rev Neurol* 2010; 6(7): 383-92.

Jarius S, Wildemann B, Paul F. Neuromyelitis optica: clinical features, immunopathogenesis and treatment. *Clin Exp Immunol* 2014; 176(2): 149-64.

Johns TG, Bernard CC. Binding of complement component C1q to myelin oligodendrocyte glycoprotein: a novel mechanism for regulating CNS inflammation. *Mol Immunol* 1997; 34(1): 33-8.

Johns TG, Bernard CC. The structure and function of myelin oligodendrocyte glycoprotein. *J Neurochem* 1999; 72(1): 1-9.

Jurynczyk M, Gerales R, Probert F, Woodhall MR, Waters P, Tackley G, *et al.* Distinct brain imaging characteristics of autoantibody-mediated CNS conditions and multiple sclerosis. *Brain* 2017a; 140(3): 617-27.

Jurynczyk M, Jacob A, Fujihara K, Palace J. Myelin oligodendrocyte glycoprotein (MOG) antibody-associated disease: practical considerations. *Pract Neurol* 2019; 19(3): 187-95.

Jurynczyk M, Probert F, Yeo T, Tackley G, Claridge TDW, Cavey A, *et al.* Metabolomics reveals distinct, antibody-independent, molecular signatures of MS, AQP4-antibody and MOG-antibody disease. *Acta Neuropathol Commun* 2017b; 5(1): 95.

Karni A, Bakimer-Kleiner R, Abramsky O, Ben-Nun A. Elevated levels of antibody to myelin oligodendrocyte glycoprotein is not specific for patients with multiple sclerosis. *Arch Neurol* 1999; 56(3): 311-5.

Kearney H, Altmann DR, Samson RS, Yiannakas MC, Wheeler-Kingshott CA, Ciccarelli O, *et al.* Cervical cord lesion load is associated with disability independently from atrophy in MS. *Neurology* 2015; 84(4): 367-73.

Kim T, Pfeiffer SE. Myelin glycosphingolipid/cholesterol-enriched microdomains selectively sequester the non-compact myelin proteins CNP and MOG. *Journal of neurocytology* 1999; 28(4-5): 281-93.

Kinzel S, Lehmann-Horn K, Torke S, Hausler D, Winkler A, Stadelmann C, *et al.* Myelin-reactive antibodies initiate T cell-mediated CNS autoimmune disease by opsonization of endogenous antigen. *Acta Neuropathol* 2016; 132(1): 43-58.

Kitley J, Waters P, Woodhall M, Leite MI, Murchison A, George J, *et al.* Neuromyelitis optica spectrum disorders with aquaporin-4 and myelin-oligodendrocyte glycoprotein antibodies: a comparative study. *JAMA Neurol* 2014; 71(3): 276-83.

Kleiter I, Gahlen A, Borisow N, Fischer K, Wernecke KD, Wegner B, *et al.* Neuromyelitis optica: Evaluation of 871 attacks and 1,153 treatment courses. *Ann Neurol* 2016; 79(2): 206-16.

Koch-Henriksen N, Sorensen PS. The changing demographic pattern of multiple sclerosis epidemiology. *Lancet Neurol* 2010; 9(5): 520-32.

Kroepfl JF, Viise LR, Charron AJ, Linington C, Gardinier MV. Investigation of myelin/oligodendrocyte glycoprotein membrane topology. *J Neurochem* 1996; 67(5): 2219-22.

Krupp LB, Banwell B, Tenenbaum S, International Pediatric MSSG. Consensus definitions proposed for pediatric multiple sclerosis and related disorders. *Neurology* 2007; 68(16 Suppl 2): S7-12.

Kuhle J, Pohl C, Mehling M, Edan G, Freedman MS, Hartung HP, *et al.* Lack of association between antimyelin antibodies and progression to multiple sclerosis. *N Engl J Med* 2007; 356(4): 371-8.

Lalive PH, Menge T, Delarasse C, Della Gaspera B, Pham-Dinh D, Villoslada P, *et al.* Antibodies to native myelin oligodendrocyte glycoprotein are serologic markers of early inflammation in multiple sclerosis. *Proc Natl Acad Sci U S A* 2006; 103(7): 2280-5.

Landis DM, Reese TS. Arrays of particles in freeze-fractured astrocytic membranes. *J Cell Biol* 1974; 60(1): 316-20.

Lassmann H, Brunner C, Bradl M, Linington C. Experimental allergic encephalomyelitis: the balance between encephalitogenic T lymphocytes and demyelinating antibodies determines size and structure of demyelinated lesions. *Acta Neuropathol* 1988; 75(6): 566-76.

Lebar R, Baudrimont M, Vincent C. Chronic experimental autoimmune encephalomyelitis in the guinea pig. Presence of anti-M2 antibodies in central nervous system tissue and the possible role of M2 autoantigen in the induction of the disease. *J Autoimmun* 1989; 2(2): 115-32.

Lebar R, Boutry JM, Vincent C, Robineaux R, Voisin GA. Studies on autoimmune encephalomyelitis in the guinea pig. II. An in vitro investigation on the nature, properties, and specificity of the serum-demyelinating factor. *J Immunol* 1976; 116(5): 1439-46.

Lebar R, Vincent C, Fischer-le Boubennec E. Studies on autoimmune encephalomyelitis in the guinea pig--III. A comparative study of two autoantigens of central nervous system myelin. *J Neurochem* 1979; 32(5): 1451-60.

Lennon VA, Kryzer TJ, Pittock SJ, Verkman AS, Hinson SR. IgG marker of optic-spinal multiple sclerosis binds to the aquaporin-4 water channel. *J Exp Med* 2005; 202(4): 473-7.

Lennon VA, Wingerchuk DM, Kryzer TJ, Pittock SJ, Lucchinetti CF, Fujihara K, *et al.* A serum autoantibody marker of neuromyelitis optica: distinction from multiple sclerosis. *Lancet* 2004; 364(9451): 2106-12.

Li L, Zhang H, Varrin-Doyer M, Zamvil SS, Verkman AS. Proinflammatory role of aquaporin-4 in autoimmune neuroinflammation. *FASEB J* 2011; 25(5): 1556-66.

Linnington C, Bradl M, Lassmann H, Brunner C, Vass K. Augmentation of demyelination in rat acute allergic encephalomyelitis by circulating mouse monoclonal antibodies directed against a myelin/oligodendrocyte glycoprotein. *Am J Pathol* 1988; 130(3): 443-54.

Linnington C, Webb M, Woodhams PL. A novel myelin-associated glycoprotein defined by a mouse monoclonal antibody. *J Neuroimmunol* 1984; 6(6): 387-96.

Lopez-Chiriboga AS, Majed M, Fryer J, Dubey D, McKeon A, Flanagan EP, *et al.* Association of MOG-IgG Serostatus With Relapse After Acute Disseminated Encephalomyelitis and Proposed Diagnostic Criteria for MOG-IgG-Associated Disorders. *JAMA Neurol* 2018; 75(11): 1355-63.

Lovato L, Willis SN, Rodig SJ, Caron T, Almendinger SE, Howell OW, *et al.* Related B cell clones populate the meninges and parenchyma of patients with multiple sclerosis. *Brain* 2011; 134(Pt 2): 534-41.

Lu M, Lee MD, Smith BL, Jung JS, Agre P, Verdijk MA, *et al.* The human AQP4 gene: definition of the locus encoding two water channel polypeptides in brain. *Proc Natl Acad Sci U S A* 1996; 93(20): 10908-12.

Lucchinetti C, Bruck W, Parisi J, Scheithauer B, Rodriguez M, Lassmann H. Heterogeneity of multiple sclerosis lesions: implications for the pathogenesis of demyelination. *Ann Neurol* 2000; 47(6): 707-17.

Lucchinetti CF, Guo Y, Popescu BF, Fujihara K, Itoyama Y, Misu T. The pathology of an autoimmune astrocytopathy: lessons learned from neuromyelitis optica. *Brain Pathol* 2014; 24(1): 83-97.

Macrini C, Gerhards R, Winklmeier S, Bergmann L, Mader S, Spadaro M, *et al.* Features of MOG required for recognition by patients with MOG antibody-associated disorders. *Brain* 2021.

Mader S, Gredler V, Schanda K, Rostasy K, Dujmovic I, Pfaller K, *et al.* Complement activating antibodies to myelin oligodendrocyte glycoprotein in neuromyelitis optica and related disorders. *J Neuroinflammation* 2011; 8: 184.

Mader S, Kumpfel T, Meinl E. Novel insights into pathophysiology and therapeutic possibilities reveal further differences between AQP4-IgG- and MOG-IgG-associated diseases. *Curr Opin Neurol* 2020; 33(3): 362-71.

Mader S, Lutterotti A, Di Pauli F, Kuenz B, Schanda K, Aboul-Enein F, *et al.* Patterns of antibody binding to aquaporin-4 isoforms in neuromyelitis optica. *PLoS One* 2010; 5(5): e10455.

Mantegazza R, Cristaldini P, Bernasconi P, Baggi F, Pedotti R, Piccini I, *et al.* Anti-MOG autoantibodies in Italian multiple sclerosis patients: specificity, sensitivity and clinical association. *Int Immunol* 2004; 16(4): 559-65.

Marchioni E, Ravaglia S, Piccolo G, Furione M, Zardini E, Franciotta D, *et al.* Postinfectious inflammatory disorders: subgroups based on prospective follow-up. *Neurology* 2005; 65(7): 1057-65.

Marta CB, Montano MB, Taylor CM, Taylor AL, Bansal R, Pfeiffer SE. Signaling cascades activated upon antibody cross-linking of myelin oligodendrocyte glycoprotein: potential implications for multiple sclerosis. *J Biol Chem* 2005; 280(10): 8985-93.

Marta CB, Taylor CM, Coetzee T, Kim T, Winkler S, Bansal R, *et al.* Antibody cross-linking of myelin oligodendrocyte glycoprotein leads to its rapid repartitioning into detergent-insoluble fractions, and altered protein phosphorylation and cell morphology. *J Neurosci* 2003; 23(13): 5461-71.

Marti Fernandez I, Macrini C, Krumbholz M, Hensbergen PJ, Hipgrave Ederveen AL, Winklmeier S, *et al.* The Glycosylation Site of Myelin Oligodendrocyte Glycoprotein Affects Autoantibody Recognition in a Large Proportion of Patients. *Front Immunol* 2019; 10: 1189.

Mayer MC, Breithaupt C, Reindl M, Schanda K, Rostasy K, Berger T, *et al.* Distinction and temporal stability of conformational epitopes on myelin oligodendrocyte glycoprotein recognized by patients with different inflammatory central nervous system diseases. *J Immunol* 2013; 191(7): 3594-604.

Mayer MC, Meinl E. Glycoproteins as targets of autoantibodies in CNS inflammation: MOG and more. *Ther Adv Neurol Disord* 2012; 5(3): 147-59.

McDonald WI, Compston A, Edan G, Goodkin D, Hartung HP, Lublin FD, *et al.* Recommended diagnostic criteria for multiple sclerosis: guidelines from the International Panel on the diagnosis of multiple sclerosis. *Ann Neurol* 2001; 50(1): 121-7.

McLaughlin KA, Chitnis T, Newcombe J, Franz B, Kennedy J, McArdel S, *et al.* Age-dependent B cell autoimmunity to a myelin surface antigen in pediatric multiple sclerosis. *J Immunol* 2009; 183(6): 4067-76.

Menge T, Hemmer B, Nessler S, Wiendl H, Neuhaus O, Hartung HP, *et al.* Acute disseminated encephalomyelitis: an update. *Arch Neurol* 2005; 62(11): 1673-80.

Menge T, Kieseier BC, Nessler S, Hemmer B, Hartung HP, Stuve O. Acute disseminated encephalomyelitis: an acute hit against the brain. *Curr Opin Neurol* 2007a; 20(3): 247-54.

Menge T, von Budingen HC, Lalive PH, Genain CP. Relevant antibody subsets against MOG recognize conformational epitopes exclusively exposed in solid-phase ELISA. *Eur J Immunol* 2007b; 37(11): 3229-39.

Mikaeloff Y, Adamsbaum C, Husson B, Vallee L, Ponsot G, Confavreux C, *et al.* MRI prognostic factors for relapse after acute CNS inflammatory demyelination in childhood. *Brain* 2004; 127(Pt 9): 1942-7.

Miller DH, Chard DT, Ciccarelli O. Clinically isolated syndromes. *Lancet Neurol* 2012; 11(2): 157-69.

Misu T, Hoftberger R, Fujihara K, Wimmer I, Takai Y, Nishiyama S, *et al.* Presence of six different lesion types suggests diverse mechanisms of tissue injury in neuromyelitis optica. *Acta Neuropathol* 2013; 125(6): 815-27.

Munger KL, Zhang SM, O'Reilly E, Hernan MA, Olek MJ, Willett WC, *et al.* Vitamin D intake and incidence of multiple sclerosis. *Neurology* 2004; 62(1): 60-5.

Murthy SN, Faden HS, Cohen ME, Bakshi R. Acute disseminated encephalomyelitis in children. *Pediatrics* 2002; 110(2 Pt 1): e21.

Nielsen S, Nagelhus EA, Amiry-Moghaddam M, Bourque C, Agre P, Ottersen OP. Specialized membrane domains for water transport in glial cells: high-resolution immunogold cytochemistry of aquaporin-4 in rat brain. *J Neurosci* 1997; 17(1): 171-80.

Nielsen TR, Pedersen M, Rostgaard K, Frisch M, Hjalgrim H. Correlations between Epstein-Barr virus antibody levels and risk factors for multiple sclerosis in healthy individuals. *Mult Scler* 2007; 13(3): 420-3.

Nilsson I, Saaf A, Whitley P, Gafvelin G, Waller C, von Heijne G. Proline-induced disruption of a transmembrane alpha-helix in its natural environment. *J Mol Biol* 1998; 284(4): 1165-75.

Noseworthy JH, Lucchinetti C, Rodriguez M, Weinshenker BG. Multiple sclerosis. *N Engl J Med* 2000; 343(13): 938-52.

O'Connor KC, Bar-Or A, Hafler DA. The neuroimmunology of multiple sclerosis: possible roles of T and B lymphocytes in immunopathogenesis. *J Clin Immunol* 2001; 21(2): 81-92.

O'Connor KC, McLaughlin KA, De Jager PL, Chitnis T, Bettelli E, Xu C, *et al.* Self-antigen tetramers discriminate between myelin autoantibodies to native or denatured protein. *Nat Med* 2007; 13(2): 211-7.

Obermeier B, Lovato L, Mentele R, Bruck W, Forne I, Imhof A, *et al.* Related B cell clones that populate the CSF and CNS of patients with multiple sclerosis produce CSF immunoglobulin. *J Neuroimmunol* 2011; 233(1-2): 245-8.

Owens GP, Ritchie AM, Burgoon MP, Williamson RA, Corboy JR, Gildea DH. Single-cell repertoire analysis demonstrates that clonal expansion is a prominent feature of the B cell response in multiple sclerosis cerebrospinal fluid. *J Immunol* 2003; 171(5): 2725-33.

Pandit L, Asgari N, Apiwattanakul M, Palace J, Paul F, Leite MI, *et al.* Demographic and clinical features of neuromyelitis optica: A review. *Mult Scler* 2015; 21(7): 845-53.

Pandit L, Mustafa S. Spontaneous remission lasting more than a decade in untreated AQP4 antibody-positive NMOSD. *Neurol Neuroimmunol Neuroinflamm* 2017; 4(4): e351.

Papadopoulos MC, Manley GT, Krishna S, Verkman AS. Aquaporin-4 facilitates reabsorption of excess fluid in vasogenic brain edema. *FASEB J* 2004; 18(11): 1291-3.

Parker Harp CR, Archambault AS, Sim J, Ferris ST, Mikesell RJ, Koni PA, *et al.* B cell antigen presentation is sufficient to drive neuroinflammation in an animal model of multiple sclerosis. *J Immunol* 2015; 194(11): 5077-84.

Peschl P, Bradl M, Hoftberger R, Berger T, Reindl M. Myelin Oligodendrocyte Glycoprotein: Deciphering a Target in Inflammatory Demyelinating Diseases. *Front Immunol* 2017a; 8: 529.

Peschl P, Schanda K, Zeka B, Given K, Bohm D, Ruprecht K, *et al.* Human antibodies against the myelin oligodendrocyte glycoprotein can cause complement-dependent demyelination. *J Neuroinflammation* 2017b; 14(1): 208.

Pham-Dinh D, Mattei MG, Nussbaum JL, Roussel G, Pontarotti P, Roedel N, *et al.* Myelin/oligodendrocyte glycoprotein is a member of a subset of the immunoglobulin superfamily encoded within the major histocompatibility complex. *Proc Natl Acad Sci U S A* 1993; 90(17): 7990-4.

Pittock SJ, Berthele A, Fujihara K, Kim HJ, Levy M, Palace J, *et al.* Eculizumab in Aquaporin-4-Positive Neuromyelitis Optica Spectrum Disorder. *N Engl J Med* 2019; 381(7): 614-25.

Popescu BF, Pirko I, Lucchinetti CF. Pathology of multiple sclerosis: where do we stand? *Continuum (Minneapolis)* 2013; 19(4 Multiple Sclerosis): 901-21.

Probstel AK, Dornmair K, Bittner R, Sperl P, Jenne D, Magalhaes S, *et al.* Antibodies to MOG are transient in childhood acute disseminated encephalomyelitis. *Neurology* 2011; 77(6): 580-8.

Rammohan KW. Cerebrospinal fluid in multiple sclerosis. *Ann Indian Acad Neurol* 2009; 12(4): 246-53.

Rash JE, Yasumura T, Hudson CS, Agre P, Nielsen S. Direct immunogold labeling of aquaporin-4 in square arrays of astrocyte and ependymocyte plasma membranes in rat brain and spinal cord. *Proc Natl Acad Sci U S A* 1998; 95(20): 11981-6.

Ratelade J, Asavapanumas N, Ritchie AM, Wemlinger S, Bennett JL, Verkman AS. Involvement of antibody-dependent cell-mediated cytotoxicity in

inflammatory demyelination in a mouse model of neuromyelitis optica. *Acta Neuropathol* 2013; 126(5): 699-709.

Reindl M, Linington C, Brehm U, Egg R, Dilitz E, Deisenhammer F, *et al.* Antibodies against the myelin oligodendrocyte glycoprotein and the myelin basic protein in multiple sclerosis and other neurological diseases: a comparative study. *Brain* 1999; 122 (Pt 11): 2047-56.

Reindl M, Schanda K, Woodhall M, Tea F, Ramanathan S, Sagen J, *et al.* International multicenter examination of MOG antibody assays. 2020; 7(2).

Reindl M, Waters P. Myelin oligodendrocyte glycoprotein antibodies in neurological disease. *Nat Rev Neurol* 2019; 15(2): 89-102.

Rossi A, Moritz TJ, Ratelade J, Verkman AS. Super-resolution imaging of aquaporin-4 orthogonal arrays of particles in cell membranes. *J Cell Sci* 2012; 125(Pt 18): 4405-12.

Saadoun S, Bridges LR, Verkman AS, Papadopoulos MC. Paucity of natural killer and cytotoxic T cells in human neuromyelitis optica lesions. *Neuroreport* 2012a; 23(18): 1044-7.

Saadoun S, Waters P, Bell BA, Vincent A, Verkman AS, Papadopoulos MC. Intra-cerebral injection of neuromyelitis optica immunoglobulin G and human complement produces neuromyelitis optica lesions in mice. *Brain* 2010; 133(Pt 2): 349-61.

Saadoun S, Waters P, MacDonald C, Bell BA, Vincent A, Verkman AS, *et al.* Neutrophil protease inhibition reduces neuromyelitis optica-immunoglobulin G-induced damage in mouse brain. *Ann Neurol* 2012b; 71(3): 323-33.

Saadoun S, Waters P, Owens GP, Bennett JL, Vincent A, Papadopoulos MC. Neuromyelitis optica MOG-IgG causes reversible lesions in mouse brain. *Acta Neuropathol Commun* 2014; 2(1): 35.

Salama S, Khan M, Shanechi A, Levy M, Izbudak I. MRI differences between MOG antibody disease and AQP4 NMOSD. *Mult Scler* 2020: 1352458519893093.

Sato DK, Callegaro D, Lana-Peixoto MA, Waters PJ, de Haidar Jorge FM, Takahashi T, *et al.* Distinction between MOG antibody-positive and AQP4 antibody-positive NMO spectrum disorders. *Neurology* 2014; 82(6): 474-81.

Seil FJ, Falk GA, Kies MW, Alvord EC, Jr. The in vitro demyelinating activity of sera from guinea pigs sensitized with whole CNS and with purified encephalitogen. *Exp Neurol* 1968; 22(4): 545-55.

Serafini B, Rosicarelli B, Magliozzi R, Stigliano E, Aloisi F. Detection of ectopic B-cell follicles with germinal centers in the meninges of patients with secondary progressive multiple sclerosis. *Brain Pathol* 2004; 14(2): 164-74.

Shaw A, Hoffecker IT, Smyrlaki I, Rosa J, Grevys A, Bratlie D, *et al.* Binding to nanopatterned antigens is dominated by the spatial tolerance of antibodies. *Nat Nanotechnol* 2019; 14(2): 184-90.

Soltys J, Liu Y, Ritchie A, Wemlinger S, Schaller K, Schumann H, *et al.* Membrane assembly of aquaporin-4 autoantibodies regulates classical complement activation in neuromyelitis optica. *J Clin Invest* 2019; 129(5): 2000-13.

Sospedra M, Martin R. Immunology of multiple sclerosis. *Annu Rev Immunol* 2005; 23: 683-747.

Spadaro M, Gerdes LA, Krumbholz M, Ertl-Wagner B, Thaler FS, Schuh E, *et al.* Autoantibodies to MOG in a distinct subgroup of adult multiple sclerosis. *Neurol Neuroimmunol Neuroinflamm* 2016; 3(5): e257.

Spadaro M, Gerdes LA, Mayer MC, Ertl-Wagner B, Laurent S, Krumbholz M, *et al.* Histopathology and clinical course of MOG-antibody associated encephalomyelitis. *Annals of Clinical and Translational Neurology* 2015; 2: 295-301.

Spadaro M, Meinl E. Detection of Autoantibodies Against Myelin Oligodendrocyte Glycoprotein in Multiple Sclerosis and Related Diseases. *Methods Mol Biol* 2016; 1304: 99-104.

Spadaro M, Winklmeier S, Beltran E, Macrini C, Hoftberger R, Schuh E, *et al.* Pathogenicity of human antibodies against myelin oligodendrocyte glycoprotein. *Ann Neurol* 2018; 84(2): 315-28.

Stangel M, Fredrikson S, Meinl E, Petzold A, Stuve O, Tumani H. The utility of cerebrospinal fluid analysis in patients with multiple sclerosis. *Nat Rev Neurol* 2013; 9(5): 267-76.

Sutherland BW, Toews J, Kast J. Utility of formaldehyde cross-linking and mass spectrometry in the study of protein-protein interactions. *J Mass Spectrom* 2008; 43(6): 699-715.

Takai Y, Misu T, Kaneko K, Chihara N, Narikawa K, Tsuchida S, *et al.* Myelin oligodendrocyte glycoprotein antibody-associated disease: an immunopathological study. *Brain* 2020; 143(5): 1431-46.

Tea F, Lopez JA, Ramanathan S, Merheb V, Lee FXZ, Zou A, *et al.* Characterization of the human myelin oligodendrocyte glycoprotein antibody response in demyelination. *Acta Neuropathol Commun* 2019; 7(1): 145.

Tenembaum S, Chamoles N, Fejerman N. Acute disseminated encephalomyelitis: a long-term follow-up study of 84 pediatric patients. *Neurology* 2002; 59(8): 1224-31.

Tenembaum S, Chitnis T, Ness J, Hahn JS, International Pediatric MSSG. Acute disseminated encephalomyelitis. *Neurology* 2007; 68(16 Suppl 2): S23-36.

Thompson AJ, Banwell BL, Barkhof F, Carroll WM, Coetzee T, Comi G, *et al.* Diagnosis of multiple sclerosis: 2017 revisions of the McDonald criteria. *Lancet Neurol* 2018; 17(2): 162-73.

Toews J, Rogalski JC, Kast J. Accessibility governs the relative reactivity of basic residues in formaldehyde-induced protein modifications. *Anal Chim Acta* 2010; 676(1-2): 60-7.

van der Mei IA, Ponsonby AL, Dwyer T, Blizzard L, Simmons R, Taylor BV, *et al.* Past exposure to sun, skin phenotype, and risk of multiple sclerosis: case-control study. *BMJ* 2003; 327(7410): 316.

Verkman AS, Binder DK, Bloch O, Auguste K, Papadopoulos MC. Three distinct roles of aquaporin-4 in brain function revealed by knockout mice. *Biochim Biophys Acta* 2006; 1758(8): 1085-93.

von Budingen HC, Hauser SL, Ouallet JC, Tanuma N, Menge T, Genain CP. Frontline: Epitope recognition on the myelin/oligodendrocyte glycoprotein differentially influences disease phenotype and antibody effector functions in autoimmune demyelination. *Eur J Immunol* 2004; 34(8): 2072-83.

von Budingen HC, Mei F, Greenfield A, Jahn S, Shen YA, Reid HH, *et al.* The myelin oligodendrocyte glycoprotein directly binds nerve growth factor to modulate central axon circuitry. *J Cell Biol* 2015; 210(6): 891-8.

von Heijne G. Proline kinks in transmembrane alpha-helices. *J Mol Biol* 1991; 218(3): 499-503.

Wang H, Munger KL, Reindl M, O'Reilly EJ, Levin LI, Berger T, *et al.* Myelin oligodendrocyte glycoprotein antibodies and multiple sclerosis in healthy young adults. *Neurology* 2008; 71(15): 1142-6.

Wang JJ, Jaunmuktane Z, Mummery C, Brandner S, Leary S, Trip SA. Inflammatory demyelination without astrocyte loss in MOG antibody-positive NMOSD. *Neurology* 2016; 87(2): 229-31.

Waters P, Fadda G, Woodhall M, O'Mahony J, Brown RA, Castro DA, *et al.* Serial Anti-Myelin Oligodendrocyte Glycoprotein Antibody Analyses and Outcomes in Children With Demyelinating Syndromes. *JAMA Neurol* 2019.

Waters P, Woodhall M, O'Connor KC, Reindl M, Lang B, Sato DK, *et al.* MOG cell-based assay detects non-MS patients with inflammatory neurologic disease. *Neurol Neuroimmunol Neuroinflamm* 2015; 2(3): e89.

Waters PJ, McKeon A, Leite MI, Rajasekharan S, Lennon VA, Villalobos A, *et al.* Serologic diagnosis of NMO: a multicenter comparison of aquaporin-4-IgG assays. *Neurology* 2012; 78(9): 665-71; discussion 9.

Weber MS, Derfuss T, Metz I, Bruck W. Defining distinct features of anti-MOG antibody associated central nervous system demyelination. *Ther Adv Neurol Disord* 2018; 11: 1756286418762083.

Weinshenker BG, Wingerchuk DM. Neuromyelitis Spectrum Disorders. *Mayo Clin Proc* 2017; 92(4): 663-79.

Wingerchuk DM. Smoking: effects on multiple sclerosis susceptibility and disease progression. *Ther Adv Neurol Disord* 2012; 5(1): 13-22.

Wingerchuk DM, Lennon VA, Lucchinetti CF, Pittock SJ, Weinshenker BG. The spectrum of neuromyelitis optica. *Lancet Neurol* 2007a; 6(9): 805-15.

Wingerchuk DM, Lennon VA, Pittock SJ, Lucchinetti CF, Weinshenker BG. Revised diagnostic criteria for neuromyelitis optica. *Neurology* 2006; 66(10): 1485-9.

Wingerchuk DM, Pittock SJ, Lucchinetti CF, Lennon VA, Weinshenker BG. A secondary progressive clinical course is uncommon in neuromyelitis optica. *Neurology* 2007b; 68(8): 603-5.

Wolburg H, Wolburg-Buchholz K, Fallier-Becker P, Noell S, Mack AF. Structure and functions of aquaporin-4-based orthogonal arrays of particles. *Int Rev Cell Mol Biol* 2011; 287: 1-41.

Woodhall M, Coban A, Waters P, Ekizoglu E, Kurtuncu M, Shugaiv E, *et al.* Glycine receptor and myelin oligodendrocyte glycoprotein antibodies in Turkish patients with neuromyelitis optica. *J Neurol Sci* 2013; 335(1-2): 221-3.

Wynford-Thomas R, Jacob A, Tomassini V. Neurological update: MOG antibody disease. *J Neurol* 2019; 266(5): 1280-6.

Yang B, Brown D, Verkman AS. The mercurial insensitive water channel (AQP-4) forms orthogonal arrays in stably transfected Chinese hamster ovary cells. *J Biol Chem* 1996; 271(9): 4577-80.

Yang B, Verkman AS. Water and glycerol permeabilities of aquaporins 1-5 and MIP determined quantitatively by expression of epitope-tagged constructs in *Xenopus* oocytes. *J Biol Chem* 1997; 272(26): 16140-6.

Zamvil SS, Steinman L. The T lymphocyte in experimental allergic encephalomyelitis. *Annu Rev Immunol* 1990; 8: 579-621.

Zhang H, Verkman AS. Eosinophil pathogenicity mechanisms and therapeutics in neuromyelitis optica. *J Clin Invest* 2013; 123(5): 2306-16.

Zhang X, Yu CJ, Sisodia SS. The topology of pen-2, a gamma-secretase subunit, revisited: evidence for a reentrant loop and a single pass transmembrane domain. *Mol Neurodegener* 2015; 10: 39.

Zhou D, Srivastava R, Nessler S, Grummel V, Sommer N, Bruck W, *et al.* Identification of a pathogenic antibody response to native myelin oligodendrocyte glycoprotein in multiple sclerosis. *Proc Natl Acad Sci U S A* 2006; 103(50): 19057-62.

6 ACKNOWLEDGMENTS

I would firstly like to thank Prof. Edgar Meinl for giving me a chance to work as a PhD student in his lab five years ago. I am also extremely grateful to Prof. Elisabeth Weiß to kindly agree to be my supervisor at the Biology faculty and to Dr. Florence Bareyre to be part of my thesis advisory committee. Lastly, I am so glad that since my master thesis I could count on Henri (Dr. Franquelim). His enthusiasm and his brilliant ideas had a meaningful impact on my project. All of you together guided me through my PhD years, especially when things were not working or not making sense. At the end, everything worked out and our common efforts were rewarded with a nice published manuscript.

I am also thankful to my thesis committee: Prof. Laura Busse, Prof. Angelika Böttger, Dr. Serena Schwenkert, Dr. Lars Kunz and Prof. Richard Merrill. Thank you for finding time for me and my dissertation.

A huge thank you also to Prof. H. H. Kampinga from the University of Groningen. For me he has been an amazing mentor from a scientific and human perspective. He saw the potential in me and helped me believe in myself and highlight my strength. I will never forget this.

Truth must be told, those 5 years were not always an easy ride. However, I can also say that for sure all the single years were lots of FUN. It takes a village to do a PhD, and awesome people luckily inhabit mine.

Un grazie a mamma e papa per avermi permesso di studiare senza mai farmi mancare nulla e per essere un esempio di perseveranza e ambizione. Un grazie anche a mia sorella Sveva e alle mie zie Carla e Fiorella. Nonostante la lontananza creata dal covid, riesco comunque a sentirvi vicine. Anche perché silenziose non siete mai state. Nonna Ines non è più con noi, ma insieme a nonna Rosita mi ha cresciuto. Credo non abbiano mai capito cosa studiassi, comunque mi hanno sempre mostrato il loro amore incondizionato e sono sempre state orgogliose di ogni mio traguardo.

I think you all know that I consider friendship essential for my life. Living abroad, far from your family, comes with a bit of loneliness. However, I have

been blessed with awesome friends that constitute my second family. Therefore, I will take my time to show you my love and infinite gratitude.

Grazie alle mie amiche/befane di vecchia data Carla e Giorgia. Sono 19 anni che ci conosciamo, sfortunatamente non ci vediamo spesso come vorremmo. Ma ogni volta che vi vedo siete sempre uno spasso e ci vogliamo bene come quando avevamo 11 anni. Però e per fortuna siamo MOLTO cambiate esteriormente da quando scattammo le foto a casa di Carla a 11 anni. Vi aspetto a Monaco!

Un enorme grazie va anche alle Amiche "belle e brave" che ho conosciuto in triennale a Trieste: Alessia, Gael, Giovanna e Ilaria. Mi mancate sempre tantissimo. Ci siamo state vicine in molti momenti di totale disagio e so che lo faremo anche in futuro. Anche perché al disagio non c'è fine. Non vedo l'ora di riabbracciarvi, non importa se a Trieste, Portogruaro o Londra. L'importante è potersi rivedere.

In the Netherlands, I had the huge luck to live with Iris, and thanks to her I got to know Adri. I still hope that one day we might live again in the same city. I can picture ourselves in the future with wine, junk food watching the 300th season of Grey's Anatomy. I miss you very much, but you are a constant in my life and you are both source of kindness, support, wisdom and fun. I can't wait to travel again with you!

In the Netherlands, I also met Giovanni. Even though, I was pretty desperate and I bailed last minute many gatherings/dinners you still decided to be my friend. You helped me to go through a lot and most importantly, you fed me several times. So, tanti cuoricini.

I am living since six years in Munich and I have been lucky enough to meet some special people that made want to settle here.

Per prima cosa, un grazie a Linda. Sei stata la mia prima vera amica a Monaco. E la nostra amicizia ha funzionato nonostante il fatto che l'intera U6 ci dividesse. Sono veramente felice di riaverti qui a Monaco, per fare i picnic, le cene e andare ai concerti. Grazie a Linda, ho potuto conoscere Sonia. Anche se alla fine ci siamo incrociate solo per un anetto o più, ho subito capito

quanto fossi dolce e in gamba. Insieme facciamo veramente un trio gnocco ma comunque sempre poraccio.

I am glad to have met Jonas at MPI. Even though, you gave me a nickname that I do not like, I enjoyed so much our fun office. I hope you realize that now I did write my thesis and did save it. What an accomplishment. I hope soon I will finally meet little Brianna. Seeing you and Laura starting a family filled me with joy.

Thanks to MPI, I also met Philipp G. and Melanie. You are such a nice company for trips, games and new year's eve. I hope these moments will keep happening more and more in the future. You are such a warm and welcoming couple, and Pino is so adorable and so lucky to have you.

As I said before those last five years were not always so easy. However, the Meinel group was extremely supportive and such a great source of ideas and joy. Thanks to Sarah Laurent, Melania Spadaro, Franziska Thaler, Heike Rübsamen, Katie Wong, Samantha Ho, Charlotte Schadt and all the master and bachelor students that helped us through the years. A special thank you goes to Simone Mader. You are such a great addition to our group. You will make an incredible group leader, I am sure about it.

A super mega huge thank you goes to the "Lunch group": Alina, Bella, Edu, Julia, Kathrin, Lian, Michelle, Miriam, Ramona, Stephan and of course our guest "scientist" Christian. I can consider you good friends and I hope this will continue for a long time even after I am gone from the lab. I love spending time with you; you made every lunch break so little about science and so much about HAPPINES. We became so close to plan so many activities together that most of the time we have no time to make everything happen. I have missed our breaks dearly during the lockdown. I hope soon we can travel again all together. I think the first trip on the list is Spain; otherwise, Isar will be fine too. Or Trieste. Or Mensa.

In Munich, I have got to know a very lovely lady. Miss Marucci. I am glad that I joined Interact, because there I had the chance to meet you. I feel that many times, we think the same things, and it is crazy how close we became in such little time. I miss you very much now that you are in Leipzig. However, I am happy that you are together with Mr. Erik. As sure as you will always have a

place in Munich, I am sure we will be in each other's life for a long time. I am glad that through her I've also got to know Liliana and Martina. It was a pleasure spending time with you too.

Lastly, but not at all less important, an enormous thank you to my partner Philipp. Thanks for staying next to me even when times are hard. Thanks for your positive thinking (even if I might not appreciate it in every occasion), thanks for trying to bring the best out of me and thanks for believing that I can do everything from science to artsy project. I love our cat-dominated family. I can't say anything more than: *you are my sunshine, my only sunshine, you make me happy when skies are grey*. I know, in your ears and your brain, it might sound different.

Thank you all sincerely.

7 CURRICULUM VITAE

Personal information

Name	Caterina Macrini
Date of birth	16.05.1991
Place of birth	Rome, Italy
Nationality	Italian

Scientific experience & education

08/16 – ongoing	PhD, Department of Clinical Neuroimmunology, Biomedical Center Munich, LMU Supervisor: Prof. Edgar Meinl
01/15 – 07/16	Research Collaborator and Second Master Project, Department of Molecular and Cellular Biophysics, Max Planck Institute of Biochemistry Supervisor: Prof. Petra Schwille and Dr. Henri Franquelim
11/13 – 07/14	First Master Project, Department of Cell Biology, University Medical Center Groningen (NL) Supervisor: Prof. Harm H. Kampinga
09/13 – 09/15	M.Sc. in Biomedical Sciences at the University of Groningen (NL)
03/13 – 08/13	Bachelor Project, Molecular Pathology Group, International Center for Genetic Engineering and Biotechnology, Trieste (IT) Supervisor: Dr. Maurizio Romano
09/10 – 07/13	B.Sc. in Biotechnology at the University of Trieste (IT)